e-Zine for meteor observers meteornews.net

MeteorNews

ISSN 2570-4745 VOL 5 / ISSUE 4 / JULY 2020

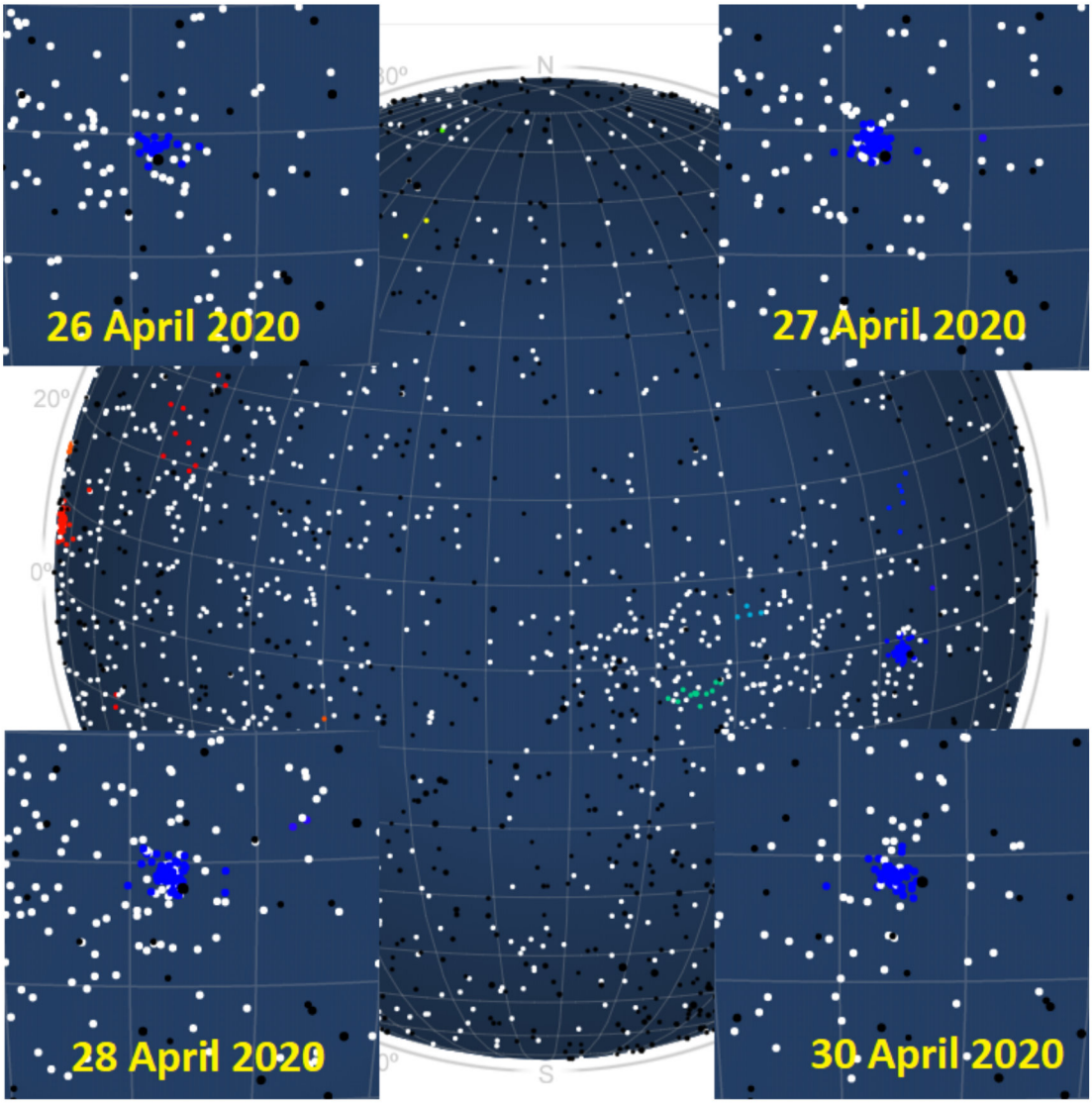

The radiant of the h Virginids appeared as a rather compact concentration of orbit points on the daily maps of the NASA Meteor shower Portal

- h Virginids
- Three Virginid showers
- CAMS reports
- Geminids 2019
- Radio observations
- Fireballs

Contents

h Virginids (HVI#343) activity enhancement in 2020

Paul Roggemans[1], **Carl Johannink**[2] **and Takashi Sekiguchi**[3]

[1] **Pijnboomstraat 25, 2800 Mechelen, Belgium**
paul.roggemans@gmail.com

[2] **Dutch Meteor Society, the Netherlands**
c.johannink@t-online.de

[3] **Nippon Meteor Society**
SonotaCo network
ts007@mtj.biglobe.ne.jp

A case study has been made on the available data for the h Virginids (HVI#343) and a reliable long-term reference orbit has been calculated. The orbits obtained by different independent video camera networks during the enhanced activity in 2020 are in perfect agreement. The orbit is a typical Jupiter family comet orbit. The HVI-meteor shower is likely a component of a complex which include some other known meteor showers.

1 Introduction

The different CAMS networks[1] registered enhanced activity from the h Virginids (HVI#343) between April 23 and 28 when Dr. Jenniskens decided to issue a CBET (Jenniskens, 2020), to announce the exceptional activity of the shower. Also, the SonotaCo Network in Japan and the Global Meteor Network could immediately confirm the enhanced activity of this shower.

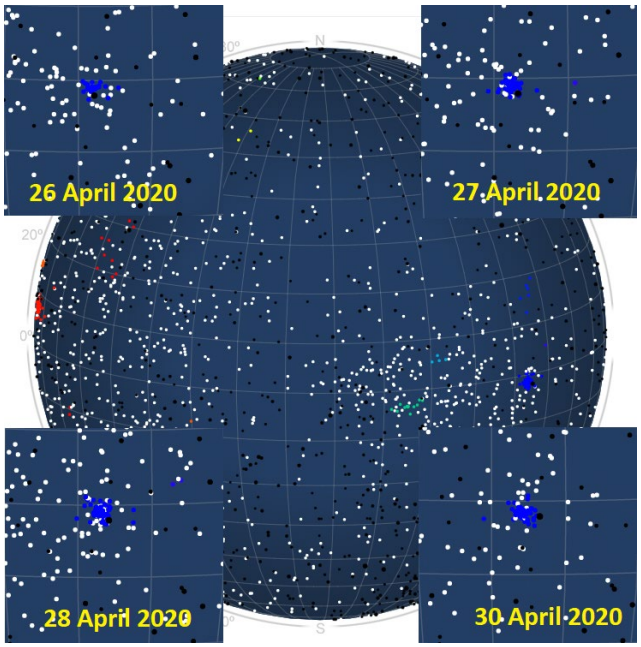

Figure 1 – The radiant of the h Virginids appeared as a rather compact concentration of orbit points on the daily maps of the NASA Meteor shower Portal. The map shows the radiant distribution on April 29, the insets show the radiant on four other nights.

The enhanced activity level lasted several nights more. The median values for the orbital elements of 13 orbits as calculated by Jenniskens (2020) were:

- $q = 0.739$ AU
- $a = 2.99$ AU
- $e = 0.755$
- $i = 0.71°$
- $\omega = 67.9°$
- $\Omega = 216.9°$
- $\Pi = 284.5°$

Which corresponds to a typical orbit of a Jupiter family comet. Using these values as reference orbit the CAMS BeNeLux network alone had 51 meteors that could be matched with this reference orbit until April 27–28. The exceptional favorable weather circumstances during this period provided perfect conditions to collect orbits during most of the activity period.

2 What do we know about HVI#343?

The shower has the status as established and the IAU working list of meteor showers[2] (Jopek and Jenniskens, 2011; Jopek and Kaňuchová, 2014, 2017) mentions three references as evidence for this meteor stream. The first refers to SonotaCo Network (2009), a publication based on the first two years of the Japanese network (*Table 1*). Hence the discovery of the h Virginids is on the account of the SonotaCo Network.

The second reference in the MDC list is based on single station video work (Molau and Rendtel, 2009). The radiant position differs 10°, the activity period is about a week

[1] http://cams.seti.org/FDL/

[2] https://www.ta3.sk/IAUC22DB/MDC2007/Roje/pojedynczy_obiekt.php?kodstrumienia=00343&colecimy=0&kodmin=00001&kodmax=01035&sortowanie=0

earlier and the velocity estimate is well above the known value for the HVI shower. The high risk for chance line-up contamination with non shower meteors and the presence of other nearby radiants are possible explanations for these differences. As the data is not based on orbits we do not consider this entry as a relevant reference for this shower.

The only evidence with a reference orbit in the IAU shower list comes from Jenniskens et al. (2016). This reference orbit was obtained from 11 HVI#343 orbits, all recorded between 27 April 2012 and 2 May 2012. The orbital elements of this reference correspond indeed with the median values for the 11 orbits, but we obtain different values for the solar longitude and radiant with $\lambda_\odot = 40.2°$, $\alpha_g = 206.4°$ and $\delta_g = –12.0°$. Working with median values to obtain an average orbit is not ideal, it is not the way to average angular values. In this particular case with 11 orbits, 7 are south of the ecliptic, 4 are north of it, which means the nodes and argument of perihelion switch with 180° whether the orbit is north or south of the ecliptic. Therefore we applied the method of Jopek et al. (2006) to compute the average orbit for these 11 orbits. This average orbit is listed in *Table 1* to be compared to the original reference. Checking for HVI orbits in the 2010–2016 CAMS orbit dataset (Jenniskens et al., 2018) which was released begin 2020, we find as many as 77 HVI orbits listed. Strange enough, only 3 of the 11 orbits that were identified as HVI in the 2010–2013 CAMS orbit dataset are still identified as HVI orbits in the new dataset. No new reference orbits have been published for the CAMS data. We compute the mean orbit for the 77 HVI orbits listed in the CAMS dataset 2010–2016, using the method of Jopek et al. (2006). The resulting orbit is listed in *Table 1*. This is a slightly different orbit than the one published by Jenniskens et al. (2016) which is listed in the IAU MDC. This explains why 8 of the original 11 HVI orbits failed to be identified in the newer dataset because a different reference orbit was derived for the shower.

Table 1 – The reference orbits listed for the HVI#343 as listed in the IAU working list of meteor showers compared to the average orbit for two CAMS datasets as computed by the authors.

	SonotaCo 2007–2008	Jenniskens et al. 2016	CAMS 2012	CAMS 2011–2016
$\lambda_\odot$	39.0°	38.0°	40.2°	40.8°
α_g	204.2°	204.8°	206.4°	204.0°
δ_g	–11.6°	–11.5°	–12.0°	–11.4°
v_g	18.7 km/s	17.2 km/s	17.2 km/s	18.2 km/s
a	–	2.28 AU	2.26 AU	2.81 AU
q	–	0.742 AU	0.750 AU	0.766 AU
e	–	0.659	0.668	0.727
ω	–	72.7°	70.9°	64.1°
Ω	–	218.2°	218.5°	220.9°
i	–	0.9°	0.6°	0.7°
N	16	11	11	77

It is obvious that apart from the SonotaCo network, the discoverer of this shower, the other references were somehow problematic. Masahiro Koseki (2020) wrote earlier: "*HVI1 is quite different from others and forms possibly a different shower with 021AVB4 and 5, 136SLE2*". It is not excluded that the HVI#343 activity has been detected earlier in other surveys and got listed under a different shower identification.

3 How did HVI perform previous years?

We have 1101924 orbits public available, 630341 combined for EDMOND and SonotaCo (2007–2019), 471583 for CAMS (2010–2016). From the 2020 orbit data we know that h Virginids must be present within the interval $30° < \lambda_\odot < 46°$, we limit our scope to this time interval which still contains 31443 orbits. The geocentric velocity range and the radiant position can help to reduce the size of the dataset further. Based on past HVI orbit data we estimate the useful velocity range to search HVI-orbits as $12 \text{ km/s} < v_g < 23 \text{ km/s}$. To limit the radiant area, we select a range in the Sun-centered ecliptic coordinates with $156° < \lambda - \lambda_\odot < 176°$ and $–7° < \beta < +5°$. This way the influence of the radiant drift due to the rotation of the Earth around the Sun is eliminated. This selection results in a workable dataset with 627 orbits.

We start a search on these 627 orbits to locate orbits that form a concentration using an iterative procedure (Roggemans et al., 2019). Using simple average values or median values for angular values is not recommended, moreover the HVI meteor stream has orbits north and south of the ecliptic what means that the nodes switch and the argument of perihelion differs 180°. We use the method of Jopek et al. (2006) to obtain average orbits for each collection of similar orbits.

To assess the degree of similarity between any orbit and the reference we use the so called discrimination criteria or D-criteria. To reduce the amount of contamination of the sample by sporadic false positives we apply the D-criteria of Southworth and Hawkins (1963), Drummond (1981) and Jopek (1993) combined. Each of these criteria has some slightly different eliminations. To distinguish between the weak similarity of the very dispersed part of the shower and the very strong similarity within the core of the shower, we define five different classes with specific threshold levels of similarity:

- Low: $D_{SH} < 0.25$ & $D_D < 0.105$ & $D_H < 0.25$;
- Medium low: $D_{SH} < 0.2$ & $D_D < 0.08$ & $D_H < 0.2$;
- Medium high: $D_{SH} < 0.15$ & $D_D < 0.06$ & $D_H < 0.15$;
- High: $D_{SH} < 0.1$ & $D_D < 0.04$ & $D_H < 0.1$.
- Very high: $D_{SH} < 0.05$ & $D_D < 0.02$ & $D_H < 0.05$.

These classes are defined arbitrary and help us to evaluate the compactness of the collection of orbits. Old and very diffuse showers should contain mainly orbits with low threshold D-criteria while young or very compact showers should have a distinct core of very high threshold orbits.

We started with the average orbit as a reference orbit for all 627 orbits in our dataset. Using the low threshold class required four iterations to reach a reference orbit for a concentration of 528 orbits within our 627 available orbits. Within this selection we got 184 orbits that fit the high threshold class, but only 28 orbits within the very high threshold class. After another six iterations we got a reference orbit for the high threshold class with 188 orbits. This selection surprisingly included a core with 70 very high threshold orbits. We decided to use this selection to iterate the final reference orbits. After another six iterations we arrived at a final reference orbit valid for the core of the HVI meteor stream.

Working with the discrimination criteria requires caution. The results indicate only a degree of similarity between the orbits. D-criteria provide no proof for any physical relationship between the meteoroids. D-criteria can be very misleading, especially if applied on short period orbits with small eccentricity. In this specific case our iterations end with a very distinct reference orbit for the very similar orbits. *Table 2* lists all the parameters obtained for the different threshold classes, using the final very high threshold orbit as reference.

Table 2 – The mean orbits for the HVI#343 meteor stream for each threshold class of similarity with the very high threshold average orbit as reference orbit.

	Low	Medium Low	Medium High	High	Very High
λ_O	39.2°	39.4°	40.0°	40.5°	41.2°
$\lambda_O{}^b$	30°	30°	30°	31°	37°
$\lambda_O{}^e$	46°	46°	46°	46°	45°
α_g	203.8°	203.6°	203.6°	203.6°	203.8°
δ_g	–11.0°	–11.1°	–11.2°	–11.3°	–11.5°
$\Delta\alpha_g$	+0.68°	+0.66°	+0.61°	+0.40°	+0.28°
$\Delta\delta_g$	–0.34°	–0.34°	–0.34°	–0.30°	–0.16°
λ–$\lambda_\odot$	167.2°	166.7°	166.4°	165.8°	164.9°
β	–1.1°	–1.2°	–1.3°	–1.3°	–1.4°
v_g	18.1 km/s	18.1 km/s	18.1 km/s	18.1 km/s	18.0 km/s
H_b	92.6 km	93.4 km	93.9 km	95.0 km	95.3 km
H_e	82.1 km	82.4 km	82.7 km	83.5 km	83.8 km
a	2.57 AU	2.67 AU	2.75 AU	2.83 AU	2.91 AU
q	0.751 AU	0.757 AU	0.759 AU	0.763 AU	0.770 AU
e	0.708	0.717	0.724	0.730	0.735
ω	66.6°	65.6°	64.4°	64.1°	63.6°
Ω	219.0°	219.2°	220.2°	220.4°	221.1°
i	0.5°	0.5°	0.5°	0.6°	0.7°
Π	285.5°	284.9°	284.8°	284.8°	284.2°
T_J	2.97	2.92	2.88	2.84	2.81
N	498	381	283	174	66

In the IAU MDC working list we find a mixture of orbits for many showers without any indication for the degree of similarity used to search for the orbits. Many authors defined shower associations using a single D-criterion like D_{SH} (Southworth and Hawkins, 1963) with a far too tolerant limit of 0.25 which produces plenty of false positives for certain types of orbits. Such meteor stream searches of the past resulted in large numbers of phantom meteor showers, defined by pure chance fitting sporadics.

Another information missing in most meteor stream searches is the time range in which the shower orbits were detected. In *Table 2* we indicate the begin and end of the interval in λ_O . $30° < \lambda_O < 46°$ is the time range we selected our orbits to search for HVI orbits. These are present from the beginning till the end, hence we took our interval rather short and the actual activity period of the h Virginids certainly extends before and after the interval we selected. However, it is not the purpose to identify the outliers of this stream. Meteor showers get dispersed and meteoroids can get separated from the main stream until the point that D-criteria or other tools of identification fail to determine their shower association.

Any indication for periodicity?

HVI orbits were detected in each year for which orbit data during the activity period was available. The largest number of HVI orbits was recorded in 2015 with 109 orbits, but the total number of video orbits available during the HVI activity period was also very high that year. If we look at the proportion HVI orbits as percentage of the total number of orbits available we see that the HVI shower appeared stronger in 2008 and 2019 than in other years. 2008 was the year the shower was first detected by SonotaCo Network, note the strong presence of high and very high threshold class orbits that year. For 2019 we have only SonotaCo Network orbits available and also this year had a significant proportion of HVI orbits. Good coverage of the activity period in the period 2011–2016 excludes that any enhanced activity was missed. Weather may have affected the years 2010, 2017 and 2018 when too few orbits were registered around the maximum of the shower. The strong presence in 2008 (*Figure 2*) may indicate a previous HVI outburst, the year the shower caught the attention when it was first discovered.

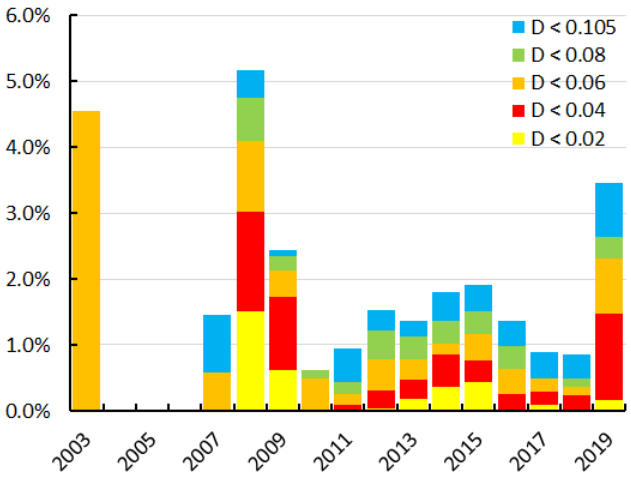

Figure 2 – The percentage of h Virginid orbits relative to the total number of orbits in the same time interval for each year.

The activity profile

When we count the total number of orbits and the number of HVI orbits in the same time bin, we can get an idea of the activity profile. We use a sliding mean counting the numbers of orbits per degree in solar longitude, moving forward in time in steps of 0.25° in solar longitude. The percentage of HVI orbits relative to the total number of orbits is a good indication for the activity level of the HVI shower. To eliminate the influence of other major sources on the total activity, we remove the orbits identified as Lyrids or as eta Aquariids.

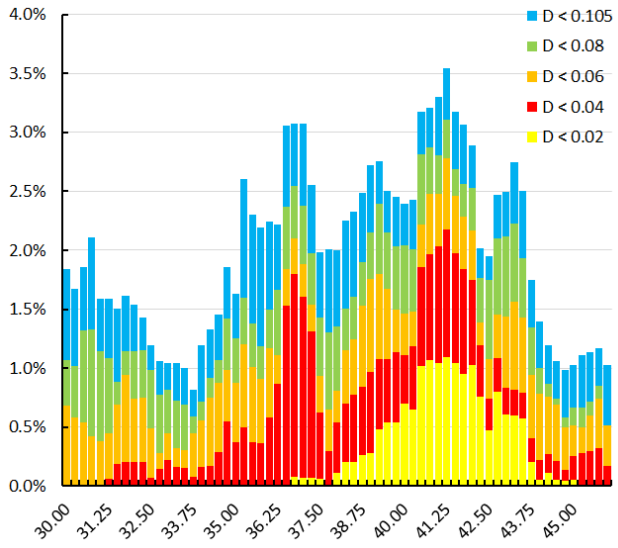

Figure 3 – HVI activity profile as percentage of the number of orbits counted per 1° in solar longitude for the different threshold classes of similarity.

First thing we notice is that HVI orbits are distinct present from the beginning until the end of the interval we searched for these orbits. This means the activity period starts earlier and ends later. There is no indication for any sharp peak in *Figure 3*, but two peaks are clearly visible, a first at $\lambda_\odot = 36.75°$ the second at $\lambda_\odot = 41.25°$ which corresponds with the very high threshold orbits of the concentration we found. The other sub-maxima that appear for the very low (blue) and low (green) threshold should be regarded as likely statistical fluctuations within the scatter of these dispersed orbits. The visible maxima in the high (red) and very high (yellow) threshold class are real.

Activity period

The time span of $30° < \lambda_\odot < 46°$ that we selected to locate the concentration of HVI orbits is shorter than the actual shower duration. To have an idea of the actual shower duration we use the high threshold orbit from *Table 2* to search for similar orbits among the 1101924 orbits we have in our dataset. The lookup with this reference orbit results in as many as 2796 possible HVI orbits that fit the minimal discrimination criteria. Determining an activity period for a shower depends on the tolerance we define for outliers. How many pure chance similarities do we allow? Most authors are not transparent at all about their criteria to identify orbits as shower orbits. Some use very low threshold similarity criteria; others use more rigid criteria. In *Table 3* we list the intervals in solar longitude between which HVI orbits were detected for the different threshold classes.

Table 3 – The solar longitudes for the first and last HVI orbit detected for each class of similarity threshold.

Similarity threshold	Begin $\lambda_\odot$	End $\lambda_\odot$	Orbits
Low	8°	75°	2773
Medium low	15°	66°	1410
Medium high	22°	57°	552
High	28°	51°	203
Very high	34°	44°	72

The HVI radiant

The number of orbits for each class is much higher than in our selection listed in *Table 2*, not only because of the much longer activity period, but also because of the much larger radiant size. In *Table 4* we list the radiant sizes obtained when all orbits are taken into account.

Table 4 – The radiant area in Sun centered ecliptic coordinates for HVI orbits, for each class of similarity threshold.

Similarity threshold	$\lambda - \lambda_\odot$ (°)	β (°)	Orbits
Low	[144°,178°]	[–27°,+27°]	2773
Medium low	[151°,175°]	[–21°,+21°]	1410
Medium high	[158°,173°]	[–17°,+14°]	552
High	[160°,171°]	[–10°,+9°]	203
Very high	[163°,169°]	[–5°,+2°]	72

Among the extra orbits we find plenty which were previously identified as alpha Virginids (AVB#021), sigma Leonids (SLE#136) and April theta Virginids (ATV#730). Most of the 'early' HVI orbits were listed as AVB and SLE which seem to be different components of one and the same meteor stream complex active for a period of at least eight weeks. This confirms what Masahiro Koseki mentioned before (Koseki, 2020).

The search on the complete dataset also revealed a number of similar orbits registered late August till mid-September, around $\lambda_\odot = 155°$ (August 28) from a radiant near $\alpha_g = 182°$ and $\delta_g = +23°$, in the region of Coma Berenices. It is rather diffuse and not worth further investigation unless more activity from this region would be confirmed.

The selection we used to locate the optimal reference orbit was limited to the interval $156° < \lambda - \lambda_\odot < 176°$ and $-7° < \beta < +5°$. The reason for this limitation in size is that a larger sampling area would include mainly outliers while the purpose is to locate a concentration of orbits to compute a mean orbit. Low velocity meteor streams near the ecliptic with short period orbits typically produce very large diffuse radiants. Using D-criteria on this type of orbits requires caution and therefore it is recommended to focus on the core of the shower. *Figure 4* shows a compact concentration of radiants of high and very high threshold orbits. *Figure 5* shows this for the inclination i in function of the length of perihelion Π.

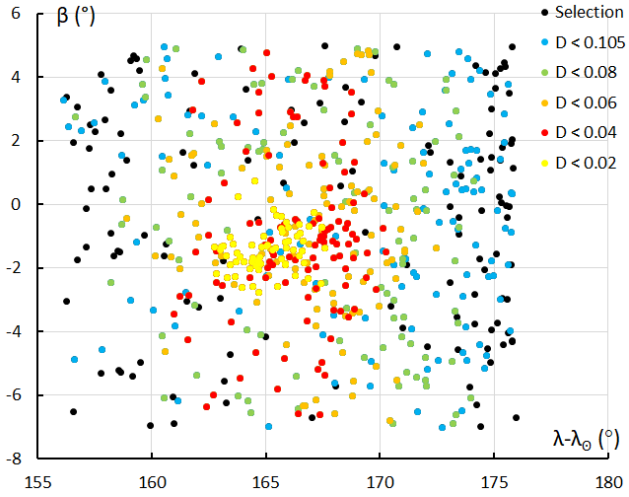

Figure 4 – The radiants for all orbits of the selection in Sun centered ecliptic coordinates, with all radiants for each similarity class mentioned in Table 2.

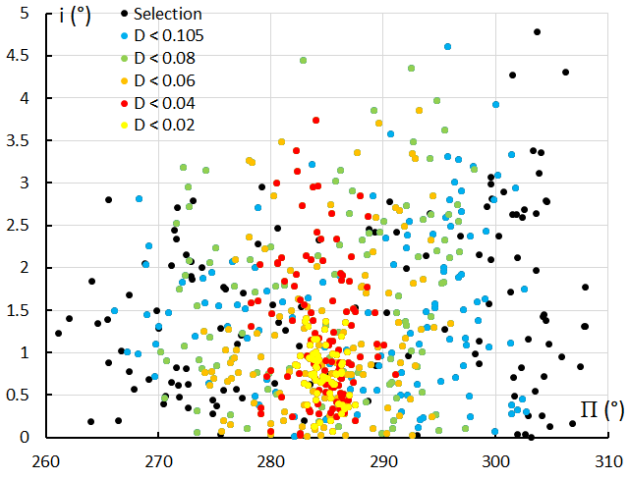

Figure 5 – The radiants for all orbits of the selection with inclination i plotted in function of the length of perihelion Π, with all radiants for each similarity class like mentioned in Table 2.

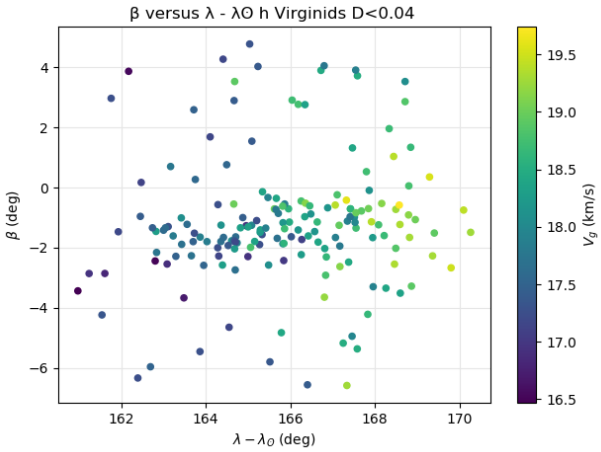

Figure 6 – HVI radiants in Sun centered ecliptic coordinates for the high threshold similarity class orbits with a color gradient for the geocentric velocity v_g.

Figure 6 shows the variation in geocentric velocity within the radiant. HVI meteors at left appeared slower than those at right. In *Figure 7* we see the increase in v_g in function of $\lambda - \lambda_\odot$. What we see is the effect of the Earth moving on its orbit around the Sun in the direction of the Apex. *Figure 6* can be seen as a close up of the HVI position in *Figure 8*, with the *x*-axis in *Figure 6* inversed.

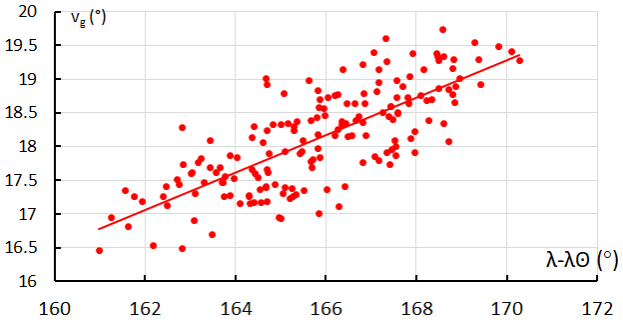

Figure 7 – The geocentric velocity v_g in function of $\lambda - \lambda_\odot$.

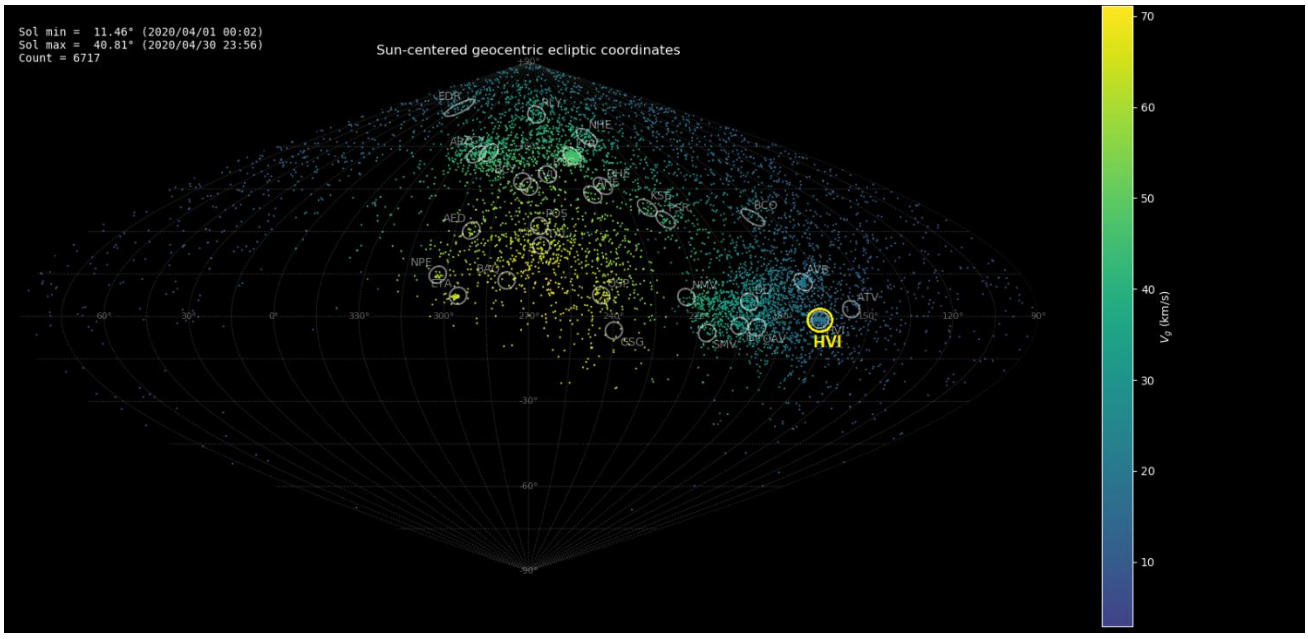

Figure 8 – The Global Meteor Network geocentric radiants in Sun-centered ecliptic coordinates for April 2020. The position of the HVI radiants is indicated relative to the entire hemisphere. (Courtesy Denis Vida).

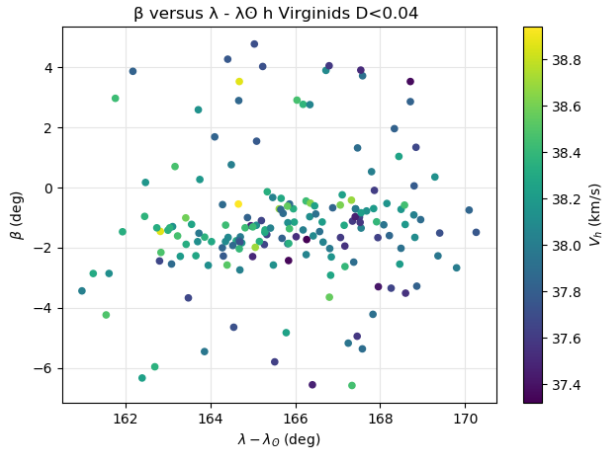

Figure 9 – HVI radiants in Sun centered ecliptic coordinates for the high threshold similarity class orbits with a color gradient for the heliocentric velocity v_h.

When we consider the spread in the heliocentric velocity v_h in *Figure 9*, no pattern in the velocity can be seen, the scatter seen is due to the error margin on the computed heliocentric velocities. No pattern appears in the plot of inclination *i* in function of the length of perihelion because of the error margins combined with the very low inclination close to zero (*Figure 10*). We also find a decrease of 0.13 km/s in the geocentric velocity per degree $\lambda_\odot$. HVI meteors appear to be faster at the begin of the activity than at the end (*Figure 11*).

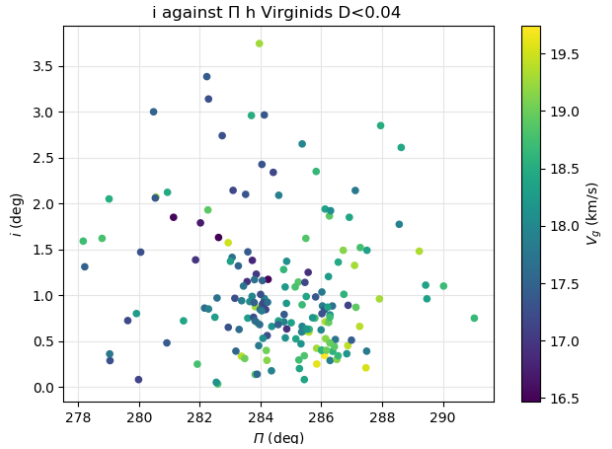

Figure 10 – Inclination i plotted in function of the length of perihelion Π for the high threshold similarity class orbits with a color gradient for the geocentric velocity v_g.

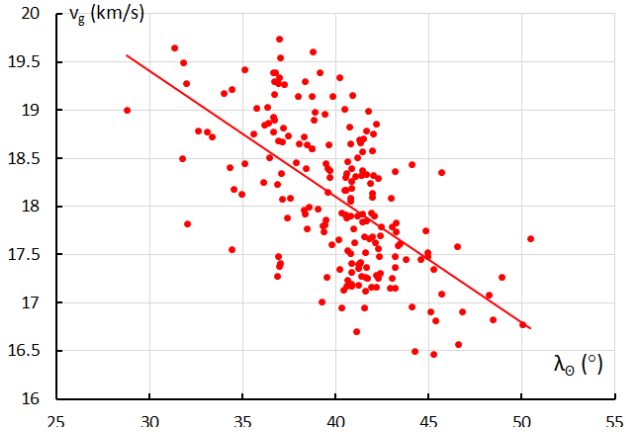

Figure 11 – Geocentric velocity v_g in function of time ($\lambda_\odot$).

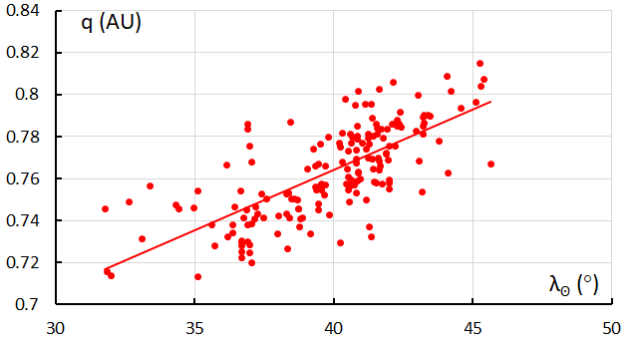

Figure 12 – Perihelion distance q in function of time ($\lambda_\odot$).

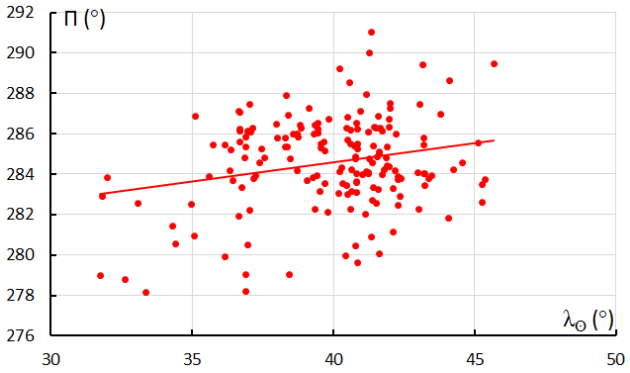

Figure 13 – Length of perihelion Π in function of time ($\lambda_\odot$).

Checking the orbital elements in function of solar longitude, we see that eccentricity *e* and the semi-major axis *a* remain stable. No trend can be derived within the error margins and scatter. The inclination *i* displays variations close to zero. The perihelion distance *q* shows an increasing trend (*Figure 12*) while the length of perihelion Π ($= \Omega + \omega$) indicates some increase but within a lot of scatter (*Figure 13*).

HVI component of a complex system?

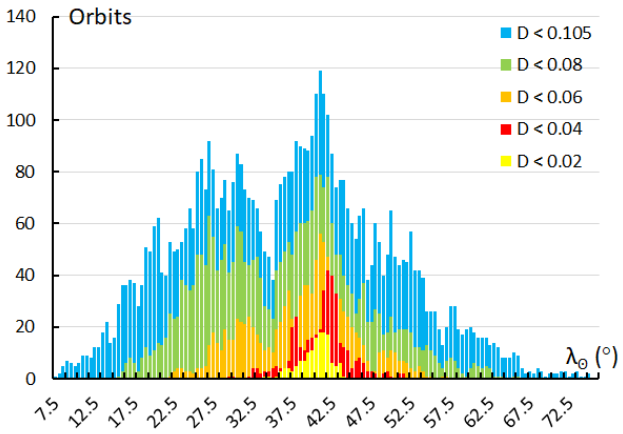

Figure 14 – Number of orbits for the different threshold classes of similarity with the high threshold mean HVI orbit as reference.

Looking at the complete activity period we established for our reference orbit, searching our dataset with 1101924 orbits, we found many more possible HVI orbits. The distribution with the number of possible HVI orbits per degree of solar longitude is plotted in *Figure 14*. The sample we used to locate the HVI concentration was limited at $30° < \lambda_\odot < 46°$. *Figure 14* suggests there is HVI-related activity with another sub-maximum going on before our

sampling window. However, caution is required with D-criteria applied with this type of orbits. To reveal the details of this earlier HVI related activity, a separate analysis should be made on the observing window $15° < \lambda_\odot < 35°$ to find the best fitting mean orbit for the concentration in this part. This study may answer the suggestion by Masahiro Koseki that some other known sources are related to this activity.

4 2020 activity by SonotaCo Network

The 2020 enhanced activity of the h Virginids has been observed by SonotaCo Network. In total 38 HVI orbits were identified. The mean orbits are listed in *Table 5*.

A simple average has been taken for the orbital parameters, 27 orbits had their radiants north of the ecliptic, 11 orbits south. This way the ascending node Ω and thus also the argument of perihelion ω switches 180°, therefore both groups were averaged separately. To compare the result with other networks, all SonotaCo Network orbits within the timelapse $31° < \lambda_\odot < 41°$ were used to calculate the mean orbit with the method of Jopek et al. (2006). The results agree well with the orbits obtained for previous years listed in *Table 2*.

Figure 15 shows clearly the radiant drift as well as the decrease in geocentric velocity v_g, also found in all previous year's orbit data (see *Figure 11*). No trend can be established for the absolute magnitude in function of time.

Figure 16 shows the radiant positions for the orbits in the nights of enhanced activity.

Figure 17 shows the orbits north and south of the ecliptic. Note the aphelia close to the orbit of Jupiter which has influence on the evolution of this shower. Mr. Yasuo Shiba[3] suggests a possible 6-year periodicity, given that the average orbital period is 5.3 years and a 2:1 resonance with Jupiter's revolution is valid.

Table 5 – The averaged HVI orbits north and south of the ecliptic compared with the mean orbit computed according to Jopek et al. (2006).

	SonotaCo $\beta > 0°$ (A)	SonotaCo $\beta < 0°$ (B)	SonotaCo $31° < \lambda_\odot < 41°$
$\lambda_\odot$	38.3°	31.2°	38.4°
α_g	202.4°	203.7°	203.0°
δ_g	–11.1°	–8.5°	–10.7°
v_g	18.7 km/s	21.2 km/s	18.8 km/s
a	2.90 AU	2.84 AU	2.86 AU
q	0.7445 AU	0.6527 AU	0.7397 AU
e	0.7394	0.7609	0.7410
ω	67.21°	259.0°	66.0°
Ω	218.23°	32.0°	219.75°
i	0.71°	0.90°	0.44°
N	27	11	34

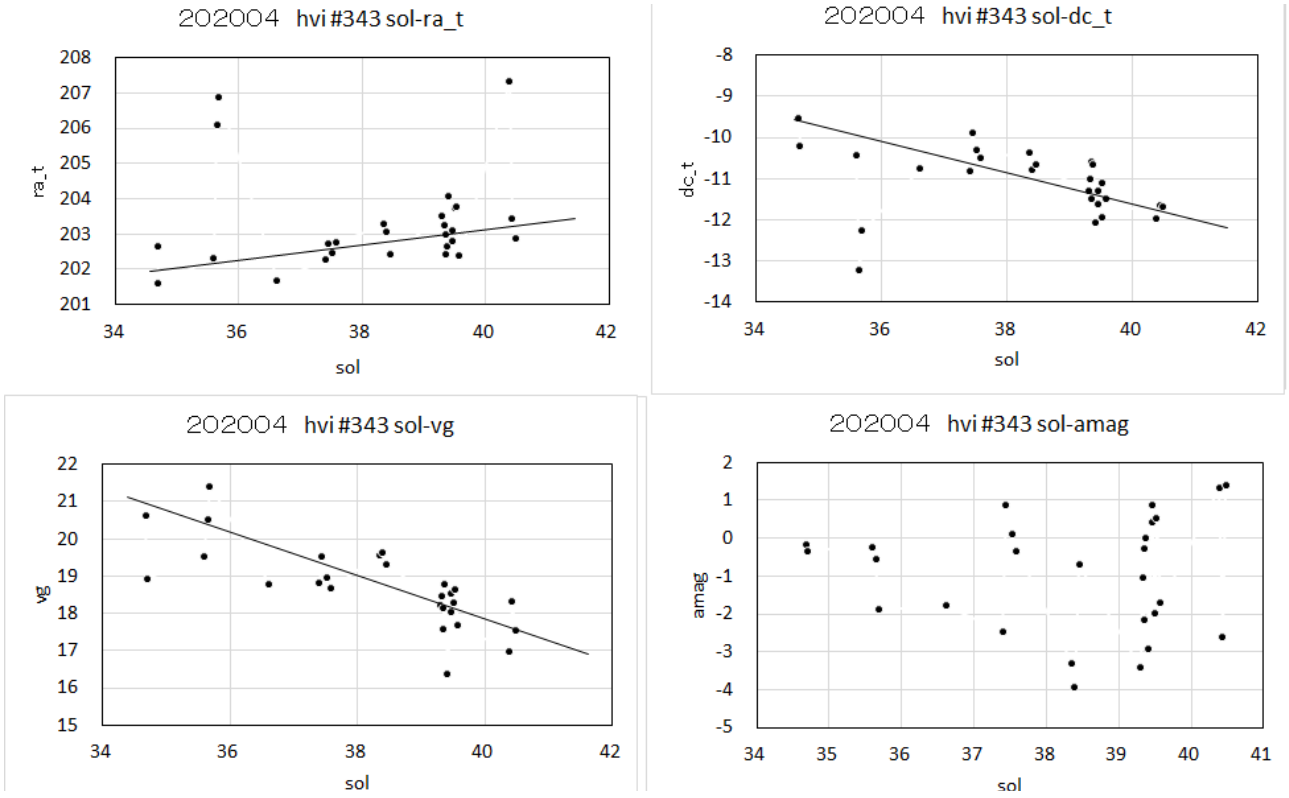

Figure 15 – The radiant drift, the variation in geocentric velocity and the distribution of the absolute magnitude for the 2020 SonotaCo orbit data.

[3] http://sonotaco.jp/forum/viewtopic.php?t=4580

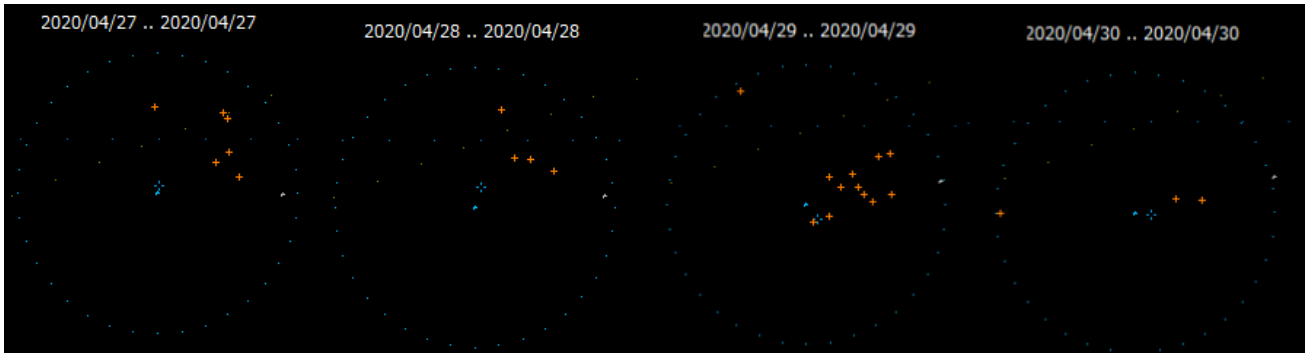

Figure 16 – The SonotaCo radiant plots during the h Virginids enhanced activity.

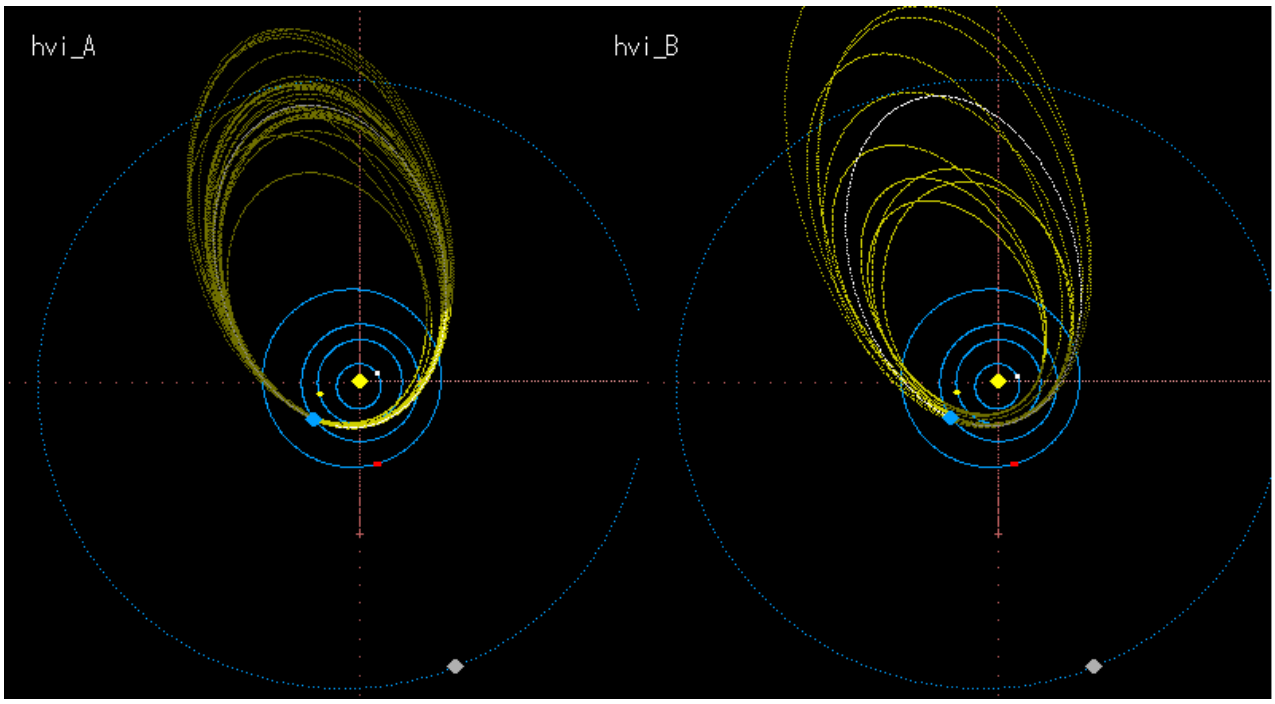

Figure 17 –The HVI orbits plotted for the orbits north of the ecliptic (A) and the orbits south of the ecliptic (B).

5 2020 activity by CAMS BeNeLux

Also CAMS BeNeLux recorded the 2020 enhanced activity. 65 orbits were selected within the interval $30.9° < \lambda_\odot < 46.9°$, $156° < \lambda - \lambda_\odot < 176°$, $-7° < \beta < +5°$ and $13 \text{ km/s} < v_g < 23 \text{ km/s}$. The reference orbit for the concentration of HVI orbits was computed with an iterative procedure for all five threshold classes of similarity.

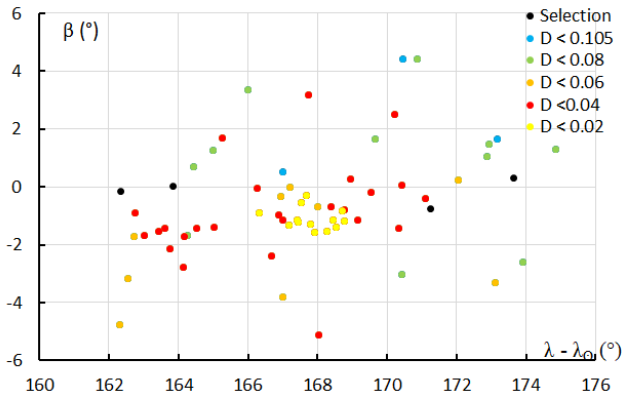

Figure 18 – The radiants for all BeNeLux HVI-orbits in Sun centered ecliptic coordinates, with all radiants for each similarity class like mentioned in Table 6.

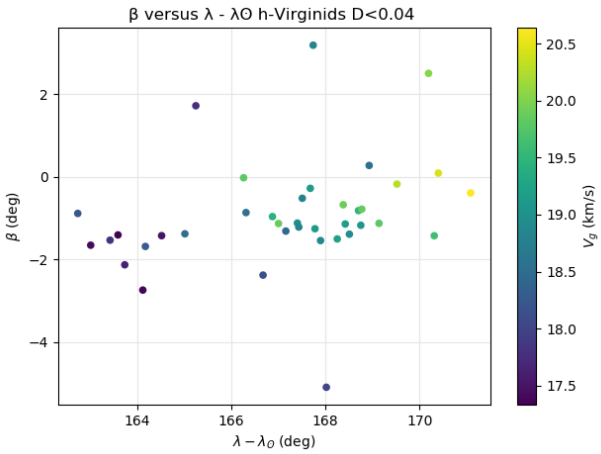

Figure 19 – HVI radiants by CAMS BeNeLux in Sun centered ecliptic coordinates for the high threshold similarity class orbits with a color gradient for the geocentric velocity v_g.

The results are listed in *Table 6* and are in good agreement. The radiant plot for Sun centered ecliptic coordinates has been plotted in *Figure 18*. The concentration of the very similar orbits is very well visible. *Figure 19* shows the increase in geocentric velocity v_g within the radiant in the direction of the apex in Sun centered ecliptic coordinates.

Using the high threshold class orbits we find a decrease in geocentric velocity with $\Delta v_g/\Delta\lambda_\odot = 0.18$ km/s, slightly higher than found for previous years (0.13 km/s per degree solar longitude) (*Figure 20*).

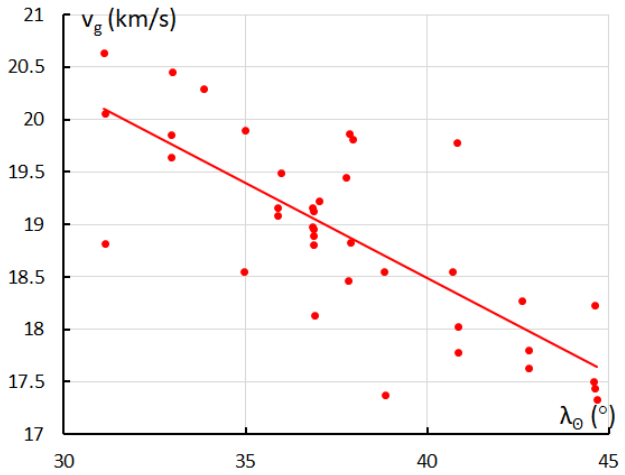

Figure 20 – Geocentric velocity v_g in function of time (solar longitude) as derived for CAMS BeNeLux.

Table 6 – The reference orbits obtained from the 2020 HVI orbits by CAMS BeNeLux, for each threshold class of similarity.

	Low	Medium Low	Medium High	High	Very High
$\lambda_\odot$	36.9°	36.9°	36.9°	37.0°	36.9°
α_g	202.5°	202.5°	202.4°	202.5°	202.5°
δ_g	–10.5°	–10.5°	–10.6°	–10.7°	–10.6°
$\Delta\alpha_g$	+0.46°	+0.48°	+0.44	+0.40°	+0.24°
$\Delta\delta_g$	–0.34°	–0.34°	–0.27°	–0.27°	–0.10°
λ–$\lambda_\odot$	167.7°	167.6°	167.4°	167.6°	167.8°
β	–1.0°	–1.1°	–1.1°	–1.1°	–1.2°
v_g	19.0 km/s	18.9 km/s	18.9 km/s	18.9 km/s	19.0 km/s
a	2.90 AU	2.94 AU	2.97 AU	2.97 AU	2.90 AU
q	0.739 AU	0.742 AU	0.746 AU	0.745 AU	0.739 AU
e	0.745	0.740	0.746	0.749	0.745
ω	62.9°	64.9°	65.3°	64.5°	68.2°
Ω	222.0°	219.8°	218.8°	220.1°	216.6°
i	0.3°	0.4°	0.6°	0.5°	0.6°
Π	284.6°	284.6°	284.5°	284.6°	284.7°
T_J	2.79	2.78	2.76	2.75	2.79
N	61	58	47	38	13

6 2020 activity by the Global Meteor Network

The Global Meteor Network online orbit data[4] for April and May 2020 includes as many as 191 orbits identified as h Virginids (HVI#343). In first instance we computed the mean orbit based on the identification as listed. GMN had significant more HVI#343 orbits than CAMS BeNeLux or SonotaCo Network. A detailed look at the dataset revealed that the list contained duplicates, slightly different orbits obtained from different camera combinations. In some cases the same camera combination yielded two orbits based on the same meteor which was detected twice on one of the cameras. Therefore it was decided to redo the analyzis on the GMN dataset after first removing all duplicate orbits.

Having done the analysis on the 2007–2019 HVI-orbits and knowing that the HVI activity covers a longer period than previously assumed, we decided to search for HVI orbits in a longer period of time taking into account a larger radiant area. Selecting all orbits obtained in the time interval $20° < \lambda_\odot < 55°$, from a radiant area with $150° < \lambda$–$\lambda_\odot < 180°$ and $-15° < \beta < +15°$, with 12 km/s $< v_g <$ 23 km/s, as many as 727 orbits were available within this selection. A mean orbit was obtained by an iterative method with 494 orbits fitting the low threshold similarity class, 371 the medium low class, 213 the medium high class and 151 the high threshold class. Before solar longitude $\lambda_\odot = 32°$ (April 22), many of these orbits were identified as α-Virginids (AVB#021) characterized by a higher inclination i with more northern radiant positions and some as April theta Virginids (ATV#730) characterized by a slightly lower velocity and higher values for the perihelion distance q. All of these are most likely components of a greater complex.

The longer the activity period of a stream, the larger the spread on the orbits of particles which must be widely dispersed in order to encounter Earth during a long period of time. Short orbit meteor streams near the ecliptic with low velocity appear from a very large radiant area and are difficult to distinguish from the sporadic background. The use of D-criteria is tricky in these cases and require caution. In this particular case with orbits north and south of the ecliptic and the inclination close to zero, the error margins on the orbits cause huge differences on both the ascending node Ω as well as the argument of perihelion ω. With inclination $i = 0°$, the orbit plane lies in the ecliptic plane and the nodes cannot be determined. Considering a long activity period and large radiant area results in mainly many more low threshold orbits with a high risk for contamination with sporadics and other nearby sources. Such large spread is not desirable to establish a mean orbit.

The real concentration of orbits within the high threshold class appears in the time interval of $30° < \lambda_\odot < 45°$. Therefore we repeat the analyzes a third time, considering only the orbits in this time interval, limiting the radiant area to $156° < \lambda - \lambda_\odot < 176°$, $-7° < \beta < +5°$. 240 orbits are available within this interval. The mean orbit of these 240 orbits is taken to launch the iteration to find the best fitting mean orbit for the concentration of similar orbits. Already after 4 iterations the procedure converges at a best fitting mean orbit for the high threshold similarity class. Next, the mean orbits are calculated for each threshold class separately using the method of Jopek et al. (2006). The final orbits for the high and very high threshold similarity class

[4] https://globalmeteornetwork.org/data/traj_summary_data/monthly/

are almost identical to those obtained for the longer activity period and larger radiant area dataset mentioned above. Also the mean orbits obtained during the first attempt on GMN data were about the same, so the duplicated orbits did not influence the result much.

The number of orbits identified as HVI members for each class of similarity are shown in *Figure 21* for each degree in solar longitude. The enhanced activity lasted during four nights from solar longitude 37 till 40° included (April 27 till May 1). The D-criteria show most of these orbits are very similar to each other. The final mean orbits for each similarity class are listed in *Table 7*. The dataset which covered a longer activity period and larger radiant area produced mainly many more low and medium low threshold class orbits with more scatter on their mean orbits, but almost identical for the high and very high class orbits.

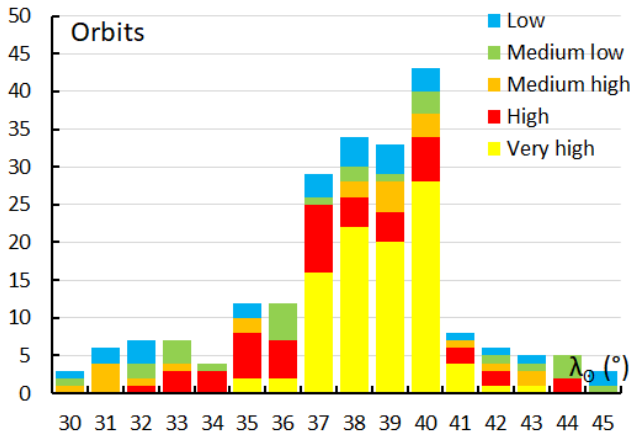

Figure 21 – Number of HVI orbits from Global Meteor Network data counted per degree in solar longitude for each similarity class.

Table 7 – The mean HVI orbits for the different similarity classes obtained from the 2020 Global Meteor Network data.

	Low	Medium Low	Medium High	High	Very High
$\lambda_\odot$	38.3°	38.3°	38.3°	38.3°	38.8°
α_g	202.8°	202.8°	202.8°	202.8°	202.8°
δ_g	–10.7°	–10.7°	–10.7°	–10.8°	–10.9°
$\Delta\alpha_g$	+0.52°	+0.45°	+0.38°	+0.34°	+0.32°
$\Delta\delta_g$	–0.31°	–0.30°	–0.36°	–0.32°	–0.30°
λ–$\lambda_\odot$	166.6°	166.6°	166.5°	166.4°	166.3°
β	–1.1°	–1.2°	–1.2°	–1.3°	–1.3°
v_g	18.5 km/s	18.5 km/s	18.5 km/s	18.5 km/s	18.5 km/s
a	2.95 AU	2.82 AU	2.89 AU	2.92 AU	2.95 AU
q	0.755 AU	0.751 AU	0.752 AU	0.753 AU	0.755 AU
e	0.744	0.733	0.740	0.742	0.744
ω	65.6°	65.8°	65.2°	65.5°	65.6°
Ω	218.6°	218.6°	219.0°	218.7°	218.6°
i	0.6°	0.7°	0.7°	0.6°	0.6°
Π	284.3°	284.6°	284.3°	284.3°	284.3°
T_J	2.81	2.80	2.79	2.78	2.77
N	217	190	165	143	96

The HVI radiants in Sun centered ecliptic coordinates are displayed in *Figure 22*. The low and medium low threshold orbits (blue and green) appear very dispersed. A compact radiant (yellow) appears as a very narrow concentration of almost identical orbits. The velocity variation within the radiant is displayed in *Figure 23,* see also *Figures 6 and 19*.

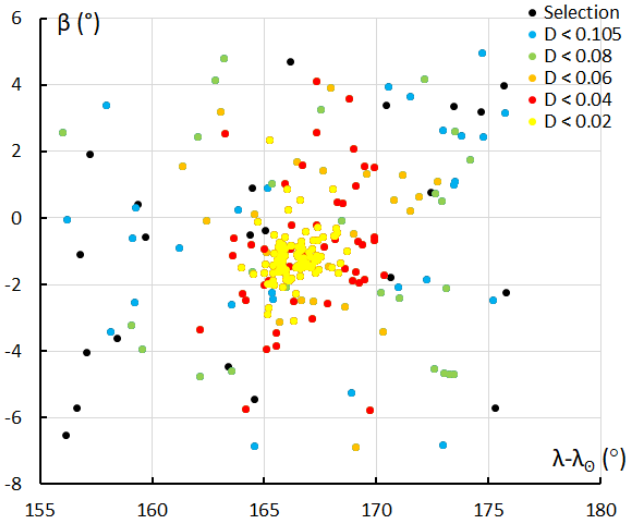

Figure 22 – The radiants for all Global Meteor Network HVI-orbits in Sun centered ecliptic coordinates, with all radiants for each similarity class like mentioned in Table 7.

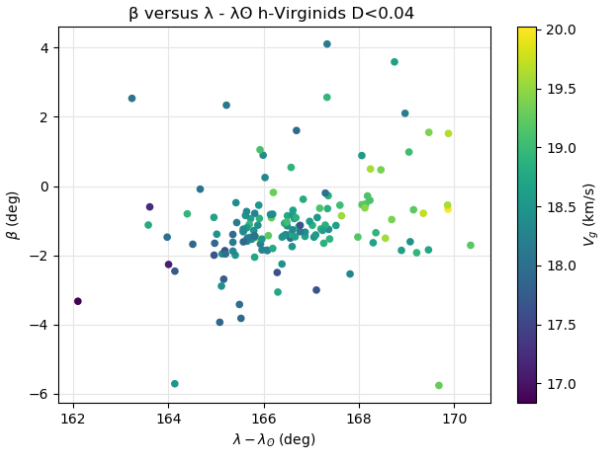

Figure 23 – HVI radiants by Global Meteor Network in Sun centered ecliptic coordinates for the high threshold similarity class orbits with a color gradient for the geocentric velocity v_g.

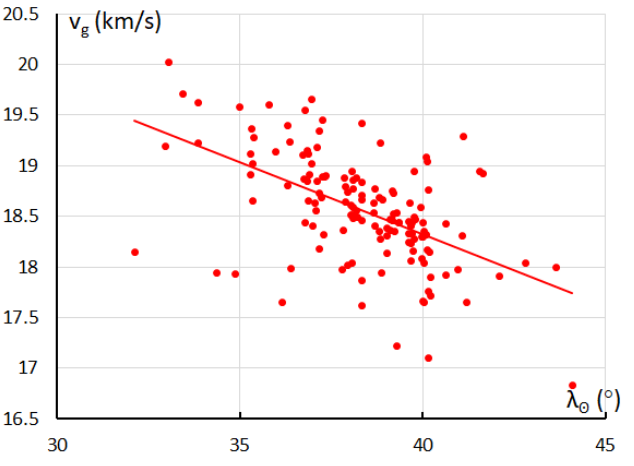

Figure 24 – Geocentric velocity v_g in function of time (solar longitude) as derived for the Global Meteor Network.

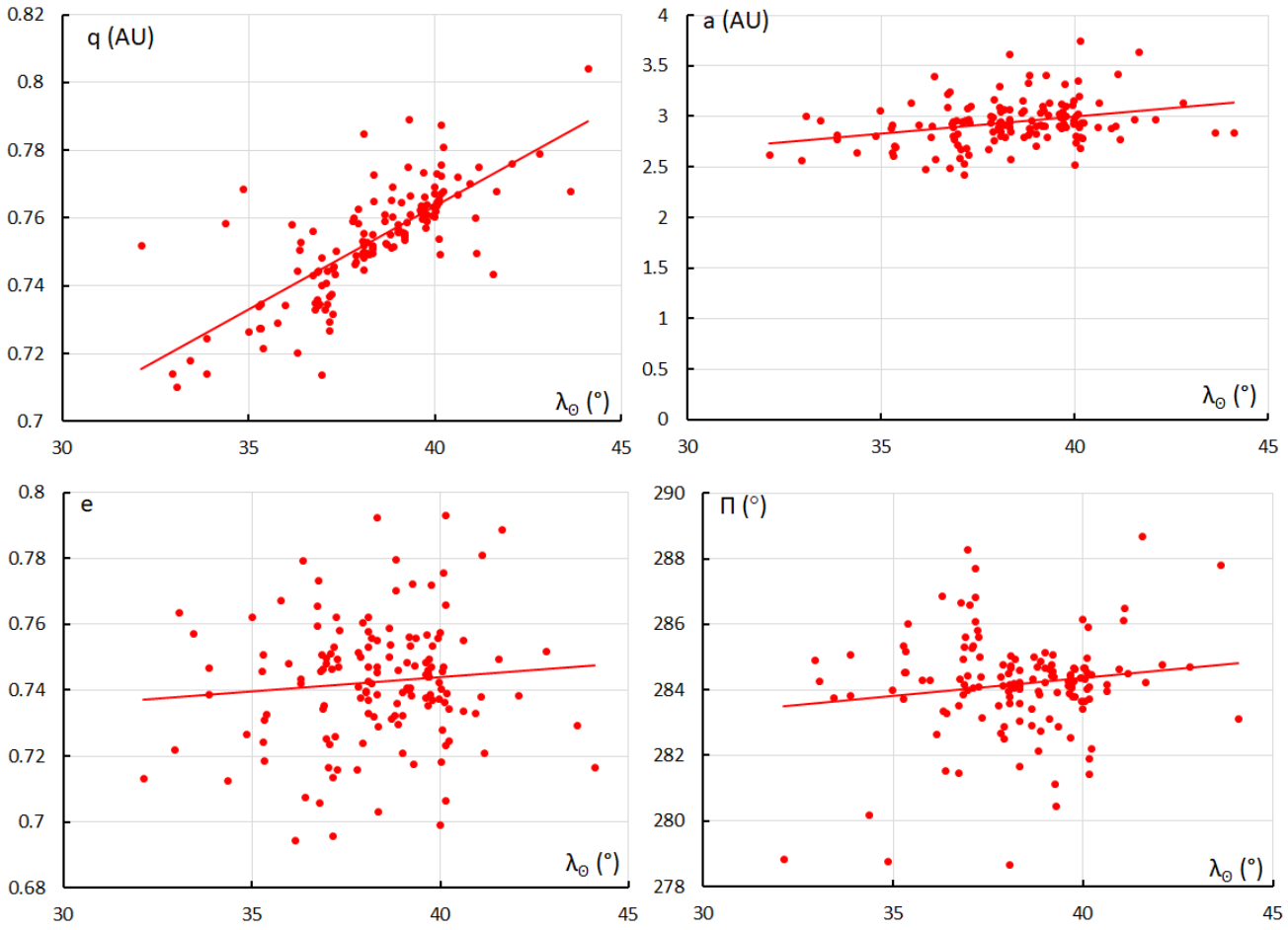

Figure 25 – The variation in the orbital elements in function of time (solar longitude).

The decrease in geocentric velocity in function of time is obvious in *Figure 24* with $\Delta v_g/\Delta\lambda_\odot = 0.14$ km/s, a bit less than found for CAMS BeNeLux, but almost identical with the long term value for this shower.

The number of HVI orbits identified in the Global Meteor Network data allows to compare the 2020 data with the long term data for the change in orbital elements in function of time (*Figure 25*). We see a clear increase in perihelion distance q while the other elements, semi major axis a, eccentricity e and length of perihelion Π, show no relevant trend within the spread on the values.

7 Conclusion

This case study has proven that the only reference orbit list in the IAU working list of meteor showers is not representative for the h Virginids (HVI#343). A new reliable reference orbit for this shower has been obtained, based on long-term orbit data obtained by EDMOND, SonotaCo Network and CAMS. The orbits for the 2020 outburst of h Virginids have been analyzed independently for the three datasets available for Sonotaco Network in Japan, CAMS BeNeLux network and the Global Meteor Network. The resulting mean orbits for the three 2020 datasets agree very well with the long term reference orbit. The final orbits are compared in *Table 8*. These orbits have a T_J value typical for Jupiter family comets. The activity period of the shower covers $28° < \lambda_\odot < 51°$ but similar orbits are found beyond these dates, identified as α-Virginids (AVB#021) before the main HVI activity and as April theta Virginids (ATV#730) after this interval. The 2020 enhanced activity may fit in some 6-year periodicity as also 2008 the year of discovery had good numbers of HVI orbits.

Table 8 – The long term reference orbit for the HVI#343 meteor stream compared to the mean orbits for 2020 as obtained by three independent video camera networks.

$\lambda_\odot$ (°)	α_g (°)	δ_g (°)	$\Delta\alpha$ (°)	$\Delta\delta$ (°)	v_g km/s	a AU	q AU	e	ω (°)	Ω (°)	i (°)	T_J	N	Dataset
40.5	203.6	–11.3	+0.40	–0.30	18.1	2.83	0.763	0.730	64.1	220.4	0.6	2.84	174	All 2003–2019
38.4	203.0	–10.7	+0.14	–0.32	18.8	2.86	0.740	0.741	66.0	219.8	0.4	2.79	34	SonotaCo 2020
37.0	202.5	–10.7	+0.40	–0.27	18.9	2.97	0.745	0.749	64.5	220.1	0.5	2.75	38	BeNeLux 2020
38.3	202.8	–10.8	+0.34	–0.32	18.5	2.92	0.753	0.742	65.5	218.7	0.6	2.78	143	GMN 2020

Acknowledgment

The authors thank *Denis Vida* for providing the scripts to plot the velocity distribution with a color gradient and to compute the average orbit according to the method of Jopek et al. (2006). We are very grateful to the volunteers who maintain the IAU working list of meteor showers (Jopek and Kaňuchová, 2014, 2017; Jopek and Jenniskens, 2011).

We used the data of the Global Meteor Network[5] which is released under the CC BY 4.0 license[6]. We thank the SonotaCo Network members in Japan who have been observing every night for more than 10 years, making it possible to consult their orbits. We thank the camera operators of the CAMS[7] networks[8]. And we thank the contributors to EDMOND[9], including: BOAM (Base des Observateurs Amateurs de Meteores, France), CEMeNt (Central European Meteor Network, cross-border network of Czech and Slovak amateur observers), CMN (Croatian Meteor Network or HrvatskaMeteorskaMreza, Croatia), FMA (Fachgruppe Meteorastronomie, Switzerland), HMN (HungarianMeteor Network or Magyar Hullocsillagok Egyesulet, Hungary), IMO VMN (IMO Video Meteor Network), MeteorsUA (Ukraine), IMTN (Italian amateur observers in Italian Meteor and TLE Network, Italy), NEMETODE (Network for Meteor Triangulation and Orbit Determination, United Kingdom), PFN (Polish Fireball Network or Pracownia Komet i Meteorow, PkiM, Poland), Stjerneskud (Danish all-sky fireball cameras network, Denmark), SVMN (Slovak Video Meteor Network, Slovakia), UKMON (UK Meteor Observation Network, United Kingdom).

References

Drummond J. D. (1981). "A test of comet and meteor shower associations". *Icarus*, **45**, 545–553.

Jenniskens P., Nénon Q., Albers J., Gural P. S., Haberman B., Holman D., Morales R., Grigsby B. J., Samuels D. and Johannink C. (2016). "The established meteor showers as observed by CAMS". *Icarus*, **266**, 331–354.

Jenniskens P., Baggaley J., Crumpton I., Aldous P., Pokorny P., Janches D., Gural P. S., Samuels D., Albers J., Howell A., Johannink C., Breukers M., Odeh M., Moskovitz N., Collison J., Ganju S. (2018). "A survey of southern hemisphere meteor showers". *Planetary Space Science*, **154**, 21–29.

Jenniskens P. (2020). "h Virginid meteor shower". CBET 4760.

Jopek T. J. (1993). "Remarks on the meteor orbital similarity D-criterion". *Icarus*, **106**, 603–607.

Jopek T. J., Rudawska R. and Pretka-Ziomek H. (2006). "Calculation of the mean orbit of a meteoroid stream". *Monthly Notices of the Royal Astronomical Society*, **371**, 1367–1372.

Jopek T. J., Jenniskens P. M. (2011). "The Working Group on Meteor Showers Nomenclature: A History, Current Status and a Call for Contributions". In, W.J. Cooke, D.E. Moser, B.F. Hardin, and D. Janches, editors, *Meteoroids: The Smallest Solar System Bodies, Proceedings of the Meteoroids Conference,* held in Breckenridge, Colorado, USA, May 24-28, 2010. Edited by, NASA/CP-2011-216469, pages 7–13.

Jopek T. J. and Kaňuchová Z. (2014). "Current status of the IAU MDC meteor showers database". In, Jopek T. J., Rietmeijer F. J. M., Watanabe J., and Williams I. P., editors, *Proceedings of the Meteoroids 2013 Conference*, Poznań, Poland, 26-30 August 2013. A.M. University Press, pages 353–364.

Jopek T. J. and Kaňuchová Z. (2017). "IAU Meteor Data Center-the shower database: A status report". *Planetary and Space Science*, **143**, 3–6.

Masahiro K. (2020). "Confusions in IAUMDC Meteor Shower Database (SD)". *eMetN*, **5**, 93–111.

Molau S., Rendtel J. (2009). "A Comprehensive List of Meteor Showers Obtained from 10 Years of Observations with the IMO Video Meteor Network". *WGN, Journal of the International Meteor Organization*, **37**, 98–121.

Roggemans P., Johannink C. and Cambell-Burns P. (2019). "October Ursae Majorids (OCU#333)". *eMetN*, **4**, 55–64.

SonotaCo (2009). "A meteor shower catalog based on video observations in 2007-2008". *WGN, Journal of the International Meteor Organization*, **37**, 55–62.

Southworth R. R. and Hawkins G. S. (1963). "Statistics of meteor streams". *Smithson. Contrib. Astrophys.*, **7**, 261–286.

[5] https://globalmeteornetwork.org/data/
[6] https://creativecommons.org/licenses/by/4.0/
[7] http://cams.seti.org/
[8] http://cams.seti.org/FDL/
[9] https://fmph.uniba.sk/microsites/daa/daa/veda-a-vyskum/meteory/edmond/

Three Virginid showers

Masahiro Koseki

NMS (The Nippon Meteor Society), 4-3-5 Annaka Annaka-shi, Gunma-ken, 379-0116 Japan
geh04301@nifty.ne.jp

Virginids were classified as an ecliptic shower or one of the ANT sources. Recent developments of video meteor observations made it possible to distinguish minor showers from the background sporadics. We investigated three such small but interesting showers of the Virginids by using SonotaCo network observations (SonotaCo, 2009); EVI#0011, AVB#0021 and HVI#0343. Observations of these showers have been carried out almost equally and we can easily see the changes in the activity year by year.
EVI#0011 and HVI#0343 have both a periodic nature and a sharp maximum. AVB#0021 is a typical ANT shower. Their radiant distributions are compact and their radii are smaller than 3 degrees from the center taking their radiant drift into consideration.

1 Introduction

"Virginids" have been noticed since the 19th century (see *Table 1*) and were described as being rich in fireballs and slow meteors (Denning, 1898). Hoffmeister and McIntosh showed the Virginids have a complex and broadened structure (Hoffmeister, 1948; McIntosh, 1935).

The development of photographic observing techniques revealed the individual components in the "Virginids". Whipple (1954) observed the EVI#0011 (η-Virginids) as the "Virginids" described earlier by Hoffmeister and these were later renamed as η-Virginids by Jenniskens (2006). McCrosky and Posen (1959) noticed the "Virginids" activity in early May and called them the "α-Virginids".

Unfortunately, further developments with especially the great amount of video data caused confusion. The IAUMDC Meteor Shower Database (SD) lists the reports from research accordingly to the naming by the authors. For example, AVB#0021 is not the original "α-Virginids" and may consist of late HVI#0343 and sporadics; HVI#0343-0 was detected by SonotaCo (2009) though was thought to be a rediscovery of the "α-Virginids" (Koseki, 2019a). AVB#0021-04, -05 and SLE#0136-02 may suggest another new meteor shower and could be called σ-Virginids as appropriate designation (Koseki, 2019a).

We try to survey the three "Virginids" mentioned above: EVI#0011 (originally Whipple's "Virginids"), AVB#0021 (newly found "σ-Virginids" and HVI#0343 (thought to be McCrosky and Posen's "α-Virginids").

2 Methods of survey

There are several sources of video meteor observations but the SonotaCo (2009)[10] database is the most suitable to research meteor shower activities, because the observations have been carried out consistently. We use their results throughout this entire study.

2.1 Estimation of the radiant drift

A meteor shower radiant usually shifts with time in equatorial coordinates but is almost stationary for the Sun centered ecliptic coordinates ($\lambda-\lambda_\odot$, β) in general. The radiant shift can be represented as a short line in the orthographic projection of the ($\lambda-\lambda_\odot$, β) coordinates even if the radiant moves in the ($\lambda-\lambda_\odot$, β) coordinates. We select the entries in the SD as representatives of each showers and calculate the linear regression of x and y on $\lambda_\odot$ for the period listed in *Table 2*; (x, y) are the coordinates of individual radiants centered at the shower radiant. The regression calculations were repeated several times to become stable.

Table 1 – The noticeable meteor showers by visual meteor observations in the 19th century (Denning, 1898).

No.	Name	α	δ	N	Remarks
136	η Virginids	180.7°	+1.7°	4	Needs further confirmation.
149	δ Virginids	192.4°	+5.6°	10	Near 154, but probably quite different.
154	o Virginids	201.7°	+7.8°	15	Well-defined shower from April to May.
158	α Virginids	205.4°	–8.7°	22	Supplies many large slow-moving meteors in April. Distinct from 166.
166	μ Viginids	216.7°	–8.6°	14	Rich shower distinct from 158. Yields many slow-moving fireballs in April and May.

[10] http://sonotaco.jp/doc/SNM/

Table 2 – Conditions for the survey; Δr is the search radius in degrees from the radiant point and $\Delta\lambda_\odot$ is the search period; originally $\lambda_\odot$ of AVB#0021-04 is 32° but the activity profile suggests that $\lambda_\odot$ = 27° is better.

Code	$\lambda_\odot$	$\lambda-\lambda_\odot$	β	Δr	$\Delta\lambda_\odot$
EVI#0011-02	357°	185.9°	+5.5	3°	7°
AVB#0021-04	27°	168.7	+11.8	3°	10°
HVI#0343-03	40.6°	165.6	–1.3	3°	5°

2.2 Activity profile based on the radiant density

We can count the number of radiant points according to the distance from the estimated radiant position in ($\lambda-\lambda_\odot$, β), compensated for the radiant drift. Nr <= 3 is the number of meteors within 3 degrees from the estimated radiant in each 1-degree bin of $\lambda_\odot$. These raw meteor numbers fluctuate widely with the observing conditions, though we use 11 years of observations of the SonotaCo network (SonotaCo, 2009). It is necessary to use other indexes to express the shower activity profiles; Koseki (2019b) proposes to use the radiant density ratios; DR3 is the density ratio within a circle of 3 degrees radius relative to a ring of 3–6 degrees; DR10 is the density ratio within a circle of 3 degrees relative to a ring of 6–10 degrees; DR15 is the density ratio within a circle of 3 degrees relative to a ring of 10–15 degrees. It is better to use the sliding mean of the radiant density ratios within bins of 3 degrees in $\lambda_\odot$ in order to avoid too low meteor numbers in the reference areas. Which index is the best is different case by case, explained in the next sections.

3 Results

We get possible candidate meteors within 3 degrees from the estimated radiant point after several iterations (*Table 3*) and we can estimate their radiant shift (*Figure 1*). We can calculate the changes of the orbital elements also and we will show in detail the results in the following sections.

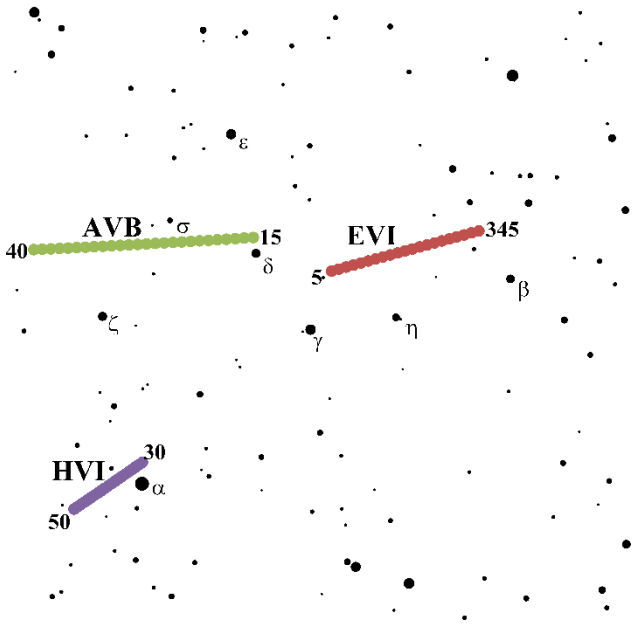

Figure 1 – Radiant shift of three "Virginids" in equatorial coordinates. Each small circles indicate the radiant point of every $\lambda_\odot$ between the estimated range (Tables 4 to 6); the start and the end values for $\lambda_\odot$ are shown in the figure.

3.1 EVI#0011

Whipple (1954) recorded four "Virginids" meteors by photographic observations (*Table 4*). These are members of the present EVI#0011 shower as shown in *Table 4* and *Figure 2*. The author pointed out that McCrosky and Posen looked over Whipple's "Virginids" (*Figure 2a* in Koseki, 2019b). The sporadic activity and the periodicity of EVI may explain why they did not notice these.

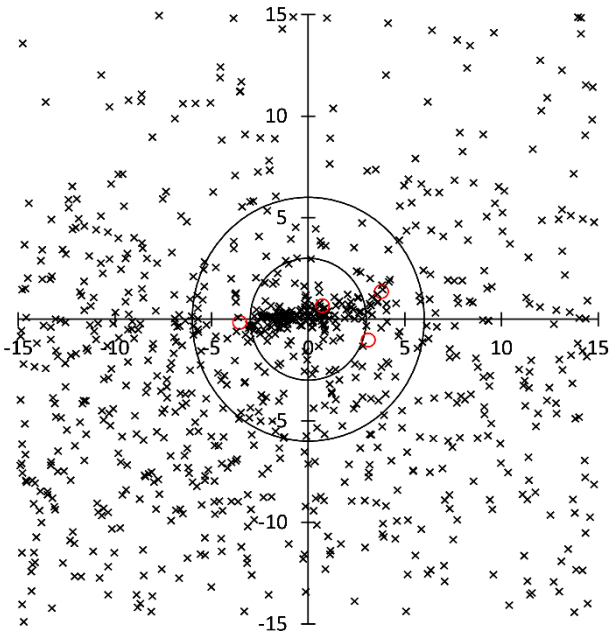

Figure 2 – The radiant distribution around the estimated EVI#0011 center; The y-axis runs through the ecliptic longitude of $\lambda-\lambda_\odot$ and the scale is in degrees. Two circles represent the distance of 3 degrees and 6 degrees from the center. Four small circles indicate Whipple's "Virginids".

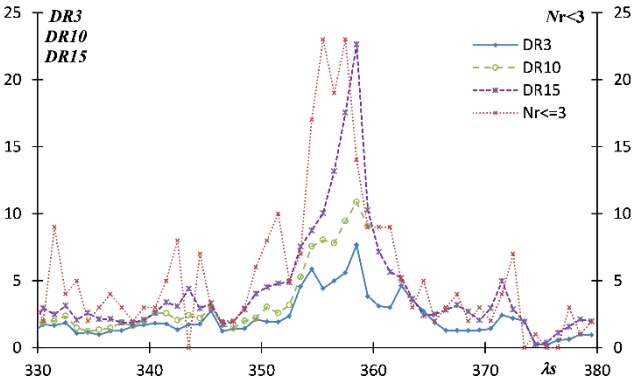

Figure 3 – Activity profile of the EVI#0011, see section 2.2 for the explanation of Nr <= 3, DR3, DR10, DR15.

Shiba (2018) pointed at a four-year periodicity of the EVI activity and *Table 3* confirmed his conclusion. He suggested that EVI is in a 3:1 resonance with Jupiter *Table 5* shows the additional evidence for his point; the orientation of the perihelion (λ_Π, β_Π) and the semi major axis *a* are almost constant.

We note that the radiant distribution of EVI is still elongated after the regression analysis (*Figure 2*) although the radiant distribution usually would be round after the process (see *Figure 5 and 10*). We selected candidate EVI meteors in the time bin of 356° <= $\lambda_\odot$ < 358° and within 3 degrees from

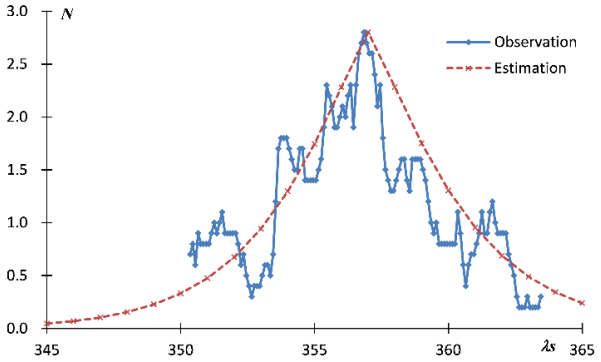

Figure 4 – Comparison between the Nr <= 3° profile of EVI#0011 and the estimation of the activity as calculated from the orbit (Koseki, 2012); Nr <= 3° is counted for each 0.1 degree bin of $\lambda_\odot$ and displayed here with a sliding mean of a 1 degree bin in $\lambda_\odot$.

the estimated radiant in ($\lambda-\lambda_\odot$, β). It becomes clear that the geocentric velocity changes with the *x*-axis in *Figure 2* and, therefore, we can calculate the difference in orbital elements between the left and right edges of the elongated radiant distribution.

It is clear that the elongated form is caused by the dispersion/rotation in the orientation of the perihelion though the semi major axis is kept constant (*Table 6*).

AVB#0021

Jenniskens et al. (2016) insists that the AVB#0021-04 are "α-Virginids" but the author showed that these observations are a newly discovered meteor shower (*Figure 4a* of Koseki, 2019a). This activity is weak but the radiant distribution shows enough concentration (*Figure 5*). The DR curves in *Figure 6* suggest that the activity peaks around $\lambda_\odot = 30°$ though the raw recorded number (Nr <= 3) fluctuates largely (*Figures 6 and 7*).

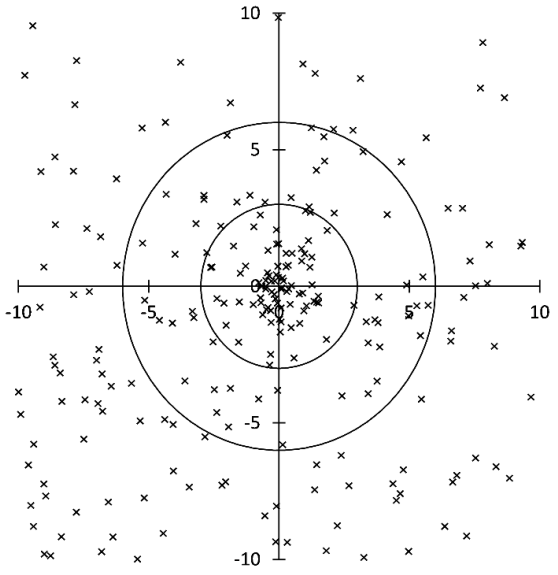

Figure 5 – The radiant distribution around the estimated AVB#0021 center.

Table 7 shows the semi major axis *a* changes a little bit but its orientation rotates with the activity period. This means AVB (it is better to call it σ-Virginids though, see *Figure 1*) is a typical ANT activity; its radiant shifts eastward with time (*Figure 1*).

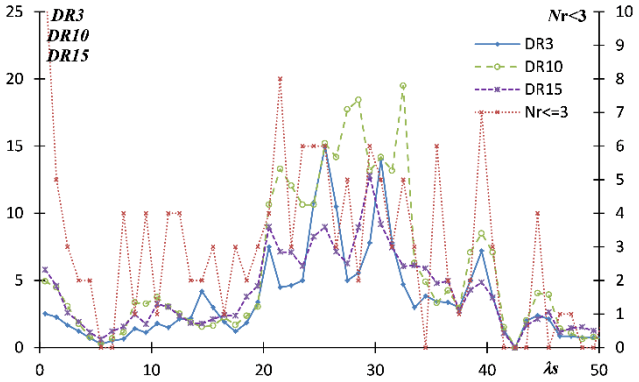

Figure 6 – Activity profile of AVB#0021.

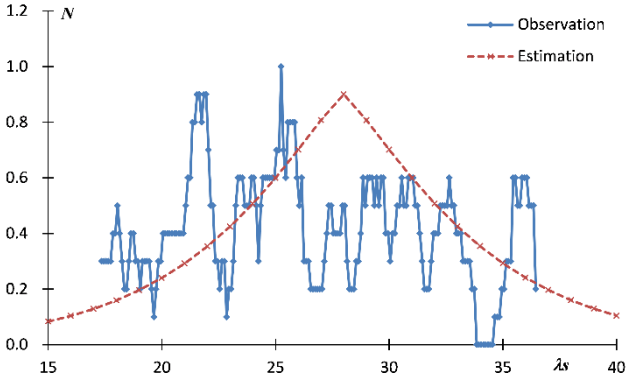

Figure 7 – Comparison between the Nr <= 3° profile of AVB#0021 with the estimation of the activity.

HVI#0343

HVI#0343 was first reported by SonotaCo (2009) and it was a very fortunate case, because the activity of HVI fluctuates a lot (*Table 3*) and their first observation coincides with its active year 2008. The discovery report was based on the observations 2007–2008.

Figure 10 clearly shows that the radiant of HVI is very compact; it is very different from the EVI case (*Figure 2*). HVI has a very sharp maximum around $\lambda_\odot = 41°$ (*Figures 8 and 9*) though our results are based mainly on 2008 and 2009 observations (*Table 3*).

Table 8 shows that the shape of the orbit and the orientation of the perihelion of HVI is stable. It confirms HVI is in resonance with Jupiter (Shiba's view; cited by Roggemans et al. 2020). Sekiguchi[11] gives 2020 observations of HVI by SonotaCo net (Roggemans et al., 2020) and his reported 27 HVI meteor are added in *Figure 11* as circles.

We know now that the HVI radiant shifts slowly in (α, δ) (*Figure 1*) but rapidly on ($\lambda-\lambda_\odot$, β), and the HVI peak is very sharp as shown in *Figures 8 and 9*. It was suggested that HVI is the rediscovery of the "α-Virginids" (Koseki, 2019a) but this assumption might be rejected. *Figure 12* shows the Harvard "α-Virginids" distribution as circles but located apart from the center and observed much later than

[11] http://sonotaco.jp/forum/viewtopic.php?t=4580

the HVI maximum shown in *Figure 9* (*Table 4a* of Koseki, 2019a).

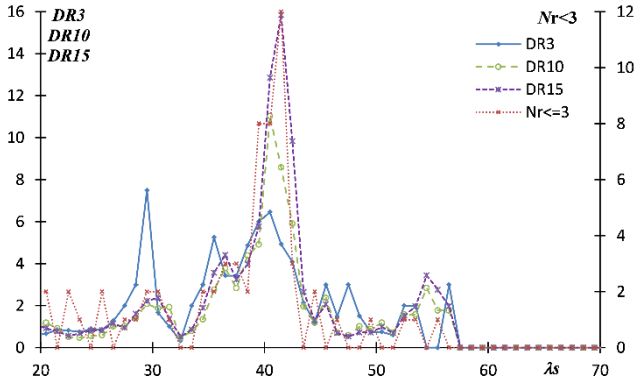

Figure 8 – Activity profile of HVI#0343.

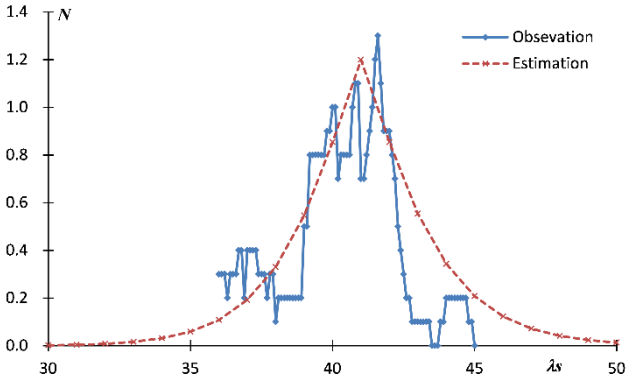

Figure 9 – Comparison of Nr <= 3° profile of HVI#0343 with the estimation of the activity.

Table 3 – Total number of radiants within 3 degrees from the estimated center.

Year	2007	2008	2009	2010	2011	2012	2013	2014	2015	2016	2017	2018	Total
EVI#0011-02	3	0	45	16	2	2	24	15	1	5	37	11	161
AVB#0021-04	1	5	9	2	9	3	7	11	5	6	13	10	81
HVI#0343-03	0	13	14	0	0	0	1	4	7	1	2	0	42

Table 4 – Whipple's "Virginids" (Whipple, 1954); (λ_Π, β_Π) are the ecliptic coordinates of the perihelion.

Code	Year	$\lambda_\odot$	α	δ	$\lambda-\lambda_\odot$	β	v_g	e	q	i	ω	Ω	λ_Π	β_Π	a
H5-2905	1951	344.7	176.2	5.1	189.8	3.2	29	0.843	0.381	3.6	290.2	344.7	274.9	–3.4	2.43
H5-1934	1950	357.9	188.9	1.6	189.7	5	29.2	0.848	0.384	5.9	289.8	357.9	287.8	–5.6	2.53
H5-828	1939	359.5	183.5	5.7	181.5	6.7	31	0.998	0.484	7.1	271.9	359.5	271.4	–7.1	2.42
H5-1158	1942	0.7	186.6	3.7	183.9	6.1	28.4	0.881	0.471	6.1	277.3	0.7	278	–6.1	3.96

Table 5 – The estimated data of the EVI resulting from the regression; (λ_Π, β_Π) are the ecliptic coordinates of the perihelion.

$\lambda_\odot$	$\lambda-\lambda_\odot$	β	α	δ	v_g	e	q	i	ω	Ω	λ_Π	β_Π	a
345	192.8	4.3	179.7	4.8	30.1	0.85	0.331	5.5	296.8	345	281.9	-4.9	2.21
346	192.3	4.3	180.1	4.7	29.9	0.847	0.34	5.5	295.6	346	281.7	-4.9	2.23
347	191.7	4.4	180.6	4.6	29.6	0.844	0.35	5.4	294.4	347	281.5	-4.9	2.25
348	191.2	4.5	181.1	4.4	29.4	0.841	0.36	5.4	293.3	348	281.4	-5	2.27
349	190.7	4.6	181.6	4.3	29.1	0.839	0.369	5.4	292.1	349	281.2	-5	2.29
350	190.2	4.6	182	4.2	28.9	0.836	0.379	5.4	291	350	281.1	-5	2.31
351	189.7	4.7	182.5	4.1	28.6	0.833	0.389	5.3	289.8	351	280.9	-5	2.33
352	189.2	4.8	183	3.9	28.3	0.83	0.398	5.3	288.7	352	280.8	-5	2.35
353	188.7	4.9	183.4	3.8	28.1	0.828	0.408	5.3	287.6	353	280.6	-5	2.37
354	188.1	4.9	183.9	3.7	27.8	0.825	0.418	5.2	286.4	354	280.5	-5	2.38
355	187.6	5	184.4	3.5	27.6	0.822	0.427	5.2	285.3	355	280.4	-5	2.4
356	187.1	5.1	184.9	3.4	27.3	0.819	0.437	5.2	284.2	356	280.2	-5	2.42
357	186.6	5.1	185.3	3.3	27	0.817	0.447	5.2	283.1	357	280.1	-5	2.44
358	186.1	5.2	185.8	3.2	26.8	0.814	0.456	5.1	281.9	358	280	-5	2.45
359	185.5	5.3	186.3	3	26.5	0.811	0.466	5.1	280.8	359	279.9	-5	2.47
0	185	5.4	186.7	2.9	26.3	0.808	0.476	5.1	279.7	0	279.8	-5	2.48
1	184.5	5.4	187.2	2.8	26	0.806	0.485	5	278.6	1	279.7	-5	2.49
2	184	5.5	187.7	2.7	25.8	0.803	0.495	5	277.5	2	279.6	-5	2.51
3	183.5	5.6	188.1	2.5	25.5	0.8	0.504	5	276.4	3	279.5	-4.9	2.52
4	183	5.6	188.6	2.4	25.2	0.797	0.513	4.9	275.4	4	279.4	-4.9	2.53
5	182.4	5.7	189.1	2.3	25	0.794	0.523	4.9	274.3	5	279.3	-4.9	2.54

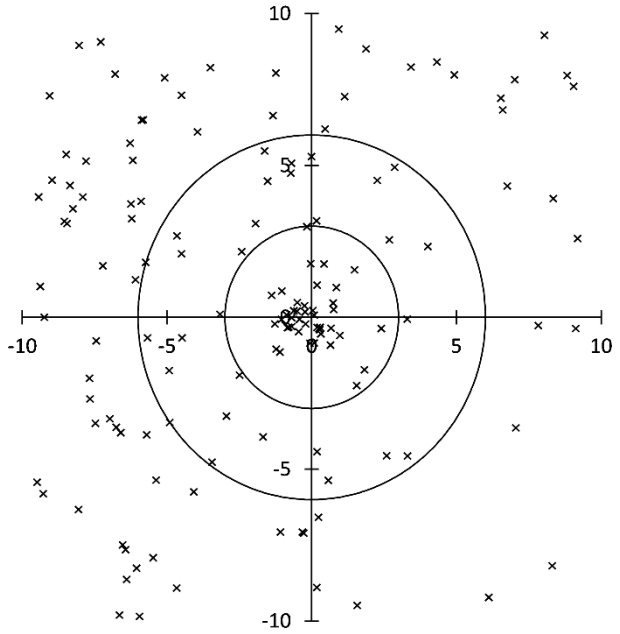

Figure 10 – The radiant distribution around the estimated HVI#0343 center.

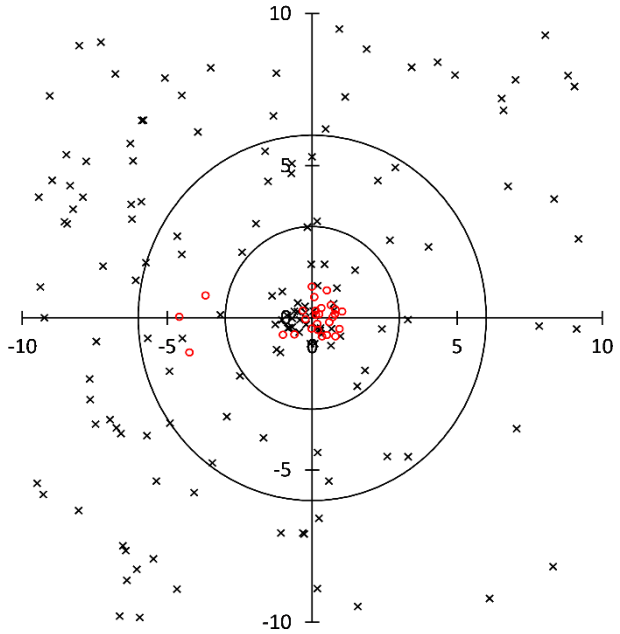

Figure 11 – 2020 HVI observations (circles) with 2007–2018 observations.

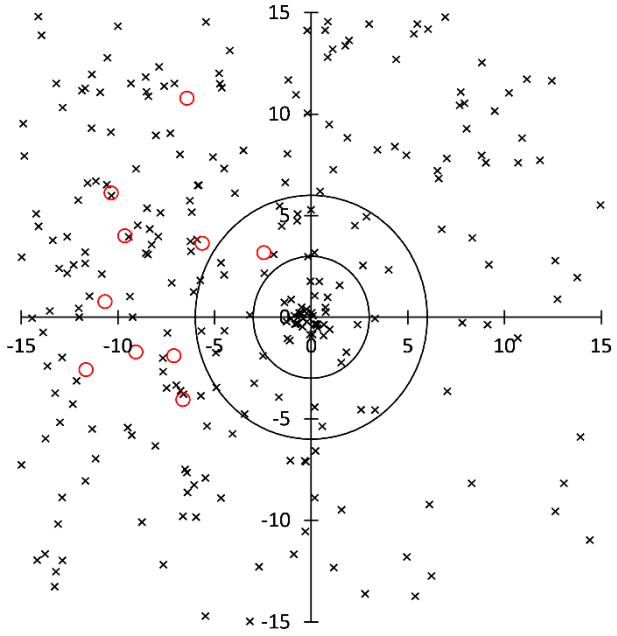

Figure 12 – Harvard photographic "α-Virginids" (circles) with 2007–2018 video observations.

Table 6 – The difference between the orbital elements of the east (left) and west (right) edges for EVI#0011.

x	y	$\lambda_\odot$	$\lambda-\lambda_\odot$	β	α	δ	v_g	e	q	i	ω	Ω	λ_Π	β_Π	a
–5	–0.2	357	190.9	5.3	189.3	1.7	29.6	0.848	0.364	6.4	292.5	357	289.6	–5.9	2.39
5	0.43	357	180.8	5.9	180.4	6.3	23.8	0.774	0.555	4.7	270.8	357	267.8	–4.7	2.46

Table 7 – The estimated data of AVB resulting from the regression; (λ_{Π}, β_{Π}) are the ecliptic coordinates of the perihelion.

$\lambda_{\odot}$	λ–$\lambda_{\odot}$	β	α	δ	v_g	e	q	i	ω	Ω	λ_{Π}	β_{Π}	a
15	176.2	9.6	194.1	4.4	21.2	0.729	0.642	6.5	261.4	15	276.3	–6.4	2.37
16	175.8	9.8	194.6	4.4	21.1	0.728	0.649	6.5	260.5	16	276.4	–6.4	2.39
17	175.3	10	195.2	4.3	20.9	0.728	0.655	6.6	259.6	17	276.6	–6.5	2.41
18	174.9	10.2	195.8	4.3	20.8	0.727	0.662	6.6	258.8	18	276.7	–6.5	2.42
19	174.4	10.4	196.4	4.3	20.6	0.727	0.668	6.7	257.9	19	276.8	–6.5	2.44
20	174	10.5	196.9	4.2	20.5	0.726	0.675	6.7	257.1	20	277	–6.5	2.46
21	173.5	10.7	197.5	4.2	20.3	0.725	0.681	6.7	256.2	21	277.1	–6.6	2.48
22	173.1	10.9	198.1	4.1	20.2	0.725	0.687	6.8	255.4	22	277.3	–6.6	2.5
23	172.6	11.1	198.6	4.1	20	0.724	0.694	6.8	254.6	23	277.5	–6.6	2.51
24	172.1	11.3	199.2	4.1	19.9	0.724	0.7	6.9	253.8	24	277.6	–6.6	2.53
25	171.7	11.5	199.8	4	19.7	0.723	0.706	6.9	252.9	25	277.8	–6.6	2.55
26	171.2	11.7	200.3	4	19.6	0.722	0.712	6.9	252.1	26	278	–6.6	2.56
27	170.8	11.8	200.9	4	19.4	0.722	0.718	6.9	251.3	27	278.2	–6.6	2.58
28	170.3	12	201.4	3.9	19.3	0.721	0.724	7	250.5	28	278.4	–6.6	2.59
29	169.9	12.2	202	3.9	19.2	0.72	0.729	7	249.7	29	278.6	–6.6	2.61
30	169.4	12.4	202.6	3.9	19	0.719	0.735	7	249	30	278.8	–6.6	2.62
31	168.9	12.6	203.1	3.8	18.9	0.718	0.741	7	248.2	31	279	–6.5	2.63
32	168.5	12.7	203.7	3.8	18.7	0.718	0.746	7.1	247.4	32	279.3	–6.5	2.64
33	168	12.9	204.2	3.8	18.6	0.717	0.752	7.1	246.7	33	279.5	–6.5	2.65
34	167.5	13.1	204.8	3.8	18.4	0.716	0.757	7.1	245.9	34	279.7	–6.5	2.66
35	167.1	13.3	205.3	3.7	18.3	0.715	0.763	7.1	245.2	35	280	–6.5	2.67
36	166.6	13.4	205.9	3.7	18.1	0.714	0.768	7.1	244.4	36	280.3	–6.4	2.68
37	166.2	13.6	206.4	3.7	18	0.713	0.773	7.1	243.7	37	280.5	–6.4	2.69
38	165.7	13.8	207	3.6	17.8	0.711	0.779	7.2	243	38	280.8	–6.4	2.7
39	165.2	14	207.5	3.6	17.7	0.71	0.784	7.2	242.2	39	281.1	–6.3	2.7
40	164.8	14.1	208.1	3.6	17.6	0.709	0.789	7.2	241.5	40	281.3	–6.3	2.71

Table 8 – The estimated data of HVI resulting from the regression; (λ_{Π}, β_{Π}) are the ecliptic coordinates of the perihelion.

$\lambda_{\odot}$	λ–$\lambda_{\odot}$	β	α	δ	v_g	e	q	i	ω	Ω	λ_{Π}	β_{Π}	a
30	173.3	-0.8	201.2	–9.8	20.2	0.73	0.675	0.5	77.2	210	287.2	0.5	2.5
31	172.5	-0.9	201.5	–10	20	0.729	0.685	0.5	75.9	211	286.9	0.5	2.53
32	171.8	-0.9	201.7	–10.1	19.8	0.729	0.694	0.6	74.6	212	286.6	0.5	2.56
33	171.1	-1	201.9	–10.3	19.5	0.728	0.704	0.6	73.2	213	286.2	0.6	2.59
34	170.3	-1	202.1	–10.4	19.3	0.727	0.713	0.6	72	214	286	0.6	2.61
35	169.6	-1.1	202.4	–10.5	19	0.726	0.723	0.6	70.7	215	285.7	0.6	2.64
36	168.8	-1.2	202.6	–10.7	18.8	0.725	0.732	0.7	69.5	216	285.5	0.6	2.66
37	168.1	-1.2	202.8	–10.8	18.6	0.724	0.741	0.7	68.2	217	285.2	0.6	2.68
38	167.4	-1.3	203	–11	18.3	0.722	0.749	0.7	67	218	285	0.6	2.7
39	166.6	-1.3	203.3	–11.1	18.1	0.721	0.758	0.7	65.8	219	284.8	0.6	2.72
40	165.9	-1.4	203.5	–11.3	17.8	0.719	0.766	0.7	64.6	220	284.6	0.6	2.73
41	165.1	-1.4	203.7	–11.4	17.6	0.718	0.775	0.7	63.5	221	284.5	0.7	2.74
42	164.4	-1.5	203.9	–11.6	17.4	0.716	0.783	0.7	62.3	222	284.3	0.7	2.75
43	163.6	-1.5	204.2	–11.7	17.1	0.714	0.79	0.8	61.2	223	284.2	0.7	2.76
44	162.9	-1.6	204.4	–11.8	16.9	0.711	0.798	0.8	60.1	224	284.1	0.7	2.76
45	162.2	-1.6	204.6	–12	16.6	0.709	0.806	0.8	59	225	284	0.7	2.77
46	161.4	-1.7	204.8	–12.1	16.4	0.706	0.813	0.8	58	226	284	0.7	2.77
47	160.7	-1.7	205.1	–12.3	16.2	0.703	0.82	0.8	56.9	227	283.9	0.7	2.76
48	159.9	-1.8	205.3	–12.4	15.9	0.7	0.827	0.8	55.9	228	283.9	0.7	2.76
49	159.2	-1.8	205.5	–12.5	15.7	0.697	0.834	0.8	54.8	229	283.8	0.7	2.75
50	158.5	-1.9	205.7	–12.7	15.5	0.693	0.84	0.8	53.8	230	283.8	0.7	2.74

References

Dennning W. F. (1899). “General Catalogue of the Radiant Points of Meteoric Showers and of Fireballs and Shooting Stars observed at more than one station”. *Memoirs of the Royal Astronomical Society*, **53**, 201–293.

Hoffmeister C. (1948). “Meteorströme”. Johann Ambrosius Bath, Verlag, Leipzig.

Jenniskens P. (2006), “Meteorshowers and Their Parent Comets”. Cambridge, UK: Cambridge University Press.

Jenniskens P., Nénon Q., Gural P. S., Albers J., Haberman B., Johnson B., Holman D., Morales R., Grigsby B. J., Samuels D., Johannink C. (2016). “CAMS confirmation of previously reported meteor showers”. *Icarus*, **266**, 355–370.

Koseki M. (2012). “A simple model of spatial structure of meteoroid streams”. *WGN, Journal of the International Meteor Organization*, **40**, 162–165.

Koseki M. (2019a). “Legendary meteor showers: Studies on Harvard photographic results”. *WGN, Journal of the International Meteor Organization*, **47**, 139–150.

Koseki M. (2019b). “Profiles of meteor shower activities inferred from the radiant Density Ratios (DR)”. *WGN, Journal of the International Meteor Organization*, **47**, 168–179.

McCrosky R. E. and Posen A. (1959). “New Photographic Meteor Shower”. *Astronomical Journal*,**64**, 25–27.

McIntosh R. A. (1935). “An Index to Southern Meteor Showers”. *Monthly Notices of the Royal Astronomical Society*, **95**, 709–718.

Roggemans P., Johannink C. and Sekiguchi T. (2020). “h Virginids (HVI#343) activity enhancement in 2020”. *eMetN*, **5**, 233–244.

Shiba Y. (2018). “Eta Virginids (EVI) four-year cycle”. *WGN, Journal of the International Meteor Organization*, **46**, 184–190.

SonotaCo (2009). “A meteor shower catalog based on video observations in 2007–2008”. *WGN, Journal of the International Meteor Organization*, **37**, 55–62.

Whipple Fred L. (1954). “Photographic meteor orbits and their distribution in space”. *Astronomical Journal*, **59**, 201–217.

D64.nl – Meteor detecting project

Rens Sparrius

Ulrum, The Netherlands

A brief description is presented of a meteor detecting setup in Groningen using a CCTV camera with software algorithms based on the Hough-transform method.

1 Introduction

While researching possibilities to support the Dutch all-sky-cam project, I realized that the airspace of the Netherlands is already adequately covered by early enthusiasts using mostly 360 degrees fish-eye cameras.

I was still curious to explore techniques behind automated detection of meteors and all the problems that come along with this exciting citizen science activity. *Richard Kacerek*, the co-founder of the UKMON group and co-founder of eMeteorNews, invited me to write an article about my setup. I'm not an astronomer and I'm very new into this field but in this article, I would like to share information about my project.

I had some reasonably good experience with the 'new' 4K IP based CCTV camera's for other projects, so I wondered if those cameras could be suitable for the sky-cam setup. After a lot of sourcing, I bought a so-called bullet camera for outdoor use with a minimum shutter speed of one-third per second. The wired network camera can be powered over 'Power over Ethernet' (PoE) or 12VDC. In my setup, I use the PoE method; this way, you only have one cable from a PoE enabled network switch to the camera itself. Maximum distance for the cable is officially 100 meter, but with a quality PoE switch and CAT-6 cable, you might even extend this easily up-to 150 meters or further.

2 My first CCTV sky cam above the kitchen door

Most IP-based CCTV cameras have an option to read the video-stream with RTSP (Real-Time Streaming Protocol) and sending interval images to a network-drive or (S)FTP server. As of now I only use the stills to detect possible meteors. To start with detecting I've configured the camera so that it will upload roughly every second an image to a local Debian SFTP server. As a 'backup' I've setup a 24-hour YouTube live-stream from the same camera, this video archive can be used to review the actual video of the detected meteors.

Using the Python programming language, the system triggers the detection algorithm on new image files in the 'receive' directory. The algorithm I use is based on the 'Hough transform' extraction technique. This method for meteor detection is described by Trayner et al. (1999). Hough-transform is 'simply' a technique to detect lines in images. This algorithm is implemented in OpenCV; an open-source 'computer vision' library written in C++ with bindings to multiple other programming languages, including Python used in my project.

Figure 1 – My first sky-cam above the kitchen door in Ulrum, Groningen, The Netherlands.

In case the algorithm detects a line it will save a copy of the image in another folder for further analyzing, then the process will wait for the next image to be checked for 'lines' etc. etc. At night this works all quite perfect, but in the daytime, there may be a lot of false positives due to planes a sporadic bird or sharp-edged clouds.

Figure 2 – One of my favorites so far; photographed on 9 April 2020, $22^h51^m39.815^s$ UTC.

Before the Hough-transform algorithm can do its 'thing' it is essential to do some preprocessing to speed things up and get more reliable results. When you take the meteor image in *Figure 2* as an example the system will first convert the picture to grey-scale. From here, my program will apply a

Gaussian blur over the image followed by a 'Canny' edge algorithm what will generate the result shown in *Figure 3*.

After the Canny-edge algorithm, the Hough-transform algorithm can easily detect any possible lines and will return the position of each detected line for further processing.

Figure 3 – Same image processed with the Canny-edge detection algorithm. As you can see there is still a lot of 'noise'; this can be eliminated with a Gaussian blur effect before applying the Canny algorithm.

3 Basic Python 3 code

A little bit basic Python 3 code to get the same result:

```
#!/usr/bin/env python3
import cv2 as cv,numpy as np
# Open a image and save the result in the
variable 'image':
image = cv.imread('./your-image.jpg')
# Make a gray-scale copy and save the
result in the variable 'gray'
gray = cv.cvtColor(image,
cv.COLOR_BGR2GRAY)
# Apply blur and save the result in the
variable 'blur'
blur = cv.GaussianBlur(gray, (5,5), 0)
# Apply the Canny edge algorithm
canny = cv.Canny(blur, 100, 200, 3)
# Save the result as 'canny.jpg'
cv2.imwrite('./canny.jpg',canny)
```

For this code to run you need to have OpenCV and Numpy installed. This can be easily done on a Debian based machine with 'apt install python3-opencv'.

To check if an image has possible lines you can simply add the following code at the end:

```
# The Hough-transform algo:
meteors = cv.HoughLinesP(canny, 1,
np.pi/180, 25, minLineLength=50,
maxLineGap=5)
if meteors is not None:
  print('I found a possible meteor')
else:
  print(':( Maybe next time better')
```

This small little script will now detect possible lines on an image and can be used to build your detection system. When you are not really into programming you may take a look on my web-based meteor detection algorithm environment; here you can adjust settings to see the effect of the algorithms on previous detected meteors.

Every morning I will check the results, remove any false positives and further process the images to merge nearby lines, calculate line length, line angles and so on. After this, the system populates a database with the results and publish it on my website.

As of now, I'm working on linking ADS-B data into my detection process to eliminate false positives by daytime planes. ADS-B is standard for radio signals sent out by most airplanes with flight information including their real-time GPS location. Those signals can be easily detected with a USB dongle and an external antenna. Knowing the location and detection window of your camera this can help you to automate the adjustment of algorithm parameters in the case of a nearby airplane.

Between 30 March 2020 and 5 May 2020, my system has detected 98 individual meteors. In a few cases, it made multiple images of the same meteor. With post-processing you can do a lot of interesting things like creating cinema-graph's, generating statistics etc. I found out that a set of verified meteor images can be valuable to adjust my algorithms further and possibly use it to train machine-learning or ai systems.

The cost break down for my one camera setup is as follows:

- 5-port PoE network switch € 60,00
- 8MP CCTV weatherproof IP camera € 264,00
- Network cable € 20,00

Besides this you need a computer to store and process the images, I got mine; a 4th generation i5 from the local Goodwill for € 100 excluding peripherals. With one computer and the 5-port PoE switch I use I can still add up-to 4 more cameras to further expand my sky coverage. Before I add more cameras, I want to work more on eliminating false positives, further automating processing and website infrastructure so that handling much more images won't be a problem.

When you like to see more of my detections, including the detection algorithm environment, some cinema-graphs of single meteors and statistics of my system check out my website[12].

References

Trayner C., Haynes B. R., and Bailey N. J. (1999). "The time-gradient Hough transform, a novel algorithm from meteor science". *IEE Colloquium on Motion Analysis and Tracking*, **103**,16/1–16/6.

[12] https://d64.nl/en/

April 2020 report CAMS BeNeLux

Paul Roggemans

Pijnboomstraat 25, 2800 Mechelen, Belgium
paul.roggemans@gmail.com

A summary of the activity of the CAMS BeNeLux network during the month of April 2020 is presented. 4128 orbits were collected during 29 nights with a maximum of 94 operational cameras at 25 different CAMS stations. Favorable weather circumstances during the Lyrid activity allowed to monitor the April Lyrid activity for a third year in a row.

1 Introduction

April is often a better month for astronomical observations after a general unfavorable first three months of the year. April also brings the Lyrids, a major annual shower with modest activity apart from some outbursts. CAMS BeNeLux got exceptional favorable observing conditions during the Lyrids 2018 and 2019, three years on a row may be too much to expect. Since March 2020 was an exceptional favorable record month the question was if the good weather would last longer into April?

2 April 2020 statistics

The weather remained stable during most of the month. As many as 16 nights had more than 100 orbits (8 in 2019), 4 nights more than 200 orbits (3 in 2019) and the record night was April 21–22 with as many as 460 orbits in a single night. Only one night, April 29–30 remained without any orbit. For a third year in a row, the CAMS BeNeLux network enjoyed clear sky during much of the Lyrid.

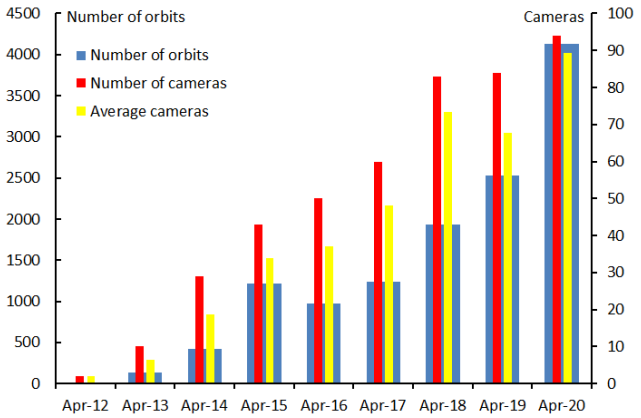

Figure 1 – Comparing April 2020 to previous months of April in the CAMS BeNeLux history. The blue bars represent the number of orbits, the red bars the maximum number of cameras running in a single night and the yellow bars the average number of cameras running per night.

CAMS BeNeLux captured 24465 meteors (14667 in 2019) of which 14924 or 61% were multiple station (7894 and 54% in 2019). April 2020 resulted in a record number of 4128 orbits (2534 in 2019). This is the best score ever for the month of April in terms of orbits. The maximum of 94 cameras available improved compared to April 2019 (84 cameras). At least 76 cameras remained operational all nights, which is a lot better than the 44 cameras in April 2019 when several camera stations experienced technical issues. On average 89.4 cameras were operational, the highest score ever, against 67.7 in April 2019.

In total CAMS BeNeLux collected 12581 orbits during 210 April nights accumulated during the past 8 years. The statistics for April 2020 are compared in *Table 1* with all previous months of April since the start of the CAMS BeNeLux network. *Figure 1* shows the increase in number of operational cameras compared to previous years.

Table 1 – April 2020 compared to previous months of April.

Year	Nights	Orbits	Stations	Max. Cams	Min. Cams	Mean Cams
2012	6	11	4	2		2.0
2013	19	140	9	10		6.5
2014	19	421	12	29		18.8
2015	27	1212	15	43		33.9
2016	26	971	17	50	15	37.0
2017	28	1235	20	60	32	48.2
2018	27	1929	21	83	59	73.3
2019	29	2534	20	84	44	67.7
2020	29	4128	25	94	76	89.4
Total	210	12581				

3 Conclusion

April 2020 brought exceptional favorable weather for the CAMS BeNeLux network. Just like in 2018 and 2019 clear nights during much of the Lyrid activity period resulted in a record number of Lyrid orbits.

Acknowledgment

Many thanks to all participants in the CAMS BeNeLux network for their dedicated efforts. The data on which this report is based has been taken from the CAMS website[13]. The CAMS BeNeLux team is operated by the following volunteers:

Hans Betlem (Leiden, Netherlands, CAMS 371, 372 and 373), Felix Bettonvil (Utrecht, Netherlands, CAMS 376 and 377), *Jean-Marie Biets* (Wilderen, Belgium, CAMS 379, 380, 381 and 382), *Martin Breukers* (Hengelo, Netherlands, CAMS 320, 321, 322, 323, 324, 325, 326 and 327, RMS 328 and 329), *Guiseppe Canonaco* (Genk, RMS 3815), *Bart Dessoy* (Zoersel, Belgium, CAMS 397, 398, 804, 805, 806 and 888), *Jean-Paul Dumoulin, Dominique Guiot and Christian Walin* (Grapfontaine, Belgium, CAMS 814 and 815, RMS 003814), *Uwe Glässner* (Langenfeld, Germany, RMS 3800), *Luc Gobin* (Mechelen, Belgium, CAMS 390, 391, 807 and 808), *Tioga Gulon* (Nancy, France, CAMS 3900 and 3901), *Robert Haas* (Alphen aan de Rijn, Netherlands, CAMS 3160, 3161, 3162, 3163, 3164, 3165, 3166 and 3167), *Robert Haas* (Texel, Netherlands, CAMS 810, 811, 812 and 813), *Robert Haas / Edwin van Dijk* (Burlage, Germany, CAMS 801, 802, 821 and 822), *Kees Habraken* (Kattendijke, Netherlands, RMS 000378), *Klaas Jobse* (Oostkapelle, Netherlands, CAMS 3030, 3031, 3032, 3033, 3034, 3035, 3036 and 3037), *Carl Johannink* (Gronau, Germany, CAMS 311, 313, 314, 315, 316, 317, 318, 3000, 3001 and 3002), *Hervé Lamy* (Dourbes, Belgium, CAMS 394 and 395), *Hervé Lamy* (Humain Belgium, CAMS 816), *Hervé Lamy* (Ukkel, Belgium, CAMS 393), *Koen Miskotte* (Ermelo, Netherlands, CAMS 351, 352, 353 and 354), *Jos Nijland* (Terschelling, Netherlands, CAMS 841 and 842), *Tim Polfliet* (Gent, Belgium, CAMS 396), *Steve Rau* (Zillebeke, Belgium, CAMS 3850 and 3852), *Paul and Adriana Roggemans* (Mechelen, Belgium, CAMS 383, 384, 388, 389, 399 and 809, RMS 003830 and 003831), *Hans Schremmer* (Niederkruechten, Germany, CAMS 803) and *Erwin van Ballegoij* (Heesch, Netherlands, CAMS 347 and 348).

[13] http://cams.seti.org/FDL/index-BeNeLux.html

May 2020 report CAMS BeNeLux

Paul Roggemans

Pijnboomstraat 25, 2800 Mechelen, Belgium
paul.roggemans@gmail.com

A summary of the activity of the CAMS BeNeLux network during the month of May 2020 is presented. 18592 meteors were detected of which 11584 were multiple station which resulted in 3226 orbits during 29 nights with a maximum of 93 operational cameras available at 24 different CAMS stations.

1 Introduction

The first weeks of May offer nice levels of meteor activity with the eta Aquariids in the early morning hours. The last couple of weeks get shorter nights while the meteor activity decreases to the lowest level of the year. With short nights, low activity and often poor weather this time of the year remains a challenge to collect orbits.

2 May 2020 statistics

May 2020 was an exceptional dry favorable month for meteor work. As many as 18 nights resulted in 100 or more orbits (against 7 in 2019), not bad at all considering the limited number of dark hours at the BeNeLux latitudes this month. Only two nights remained without any orbits, just like in May 2019. The best night of all was May 14–15 with 170 orbits, no record numbers as previous two years had several May-nights with more orbits.

As many as 18592 meteors were detected of which 11584 were multiple station (against 5886 in 2019), good for 3226 orbits (against 1825 in May 2019). 62% of all recorded meteors were multiple station and contributed to obtain orbits. Also, May 2018 offered exceptional favorable weather but then 'only' 2426 orbits were collected. More cameras that run all nights make a great difference.

Table 1 – May 2020 compared to previous months of May.

Year	Nights	Orbits	Stations	Max. Cams	Min. Cams	Mean Cams
2012	5	13	4	2		2
2013	13	69	9	13		6.8
2014	22	430	13	31		19.7
2015	25	484	15	42		24.2
2016	26	803	17	52	16	39.9
2017	24	1627	19	64	22	52.0
2018	31	2426	21	84	64	76.6
2019	29	1825	20	84	53	72.4
2020	29	3226	24	93	70	90.5
Total	204	10903				

The statistics for May 2020 are compared in *Table 1* with all previous months of May since the start of the CAMS BeNeLux network. The maximum number of operational cameras increased to 93 against 84 one year ago. The number of cameras that remained operational all nights with AutoCAMS increased to 70 against 53 in May 2019. The average number of operational cameras with 90.5 exceeded all previous years. Apart from favorable weather, the awareness to keep cameras operational 7 nights on 7 accounts to a large extent to the record number of orbits.

Since the start of CAMS BeNeLux 204 nights in May allowed to collect as many as 10903 orbits in May.

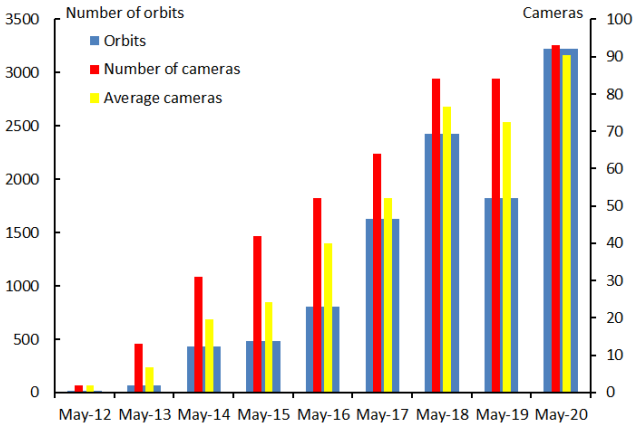

Figure 1 – Comparing May 2020 to previous months of May in the CAMS BeNeLux history. The blue bars represent the number of orbits, the red bars the maximum number of cameras running in a single night and the yellow bars the average number of cameras running per night.

Figure 1 shows the gain in camera capacity and number of orbits compared to all previous years. The key for success of a camera network is that all stations and all cameras are kept operational all nights.

3 Conclusion

May 2020 was a record month comparable to May 2018 in weather but covered with significant better camera capacity than ever before.

Acknowledgment

Many thanks to all participants in the CAMS BeNeLux network for their dedicated efforts. The data on which this report is based has been taken from the CAMS website[14]. The CAMS BeNeLux team is operated by the following volunteers:

Hans Betlem (Leiden, Netherlands, CAMS 371, 372 and 373), Felix Bettonvil (Utrecht, Netherlands, CAMS 376 and 377), *Jean-Marie Biets* (Wilderen, Belgium, CAMS 379, 380, 381 and 382), *Martin Breukers* (Hengelo, Netherlands, CAMS 320, 321, 322, 323, 324, 325, 326 and 327, RMS 328 and 329), *Guiseppe Canonaco* (Genk, RMS 3815), *Bart Dessoy* (Zoersel, Belgium, CAMS 397, 398, 804, 805, 806 and 888), *Jean-Paul Dumoulin, Dominique Guiot and Christian Walin* (Grapfontaine, Belgium, CAMS 814 and 815, RMS 003814), *Uwe Glässner* (Langenfeld, Germany, RMS 3800), *Luc Gobin* (Mechelen, Belgium, CAMS 390, 391, 807 and 808), *Tioga Gulon* (Nancy, France, CAMS 3900 and 3901), *Robert Haas* (Alphen aan de Rijn, Netherlands, CAMS 3160, 3161, 3162, 3163, 3164, 3165, 3166 and 3167), *Robert Haas* (Texel, Netherlands, CAMS 810, 811, 812 and 813), *Robert Haas / Edwin van Dijk* (Burlage, Germany, CAMS 801, 802, 821 and 822), *Kees Habraken* (Kattendijke, Netherlands, RMS 000378), *Klaas Jobse* (Oostkapelle, Netherlands, CAMS 3030, 3031, 3032, 3033, 3034, 3035, 3036 and 3037), *Carl Johannink* (Gronau, Germany, CAMS 311, 314, 317, 318, 3000, 3001, 3002, 3003, 3004 and 3005), *Hervé Lamy* (Dourbes, Belgium, CAMS 394 and 395), *Hervé Lamy* (Humain Belgium, CAMS 816), *Hervé Lamy* (Ukkel, Belgium, CAMS 393), *Koen Miskotte* (Ermelo, Netherlands, CAMS 351, 352, 353 and 354), *Tim Polfliet* (Gent, Belgium, CAMS 396), *Steve Rau* (Zillebeke, Belgium, CAMS 3850 and 3852), *Paul and Adriana Roggemans* (Mechelen, Belgium, CAMS 383, 384, 388, 389, 399 and 809, RMS 003830 and 003831), *Hans Schremmer* (Niederkruechten, Germany, CAMS 803) and *Erwin van Ballegoij* (Heesch, Netherlands, CAMS 347 and 348).

[14] http://cams.seti.org/FDL/index-BeNeLux.html

Geminids 2019 under a moonlit sky

Koen Miskotte

Dutch Meteor Society
k.miskotte@upcmail.nl

With a Full Moon on December 12 moonlight would be present all night during the Geminid maximum. So, no options for distant expeditions, but just waiting for the weather situation at home. Unfortunately, it was cloudy and rainy almost all-night December 13-14. During the day, the rain and clouds disappeared and nice open sky followed with occasional rain showers developing. However, in the evening of December 14-15, temporary clearings were expected before the next front arrived.

1 2019 December 14–15

The sky was not completely 100% clear, but around 18^h UT the clear gaps became wider. So, I started the observations at 18^h20^m UT. I observed this evening from the meteor platform on my dormer. An almost Full Moon was low in the east, and the radiant was also low. I looked northwest to keep the Moon out of the field of view. Almost every moment there were a few small clouds in my field of view, but the coverage remained very low, below 10%. The observations had to stop at 20^h55^m UT, when clouds came in from the west. The limiting magnitude decreased from +5.7 to +5.4 in that period. As the radiant was rising during this session, more and more Geminids were seen! I was counting in periods of 10–20 minutes (see *Table 1*). The numbers of Geminids increased from 4 to 10 per counting period.

Figure 1 – This magnitude –3 Geminid was captured on 14 December 2019 at 22^h09^m UT. Camera: Canon 6D with Sigma 8 mm F 4.5 fish eye lens and LC Shutter set at 16 breaks per second.

It was very nice to see some slow Earth grazing Geminids passing through Auriga and/or Camelopardalis. A nice magnitude –1 passed through Draco, a few minutes later a –1 in the Big Dipper. The most beautiful Geminid appeared at 19^h52^m UT (Geminid –2 with flare moving from Cassiopeia to Perseus) and at 20^h12^m UT (Geminid –2 in Camelopardalis).

At 20^h55^m UT most of the sky closed from the west, the next front with clouds and rain would arrive soon. The equipment simply remained on the roof and the author went to sleep, happy with the results. Despite the Moon I had still observed over 2 hours with lots of Geminids!

The images of the all sky camera show that after 21^h50^m UT the sky cleared again until 22^h40^m UT. I should have waited a bit longer. In total, I counted 55 Geminids, 1 Antihelion and 6 sporadic meteors between 18^h20^m and 20^h55^m UT (effective time 2.35 hours).

The all sky camera (Canon 6D, Sigma 8 mm F 3.5 fish eye lens and a Liquid Crystal Shutter set at 16 breaks per second) photographed four bright Geminids. See also *Table 2*.

Figure 2 – This magnitude –5 Geminid is captured on 15 December 2019 at 00^h10^m UT. Camera: Canon 6D with Sigma 8 mm F 4.5 fish eye lens and LC Shutter set at 16 breaks per second.

Table 1 – Geminid observations 14–15 December 2019 by the author.

Period UT		T_m	T_{eff}	Lm	SQM	Stream			Total	F	M
Start	End	[h]	[h]		mean	GEM	ANT	SPO			
18^h20^m	18^h36^m	18.47	0.27	5.73	18.25	4	0	1	5	1.10	C
18^h50^m	19^h10^m	19.00	0.33	5.65	~	7	0	2	9	1.07	C
19^h10^m	19^h25^m	19.29	0.25	5.6	~	5	0	1	6	1.05	C
19^h25^m	19^h35^m	19.50	0.17	5.56	~	4	0	1	5	1.05	C
19^h35^m	19^h52^m	19.73	0.28	5.56	~	5	1	0	6	1.12	C
19^h52^m	20^h12^m	20.03	0.33	5.52	~	10	0	0	10	1.04	C
20^h12^m	20^h34^m	20.38	0.37	5.52	~	10	0	1	11	1.05	C
20^h34^m	20^h55^m	20.74	0.35	5.4	~	10	0	0	10	1.10	C

Table 2 – Fireballs captured with the all sky camera EN-98 during 14–15 December 2019.

Nr.	Start UT	End UT	Time meteor	M_v	Class	Constellation
320	$22^h09^m00^s$	$22^h09^m57^s$	?	–4	GEM	PER–>AND
321	$23^h57^m00^s$	$23^h57^m57^s$	?	–6	GEM	ERI
322	$00^h10^m00^s$	$00^h10^m57^s$	?	–5	GEM	CAS
323	$06^h16^m00^s$	$06^h16^m57^s$	?	–5	GEM	HER

Figure 3 – Bright magnitude –6 Geminid captured on 14 December 2019 at 23^h57^m UT. Camera: Canon 6D with Sigma 8 mm F 4.5 fish eye lens and LC Shutter set at 16 breaks per second.

Meteor observations during the low season of meteors

Koen Miskotte

Dutch Meteor Society
k.miskotte@upcmail.nl

An overview of visual and photographic meteor observations made in March 2020 by the author.

1 Introduction

The months of January and February 2020 will enter into the books as cloudy and rainy months. Little could be observed during these periods for this reason. In addition, during that period I had to stop taking certain medicines, which led to a lack of sleep, another reason why it was decided to do nothing for visual meteor observing. In March I was through these sleepless nights and I was looking forward to a clear starry sky.

As has often happened in recent years, the weather tipped from March 15 and there were quite a number of clear nights in the 2nd half of the month. For the author, the first visual observations of 2020 in the new decade (Miskotte, 2020) could be made. March is known to be the month with the lowest meteor activity along with February. However, how much is seen in practice varies considerably and depends, among other things, on the observing conditions and the perception of the observer.

2 The observations

March 20–21

The first night in 2020 that I could observe was Friday on Saturday night March 20–21, a crystal-clear night. Because I still had to work on Saturday, I decided to observe on the meteor platform (the flat roof of my dormer), start at 00^h39^m UT. Good clear sky, lm 6.3 and an SQM of 20.37, which is a good value from the meteor platform. As expected very little activity, a +2 SPO and a nice +3 ANT were the "highlights" of this session. After an hour I realized that I didn't hear the all sky camera click. I could check what was going on: the SD card was locked. So, a bit later the camera was running again. Fortunately, no fireballs were reported this night. Anyway, no further visual observations were done after this. Between 00^h39^m and 01^h39^m UT I counted only 5 meteors, of which 1 ANT.

March 21–22

The second night was March 21–22. Again, a crystal-clear night. This time I observed from the Groevenbeekse Heide a heath just outside of Ermelo. Observations started at 01^h03^m and stopped when dusk set in at 03^h07^m UT. Lm 6.4 and SQM 20.49! The sky background was nice and dark and very transparent. Nice numbers of meteors this night: the sporadic activity was very good due to the excellent conditions: I saw resp. 9, 9 and 12 meteors per hour. Add to that the ANT activity which was also quite good this night with resp. 4, 2 and 1 meteors. So, in total I counted 37 meteors.

During the last hour the best meteors appeared: a beautiful +1 with a persistent train in Serpens, followed shortly after by a blue-white magnitude 0 sporadic meteor in Aquila with a 2-second persistent train. The most beautiful meteor appeared in the last thirty seconds of this session. At 02^h06^m UT a very slow, bright ($m_v = -2$) and red meteor moved from Corona Borealis to the southern part of Ophiuchus. Many CAMS and all sky stations recorded this meteor. This made a nice ending of this session therefore!

March 22–23

The next night March 22–23 was also clear. Again, a three-hour session from the Groevenbeekse Heide. The sky background was a bit lighter with slightly lower Lm and SQM values than in the previous night. Significantly fewer meteors were also seen. Two sporadics of +1 were the highlight of this session. In total, 23 SPO and 4 ANT were seen, making a total of 27 meteors.

March 27–28

After this night there were still some clear nights, but the haziness had increased considerably. During the night of March 27–28 I was observing again from the meteor roof. There was still some haze, resulting in a low lm (6.0) and SQM (19.91) values. Exactly 1.5 hours I was counting the meteors between 00^h37^m and 02^h08^m UT. It only yielded 7 meteors, 1 of which was ANT. That was also the brightest meteor of this session (+2).

March 30–31

March 30–31 was the last night I could observe meteors. The moon was almost in first quarter, which means moonlight during all night in the spring. I started around moonset from the meteor platform. A nice dark sky with a lm of 6.3 and SQM 20.32. I did the observations between 00^h40^m and 02^h46^m UT. During those 2 hours I counted 14 meteors. Two very beautiful meteors, the first one appeared at 01^h31^m UT near the star Kochab (in the constellation of Ursa Minor). A fast, beautiful yellow-white magnitude –2 sporadic meteor with a 2-second train. And at $02^h26^m40^s$ UT a nice slow –1 sporadic meteor moving from the Big Dipper to Cygnus. A glittery wake was visible and the color was bright red. All in all, a nice session.

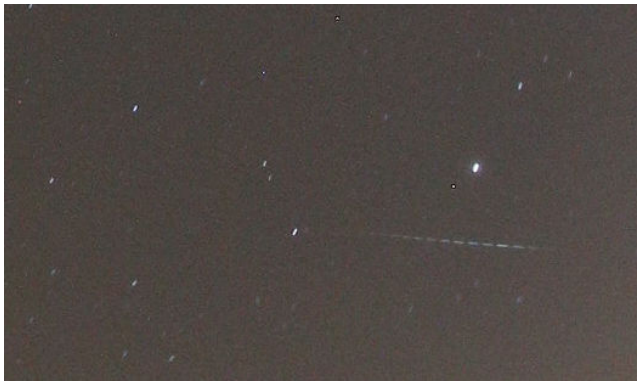

Figure 1 – Quadrantid of magnitude –4 in Bootes on 4 January 2020 at 04^h59^m UT. Camera: Canon 6D, Sigma 8 mm fish eye lens, LC shutter set at 16 breaks per second.

3 EN-98: the first quarter of 2020

Thanks to the bad weather in the first two months, only a few hits. A total of 11 fireballs were captured between January 1 and March 31, 2020. The big fireball of March 2, 2020 was of course the most spectacular! Magnitude –10 with a flare of –14 from behind (unfortunately!) the chimney. A meteorite dropping near Dortmund is almost certain (Betlem, 2020).

Figure 2 – Bright Quadrantid on 4 January 2020 at 04^h10^m UT. Camera: Canon 6D, Sigma 8 mm fish eye lens, LC shutter set at 16 breaks per second.

Table 1 – Overview of the number of fireballs photographed in the period January–March 2020.

No	Year	Month	Day	Start	End	Meteor	Mv	Shower	Constellation
326	2020	01	4	$01^h09^m00^s$	$01^h10^m27^s$		–3	QUA	Gem
327	2020	01	4	$04^h09^m00^s$	$04^h10^m27^s$		–4	QUA	Dra
328	2020	01	4	$04^h58^m30^s$	$04^h59^m57^s$		–4	QUA	Boo
329	2020	01	16	$21^h52^m30^s$	$21^h53^m57^s$		–6	SPO	Per
330	2020	02	16	$04^h52^m30^s$	$04^h53^m57^s$		–4	SPO	UMa
331	2020	03	1	$21^h02^m30^s$	$21^h03^m57^s$		–4	SPO	Per
332	2020	03	2	$01^h41^m30^s$	$01^h42^m57^s$		–3	SPO	UMa
333	2020	03	2	$23^h37^m00^s$	$23^h38^m27^s$		–10	SPO	Boo
334	2020	03	22	$04^h05^m30^s$	$04^h06^m57^s$	$04^h06^m38^s$	–2	SPO	Oph
335	2020	03	23	$00^h19^m00^s$	$00^h20^m27^s$	$00^h19^m34^s$	–7	SPO	Aur>Per
336	2020	03	26	$23^h04^m00^s$	$23^h05^m27^s$	$23^h05^m21^s$	–6	SPO	Boo

Figure 3 – This bright green fireball was captured low on the western horizon on January 16, 2020, around 21^h53^m UT. Camera: Canon 6D, Sigma 8 mm fish eye lens, LC Shutter set at 16 breaks per second.

Figure 4 – The Big Dortmund fireball of 2 March 2020 at 23^h37^m UT. Camera: Canon 6D, Sigma 8 mm fish eye lens, LC Shutter sets at 16 breaks per seconde.

Figure 5 – This beautiful fireball was captured on March 23, 2020 at $00^h19^m34^s$ UT (CAMS 351 timing). Camera: Canon 6D, Sigma 8 mm fish eye lens, LC Shutter set at 16 breaks per second.

Figure 6 – This beautiful fireball was captured on March 26, 2020 at 23^h04^m UT. Camera: Canon 6D, Sigma 8 mm fish eye lens, LC Shutter set at 16 breaks per second.

References

Miskotte Koen (2020). "Four decades of visual work: a lifetime of visual meteor observations". *eMetN*, **5**, 161–177.

Betlem H. (2020). "De superbolide van 2 maart 2020 en mogelijke meteorietval". *Radiant*, **42**, 27–32.

April-Lyrids and eta-Aquariids 2020 Radio meteor observation report in the world

Hiroshi Ogawa

h-ogawa@amro-net.jp

The meteor activity of the April-Lyrids and the eta-Aquariids were observed by radio meteor observers worldwide. The April-Lyrids showed a peak time later than in previous years. The eta-Aquariids displayed the same usual activity level as in previous years.

1 Introduction

Radio Meteor Observations in the world covered the meteor shower activity of the April-Lyrids and the eta-Aquariids 2020. Worldwide radio meteor observation data were provided by Radio Meteor Observation (RMOB) (Steyaert, 1993) and by the radio meteor observations network in Japan (Ogawa et al., 2001).

2 Method

For analyzing worldwide radio meteor observation data, meteor activities are calculated by the "Activity Level" index (Ogawa et al., 2001). The activity profile was estimated by the Lorentz activity profile (Jenniskens, 2000).

3 Results

April-Lyrids

Figure 1 shows the result for the April-Lyrids with 37 observations in 14 countries. The activity peak was estimated to occur around 12^{h} UT on 22nd of April (Solar Longitude $\lambda_{\odot}$ = 32.5°). Distinct activity was seen from 12^{h} on 21st to 12^{h} 23rd UT. The time of the maximum peak occurred later than in previous years. The long-term activity profile for the April-Lyrids for 2007–2020 is shown in

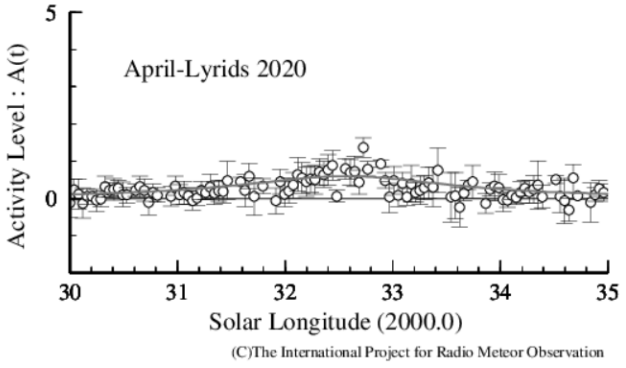

Figure 1 – April-Lyrids 2020 using worldwide radio meteor observations.

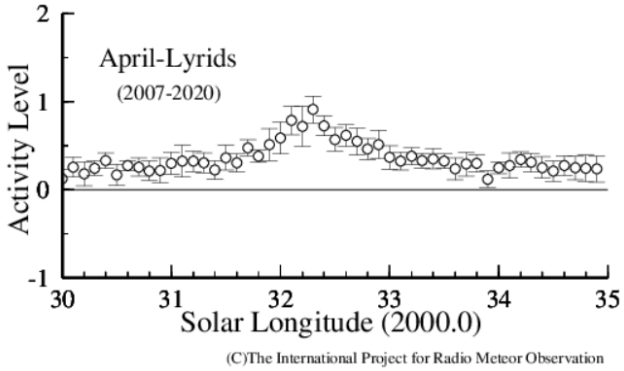

Figure 2 – The long-term activity profile of the April-Lyrids covering the period 2007–2020.

Figure 2. The peak in the long-term activity is at Solar Longitude $\lambda_{\odot}$ = 32.2° with full width half maximum (FWHM) –0.4° / +0.6°. The maximum activity level was 0.6. This is the same as in the long-term activity level.

More April-Lyrids results and information are provided on the website[15].

Eta Aquariids

One of the major meteor showers, the eta-Aquariids displayed the same activity level compared with previous years. The peak time was estimated to have occurred around 20^{h} UT, 5th May (Solar Longitude $\lambda_{\odot}$ = 45.52°) with a maximum activity level = 1.1 in 2020. Ogawa and Steyaert (2017) provided the annual activity profiles, peak solar longitude $\lambda_{\odot}$ = 45.1° with FWHM = –1.7° / +4.7°. The maximum activity level was 1.0.

Figure 3 provides two graphs, the 2020 result compared with the long-term previous years. The red line in the graph represents the long-term activity covering the period 2004–2019.

More eta-Aquariids results and information are provided on website[16].

[15] http://www.amro-net.jp/meteor-results/04_lyrids.htm

[16] http://www.amro-net.jp/meteor-results/05_aqreta.htm

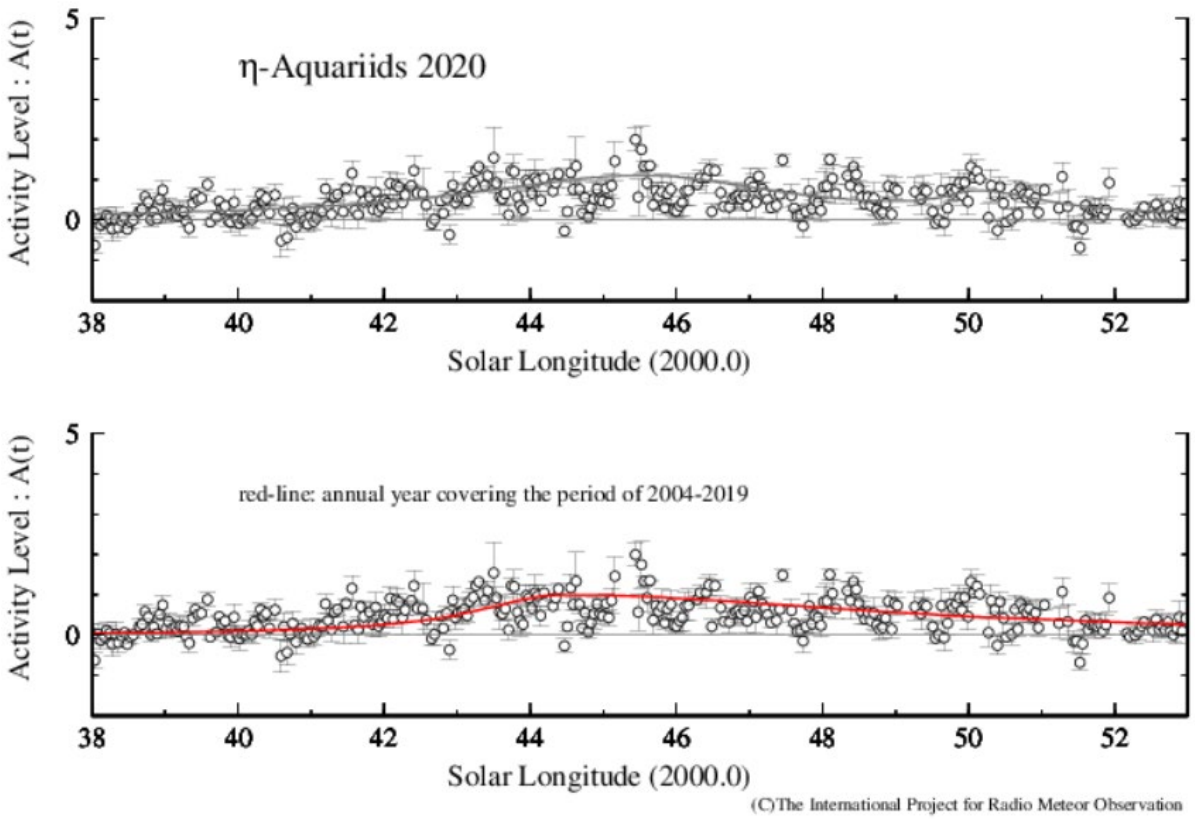

Figure 3 – eta-Aquariids 2020 compared with the long-term activity profile.

Acknowledgment

The April Lyrids and eta-Aquariids data were provided by the following observers:

Philip Norton (UK), *Phil Rourke* (UK), Felix Verbelen (Belgium), *test josephco_@_Graves* (Belgium), *Chris Steyaert* (Belgium), *Jochen Richert_1* (Switzerland), *Associazione Pontina di Astronomia* _APA (Italy), *Mario Bombardini* (Italy), *Oss_Monte_San_Lorenzo DLF* (Italy), *GAML Osservatorio_Astronomico_Gorga* (Italy), *Fabio Moschini_IN3GOO* (Italy), *AAV Planetario_di_Venezia* (Italy), *Per DL0SHF* (Germany), *Fred Espey* (Germany), *WHS Essen* (Germany), *Jean Marie F5CMQ* (France), *DanielD SAT01_DD* (France), *Jacques Molne* (France), *Kees Meteor* (Netherlands), *La Salle Radio_Club* (Spain), *Roman S58P* (Slovenia), *Stan Nelson* (USA), *Eric Smestad_KC0RDD* (USA), *ARS KF3BH_FN11ta* (USA), *Mike Otte* (USA), *Bob Mobile_K1SIX* (USA), *Salvador Aguirre* (Mexico), *Andrew Klekociuk* (Australia), *Halei Test* (China), *Kenji Fujito* (Japan), *M.Tsuboi* (Japan), *Hirofumi Sugimoto* (Japan), *Hirotaka Otsuka* (Japan), *Kazuyoshi Kanatsu* (Japan).

Worldwide data were provided by Radio Meteor Observation Bulletin (RMOB)[17].

References

Jenniskens P., Crawford C., Butow S. J., Nugent D., Koop M., Holman D., Houston J., Jobse K., Kronk G., and Beatty K. (2000). "Lorentz shaped comet dust trail cross section from new hybrid visual and video meteor counting technique imprications for future Leonid storm encounters". *Earth, Moon and Planets*, **82–83**, 191–208.

Ogawa H., Toyomasu S., Ohnishi K., and Maegawa K. (2001). "The Global Monitor of Meteor Streams by Radio Meteor Observation all over the world". In, Warmbein, Barbara, editor, *Proceeding of the Meteoroids 2001 Conference*, 6–10 August 2001, Swedish Institute of Space Physics, Kiruna, Sweden. ESA Publications Division, European Space Agency, Noordwijk, The Netherlands, pages 189–191.

Ogawa H., Steyaert C. (2017). "Major and Daytime Meteor Showers using Global Radio Meteor Observations covering the period 2001-2016". *WGN, Journal of the IMO*, **45**, 98–106.

[17] http://www.rmob.org/

Radio meteors April 2020

Felix Verbelen

Vereniging voor Sterrenkunde & Volkssterrenwacht MIRA, Grimbergen, Belgium
felix.verbelen@skynet.be

An overview of the radio observations during April 2020 is given.

1 Introduction

The graphs show both the daily totals (*Figure 1 and 2*) and the hourly numbers (*Figure 3 and 4*) of "all" reflections counted automatically, and of manually counted "overdense" reflections, overdense reflections longer than 10 seconds and longer than 1 minute, as observed here at Kampenhout (BE) on the frequency of our VVS-beacon (49.99 MHz) during the month of April 2020.

The hourly numbers, for echoes shorter than 1 minute, are weighted averages derived from:

$$N(h) = \frac{n(h-1)}{4} + \frac{n(h)}{2} + \frac{n(h+1)}{4}$$

Due to technical problems at our beacon, the observations were interrupted from 02.04.2020 at 18^h45^m UT to 08.04.2020 at 09^h33^m UT, so that the daily totals from 02 to 08 April 2020 are missing. This month there was quite some local interference and unidentified noise, and also lightning activity on three days (April 17th, 28th and 30th). No registered "sporadic E" (Es). Most unwanted signals were corrected manually in the automatic counts.

As expected, the general shower activity remained low up to 20 April, with only a brief increase on 15 April, possibly due to the phi Serpentids. As expected, the annual Lyrids were the highlight of the month. They reached their maximum here on 22 April between 04^h and 05^h UT, but between 02^h UT and 09^h UT there was increased activity. Apart from the Lyrids, between 20 April and the end of the month, there were several minor meteor showers with mostly weaker reflections (underdenses and shorter overdenses) that need further investigation.

During this month, 7 reflections longer than 1 minute were recorded, but some more may have been lost during the period the beacon was out of order. Also included are a few SpecLab recordings of interesting reflections during this month. Attached are also a few examples of the strongest reflections (*Figures 5, 6, 7, 8, 9, 10, 11 and 12*).

If you are interested in the actual figures, please send me an e-mail: felix.verbelen at skynet.be.

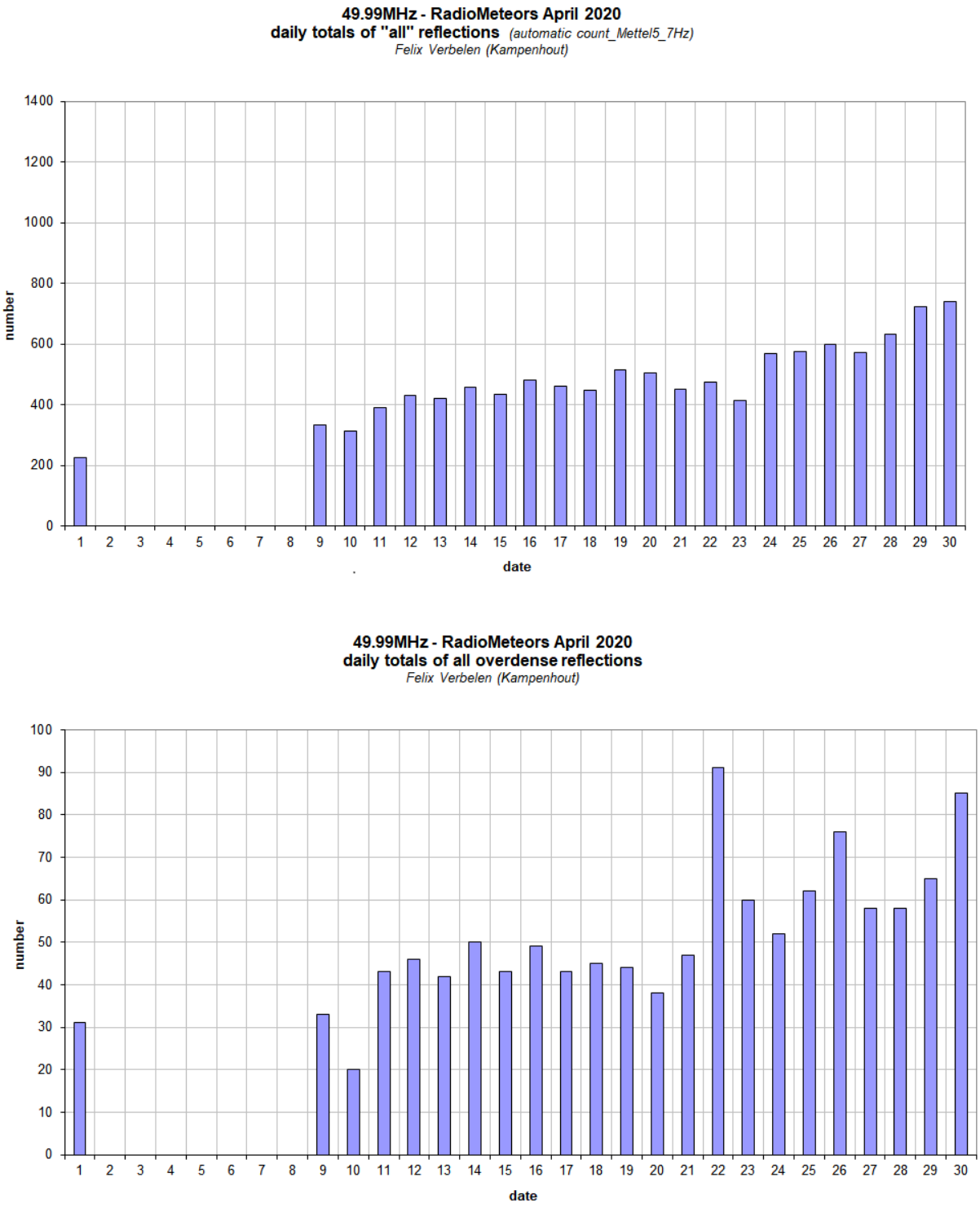

Figure 1 – The daily totals of "all" reflections counted automatically, and of manually counted "overdense" reflections, as observed here at Kampenhout (BE) on the frequency of our VVS-beacon (49.99 MHz) during April 2020.

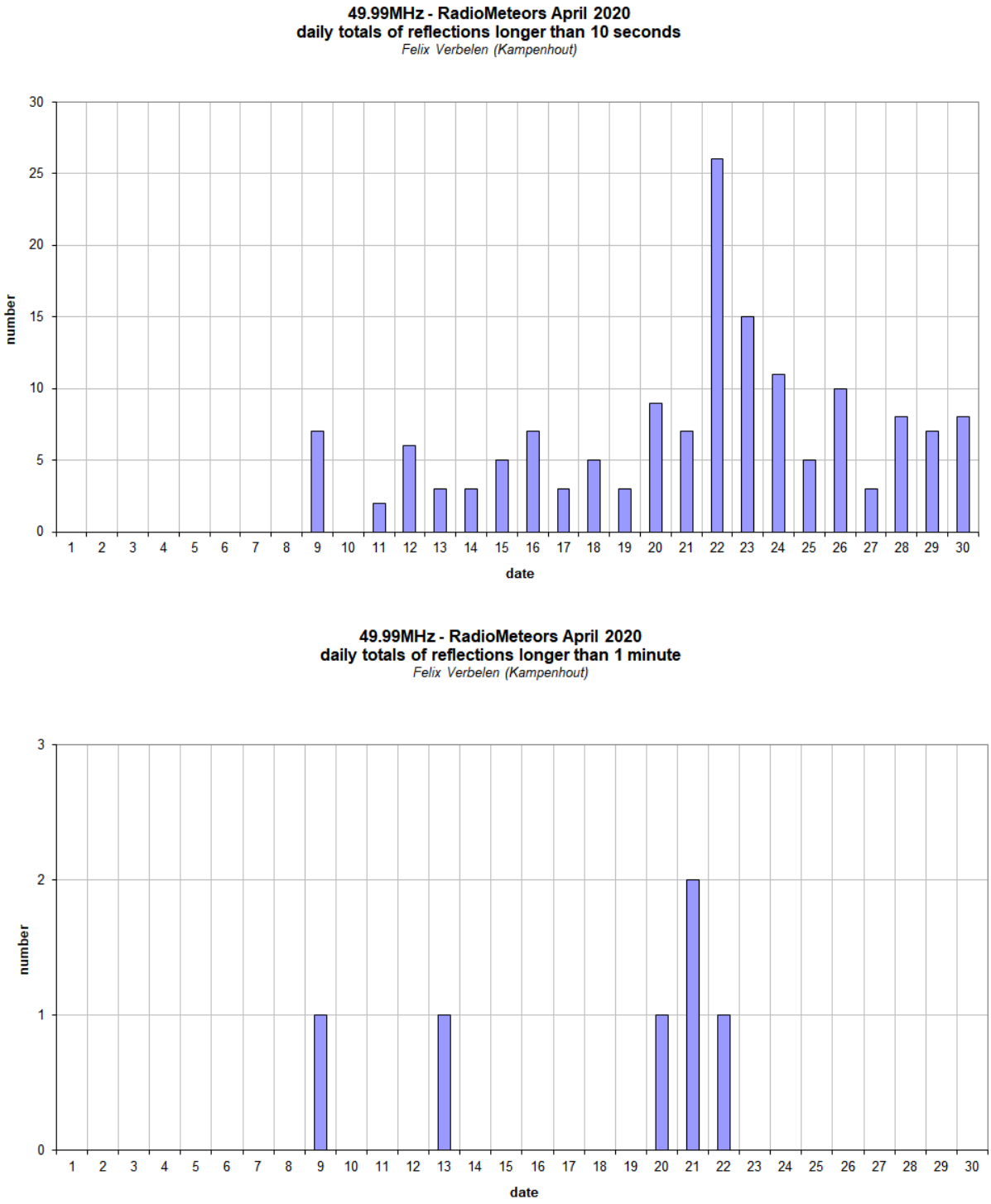

Figure 2 – The daily totals of overdense reflections longer than 10 seconds and longer than 1 minute, as observed here at Kampenhout (BE) on the frequency of our VVS-beacon (49.99 MHz) during April 2020.

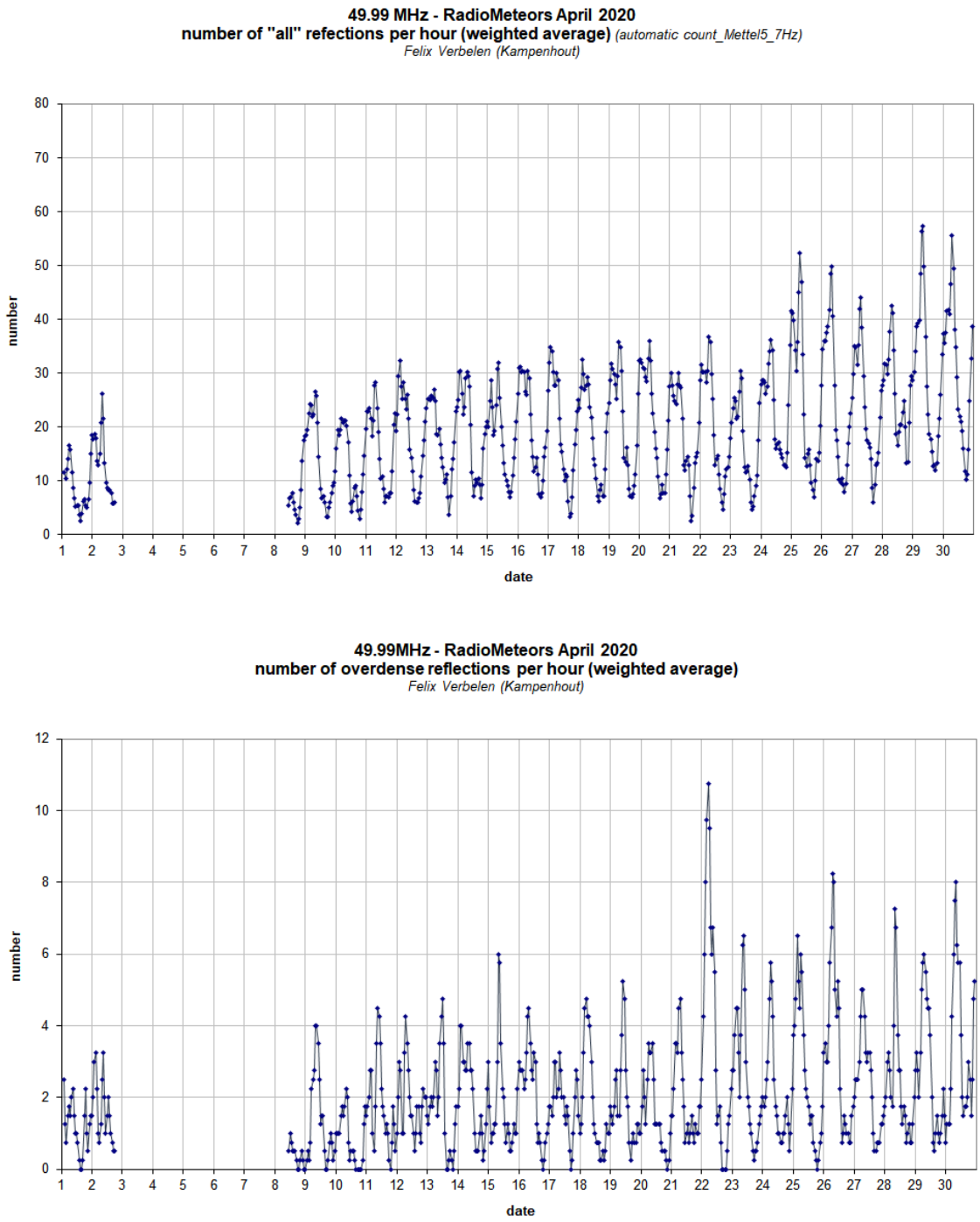

Figure 3 – The hourly numbers of "all" reflections counted automatically, and of manually counted "overdense" reflections, as observed here at Kampenhout (BE) on the frequency of our VVS-beacon (49.99 MHz) during April 2020.

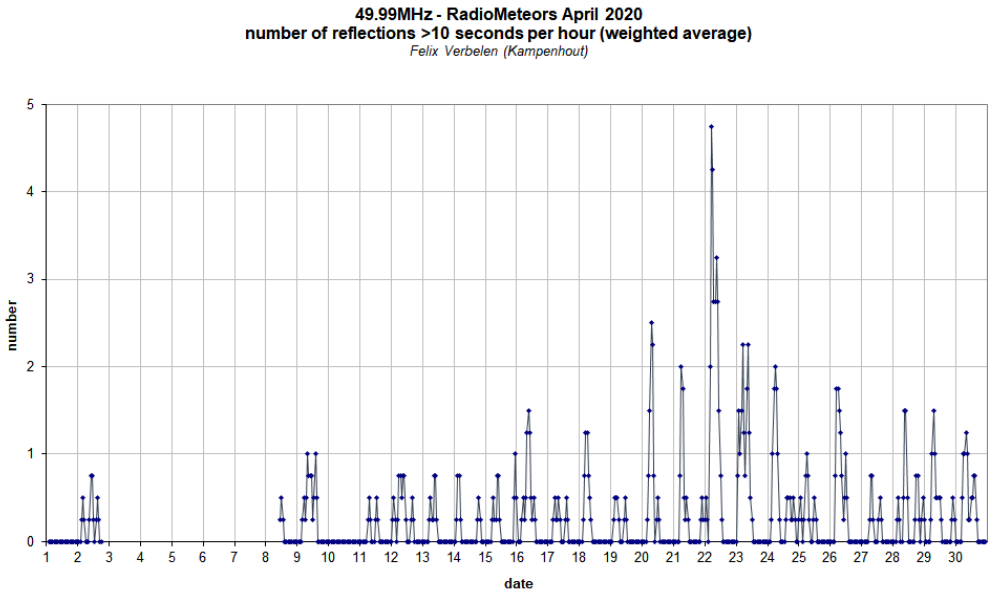

Figure 4 – The hourly numbers of overdense reflections longer than 10 seconds and longer than 1 minute, as observed here at Kampenhout (BE) on the frequency of our VVS-beacon (49.99 MHz) during April 2020.

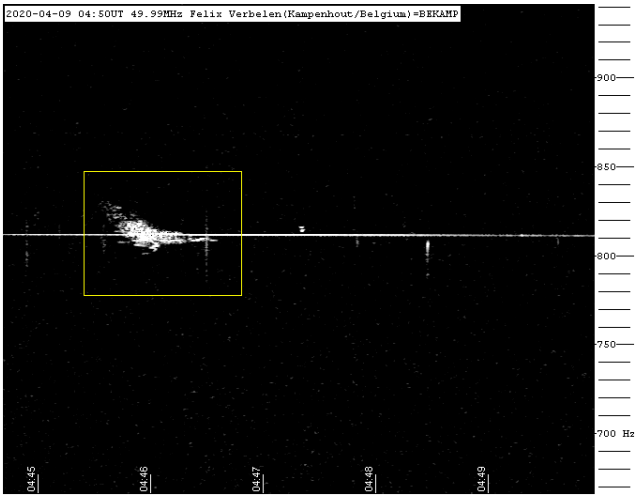

Figure 5 – 2020 April 9 at 4^h50^m UT.

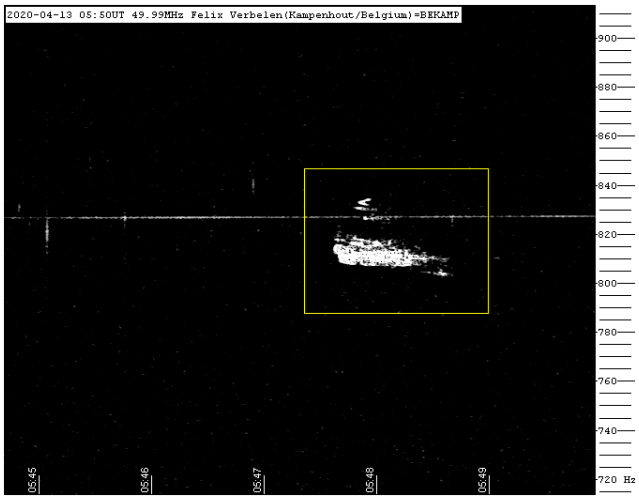

Figure 6 – 2020 April 13 at 5^h50^m UT.

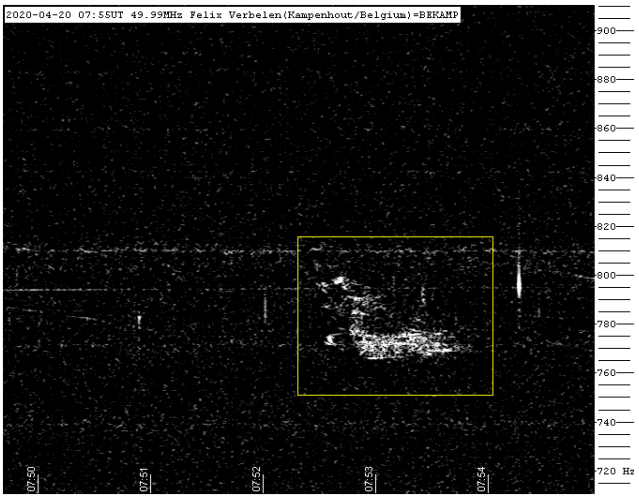

Figure 7 – 2020 April 20 at 7^h55^m UT.

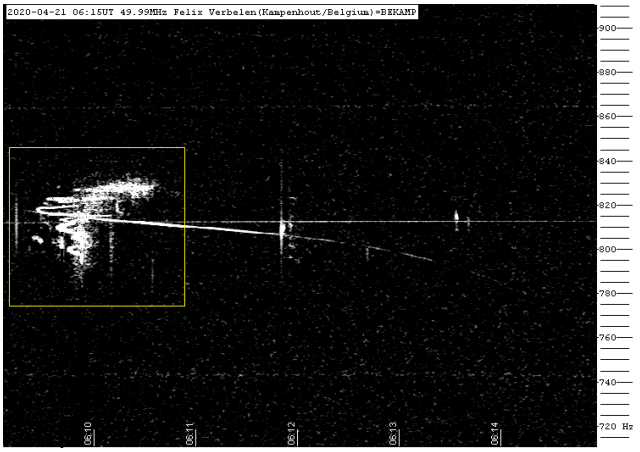

Figure 8 – 2020 April 21 at 6^h15^m UT.

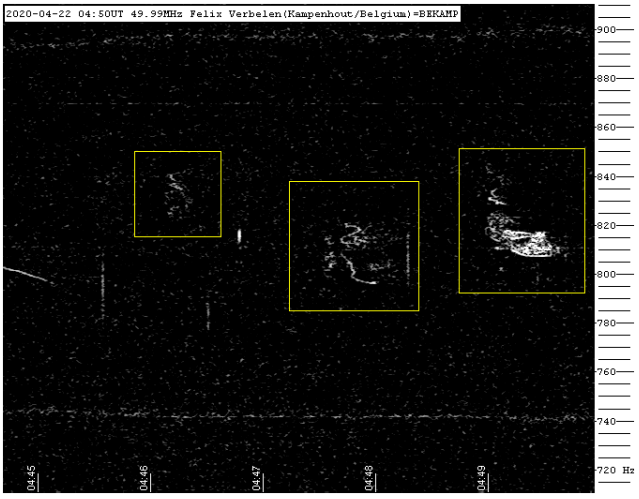

Figure 9 – 2020 April 22 at 4^h50^m UT.

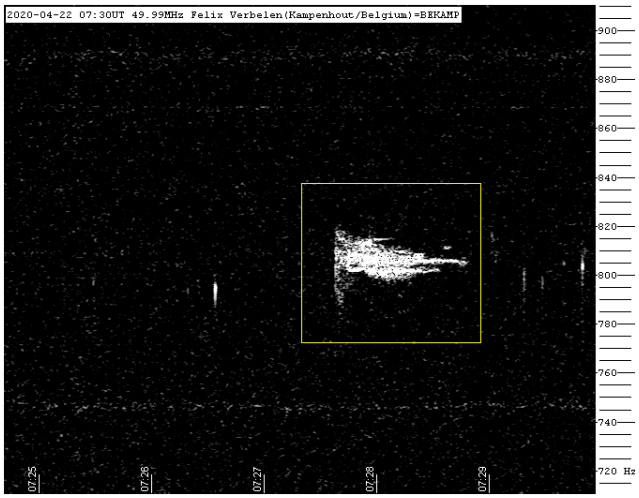

Figure 10 – 2020 April 22 at 7^h30^m UT.

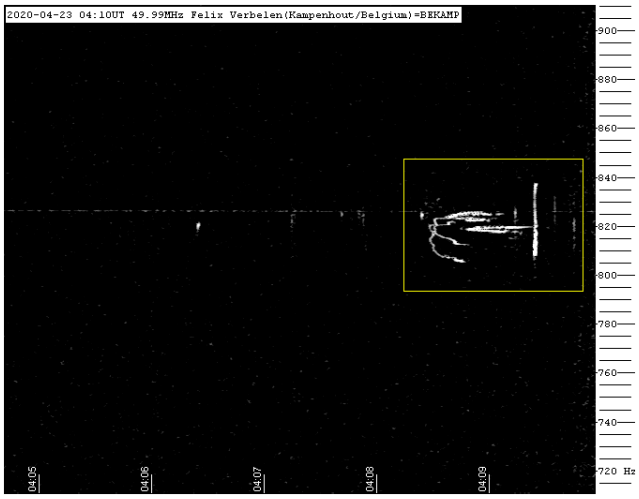

Figure 11 – 2020 April 23 at 4^h10^m UT.

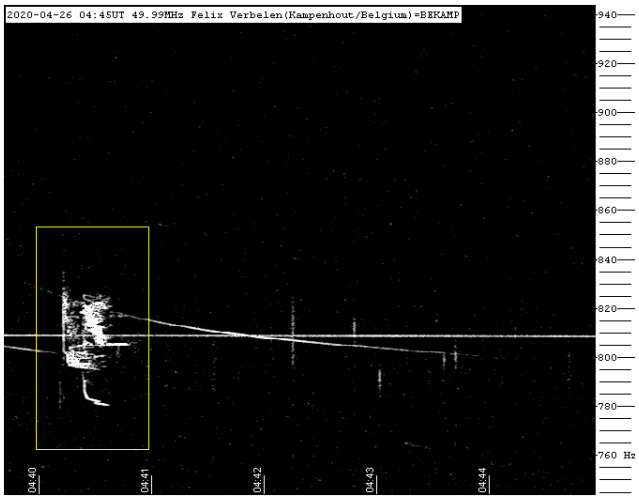

Figure 12 – 2020 April 26 at 4^h45^m UT.

Radio meteors May 2020

Felix Verbelen

Vereniging voor Sterrenkunde & Volkssterrenwacht MIRA, Grimbergen, Belgium
felix.verbelen@skynet.be

An overview of the radio observations during May 2020 is given.

1 Introduction

The graphs show both the daily totals (*Figure 1 and 2*) and the hourly numbers (*Figure 3 and 4*) of "all" reflections counted automatically, and of manually counted "overdense" reflections, overdense reflections longer than 10 seconds and longer than 1 minute, as observed here at Kampenhout (BE) on the frequency of our VVS-beacon (49.99 MHz) during the month of May 2020.

The hourly numbers, for echoes shorter than 1 minute, are weighted averages derived from:

$$N(h) = \frac{n(h-1)}{4} + \frac{n(h)}{2} + \frac{n(h+1)}{4}$$

The observations were sometimes complicated by (mainly) local interference, unidentified noise or by moderate lightning activity (on 3 different days), but the automatic counts were corrected manually in order to minimize the effects of the disturbances.

The eye-catchers of the month were, as expected, the eta-Aquariids, which apparently already reached their maximum on May 4th, but remained rather moderate overall.

During the rest of the month, there was markedly increased activity compared to previous months, with several minor showers showing higher numbers of reflections longer than 10 seconds.

Also included is a selection of SpecLab screen captures of some interesting or long meteor reflections during this month. Some of these illustrate the fact that strong or extended reflections are often accompanied by a number of underdense reflections. (*Figures 3, 4, 5, 6, 7, 8, 9, 10, 11, 12, 13, 14, 15, 16, 17 and 18*).

If you are interested in the actual figures, please send me an e-mail: felix.verbelen at skynet.be.

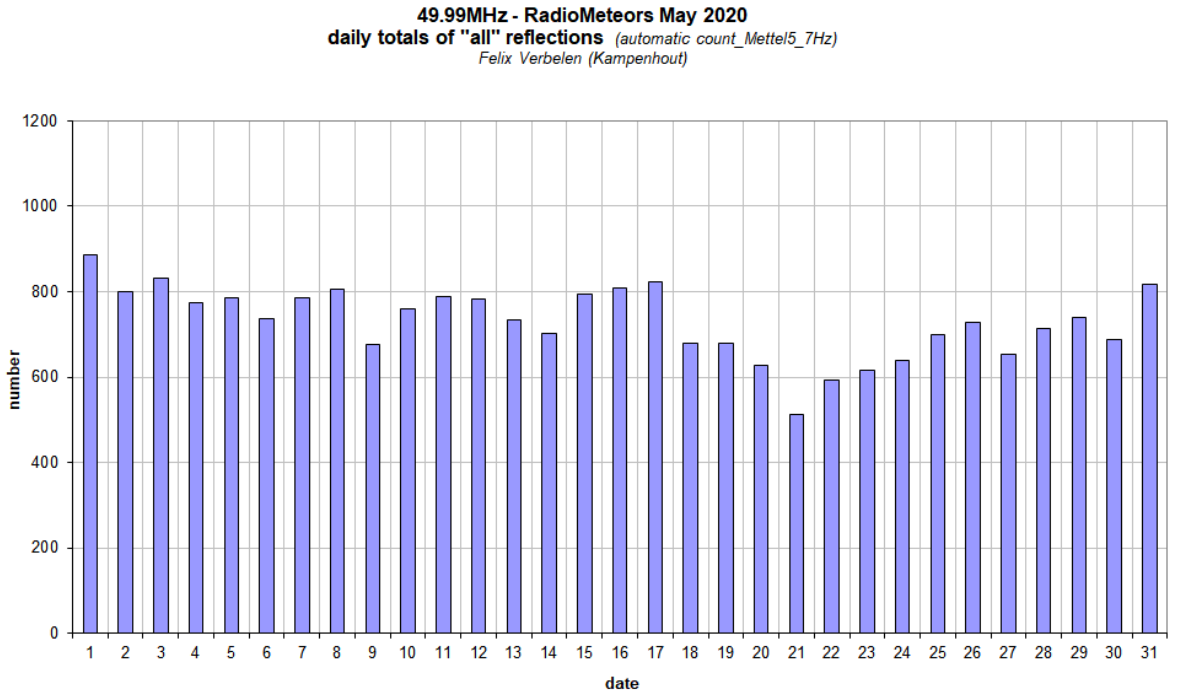

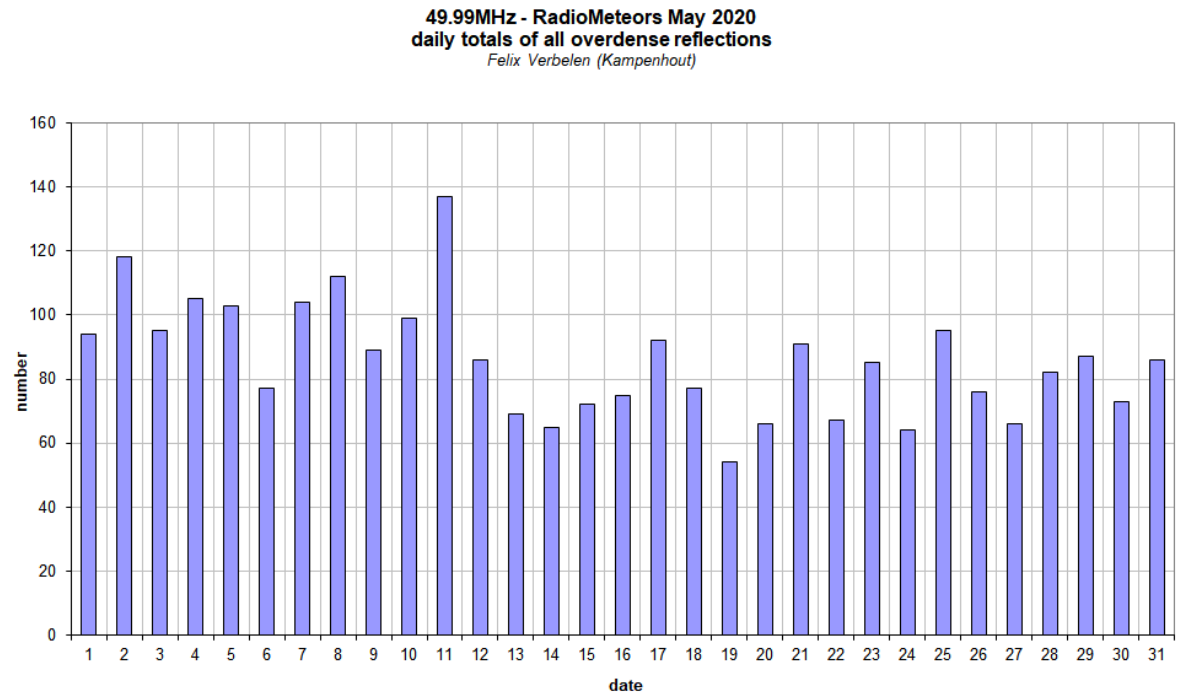

Figure 1 – The daily totals of "all" reflections counted automatically, and of manually counted "overdense" reflections, as observed here at Kampenhout (BE) on the frequency of our VVS-beacon (49.99 MHz) during May 2020.

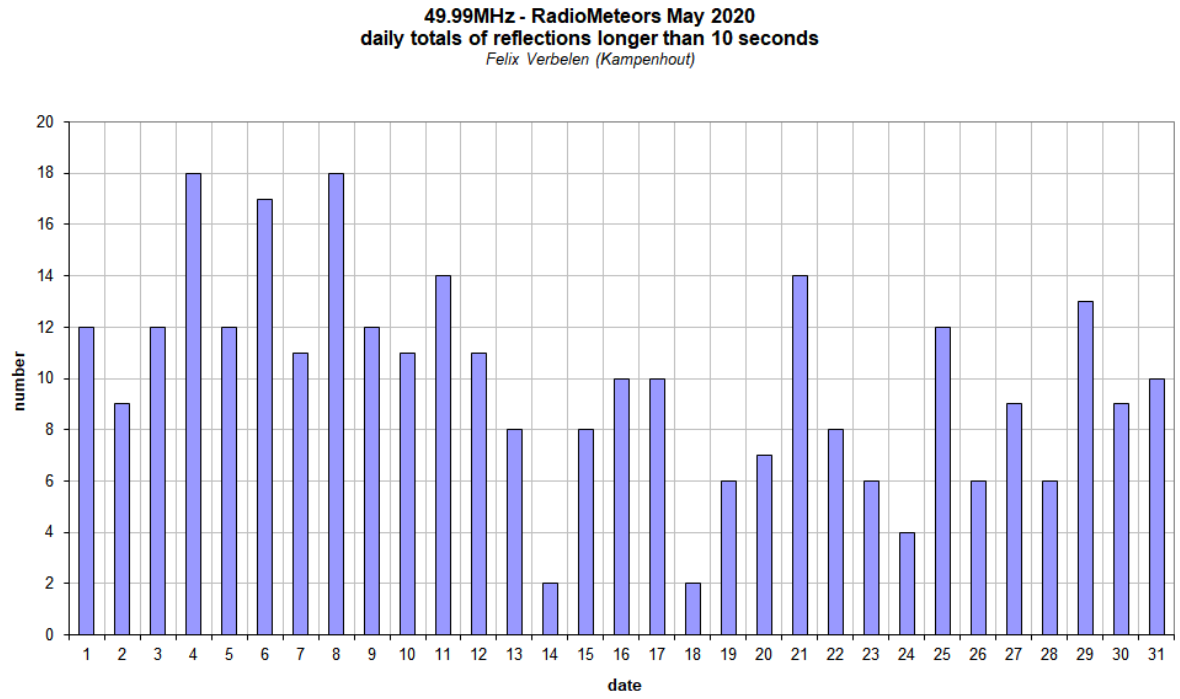

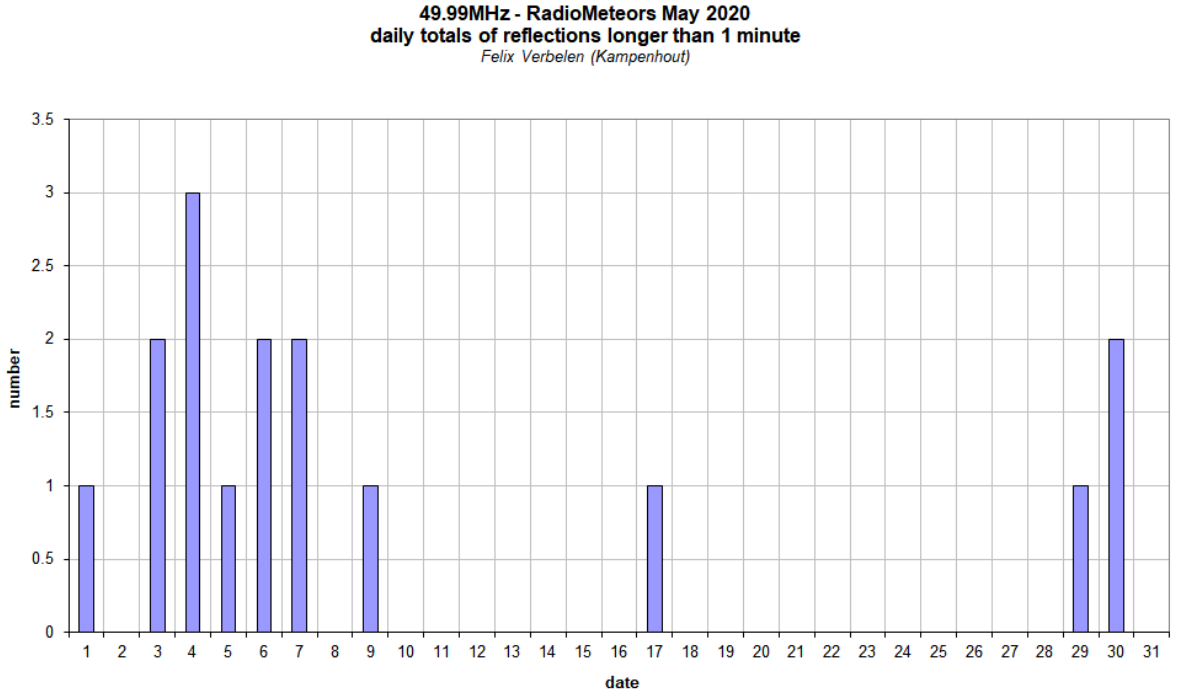

Figure 2 – The daily totals of overdense reflections longer than 10 seconds and longer than 1 minute, as observed here at Kampenhout (BE) on the frequency of our VVS-beacon (49.99 MHz) during May 2020.

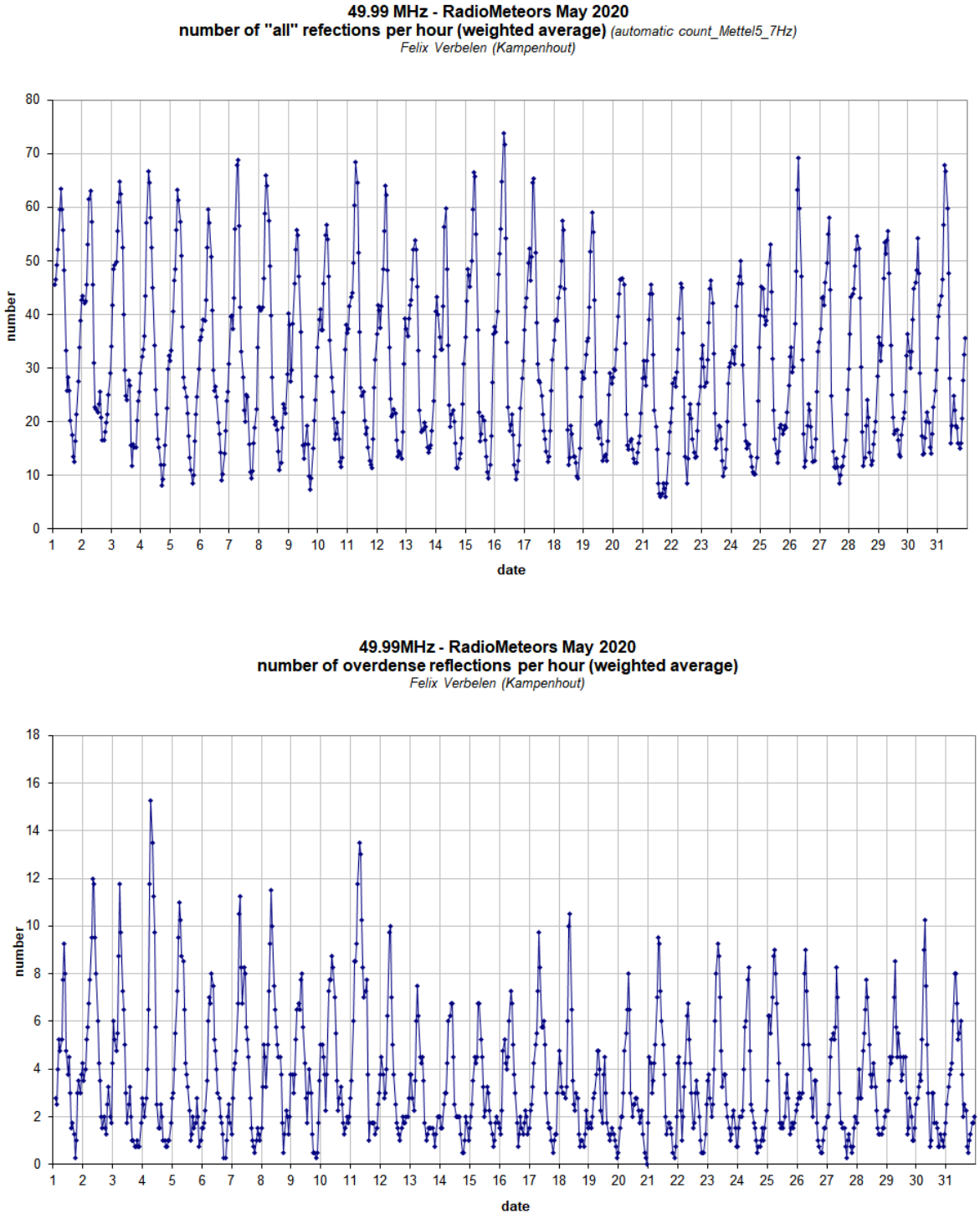

Figure 3 – The hourly numbers of "all" reflections counted automatically, and of manually counted "overdense" reflections, as observed here at Kampenhout (BE) on the frequency of our VVS-beacon (49.99 MHz) during May 2020.

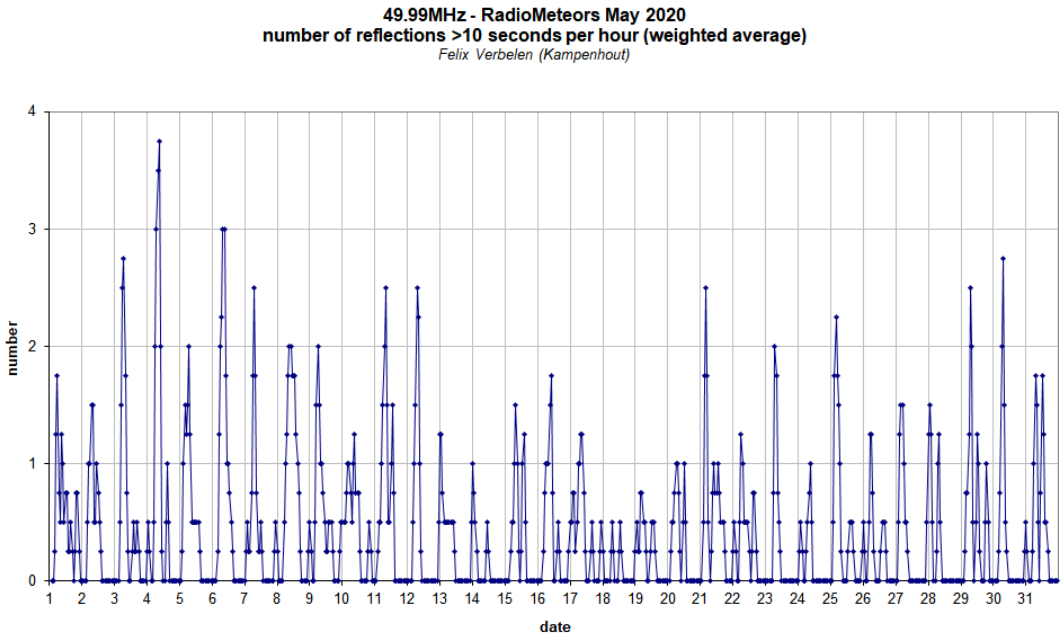

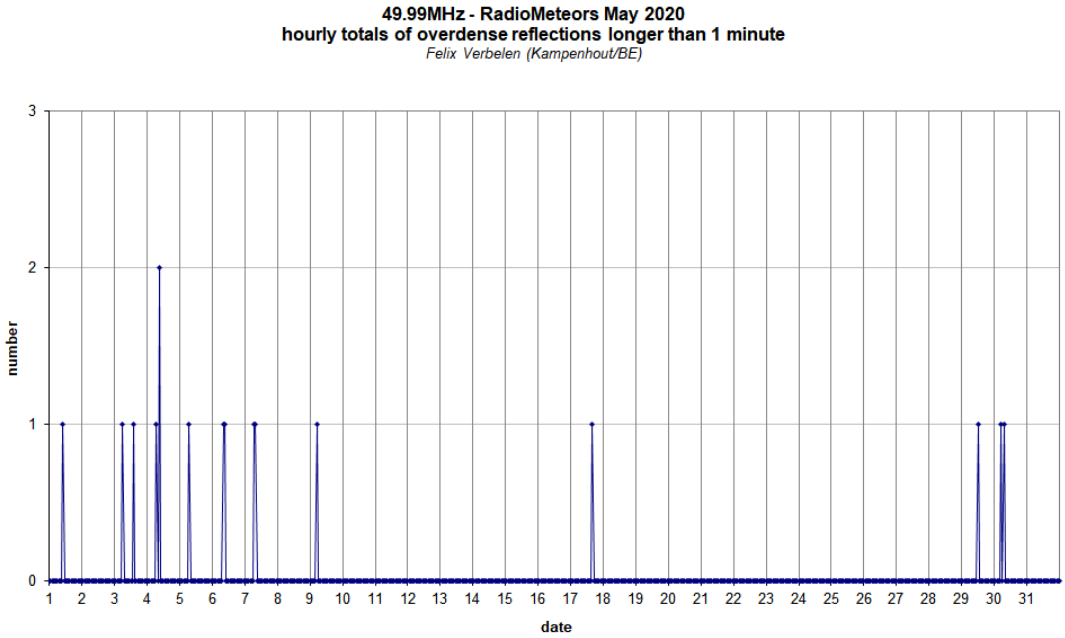

Figure 4 – The hourly numbers of overdense reflections longer than 10 seconds and longer than 1 minute, as observed here at Kampenhout (BE) on the frequency of our VVS-beacon (49.99 MHz) during April 2020

.

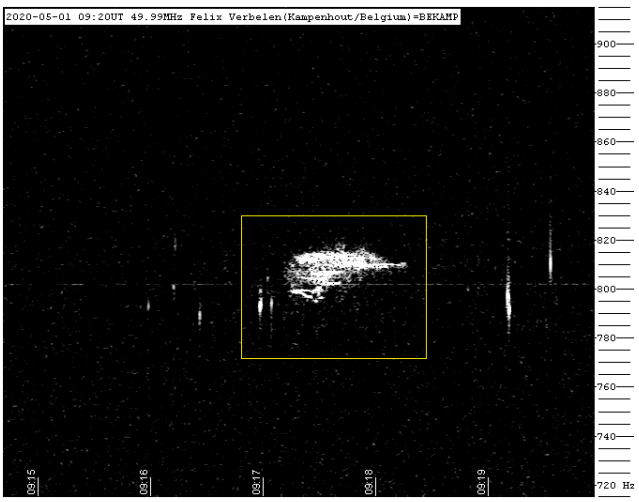

Figure 5 – 2020 May 1 at 9^h20^m UT.

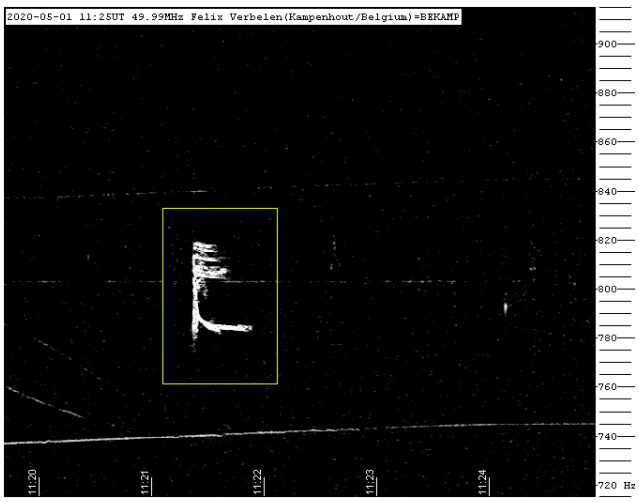

Figure 6 – 2020 May 1 at 11^h25^m UT.

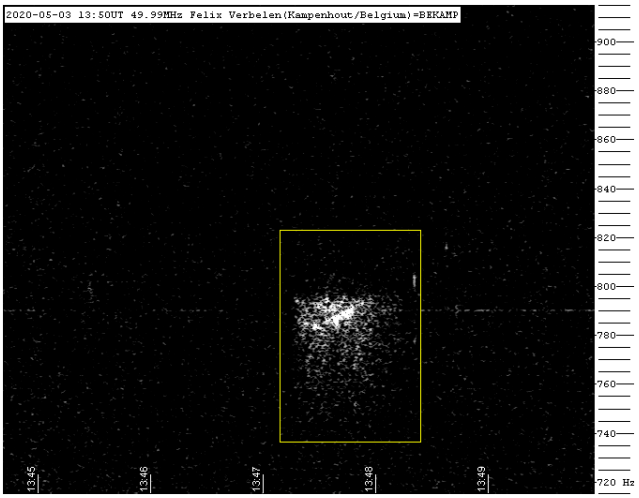

Figure 7 – 2020 May 3 at 13^{h}50^{m} UT.

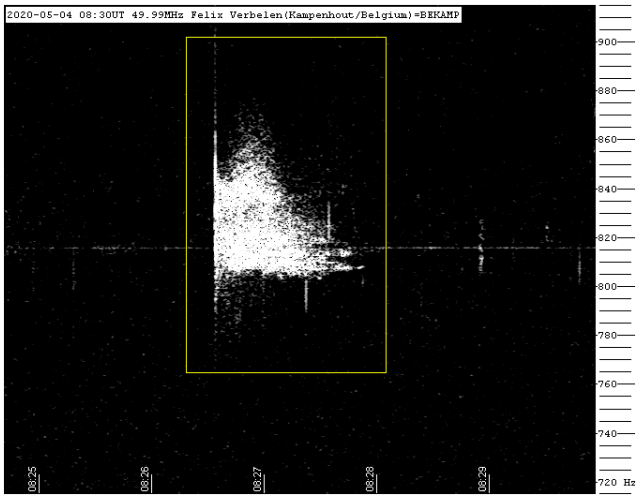

Figure 10 – 2020 May 4 at 08^{h}30^{m} UT.

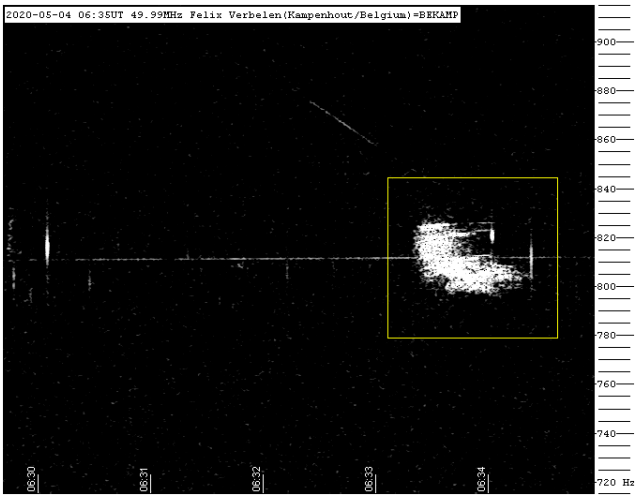

Figure 8 – 2020 May 4 at 6^{h}35^{m} UT.

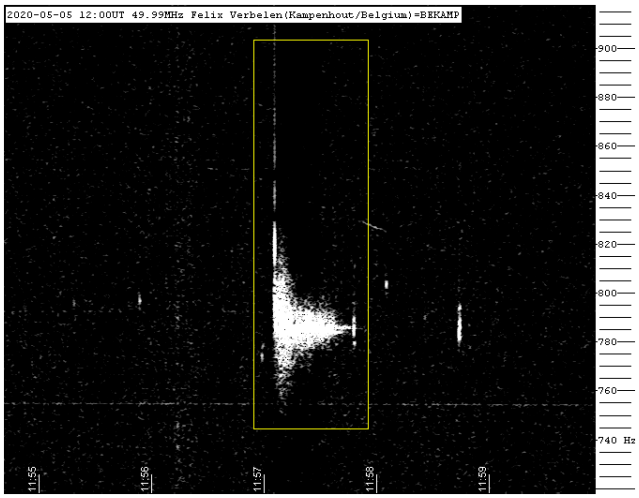

Figure 11 – 2020 May 5 at 12^{h}00^{m} UT.

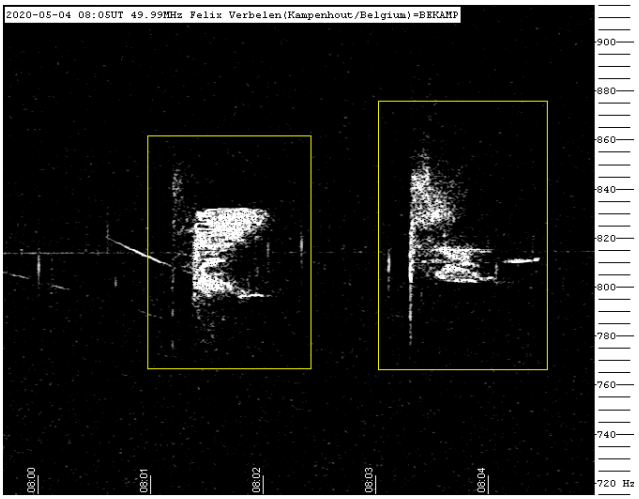

Figure 9 – 2020 May 4 at 08^{h}05^{m} UT.

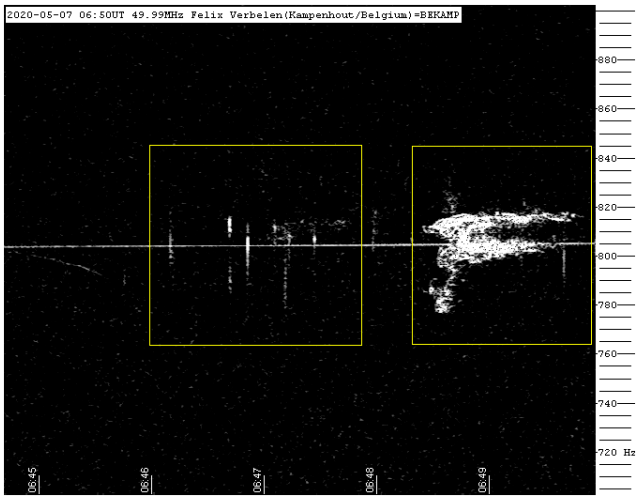

Figure 12 – 2020 May 7 at 6^{h}50^{m} UT.

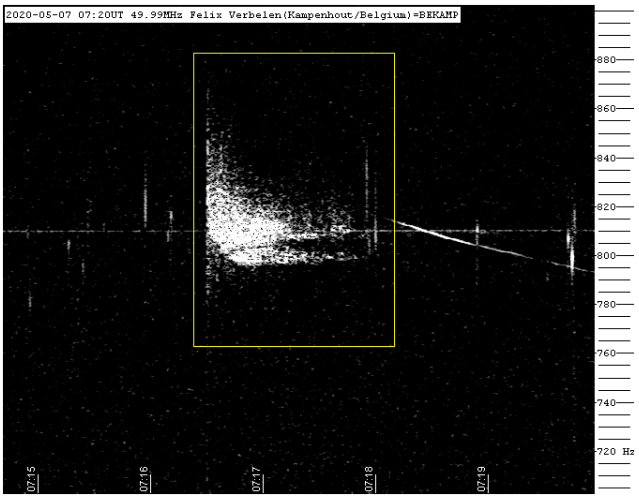

Figure 13 – 2020 May 7 at 7^h20^m UT.

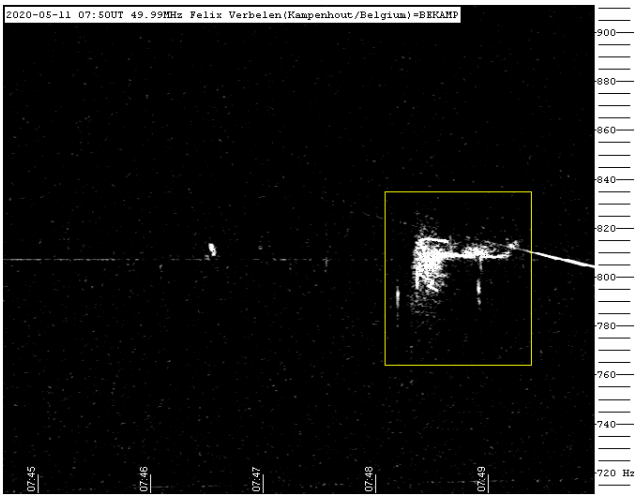

Figure 14 – 2020 May 11 at 7^h50^m UT.

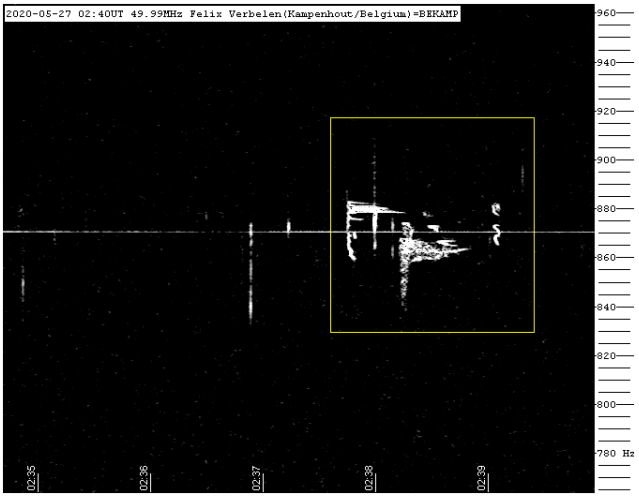

Figure 15 – 2020 May 27 at 2^h40^m UT.

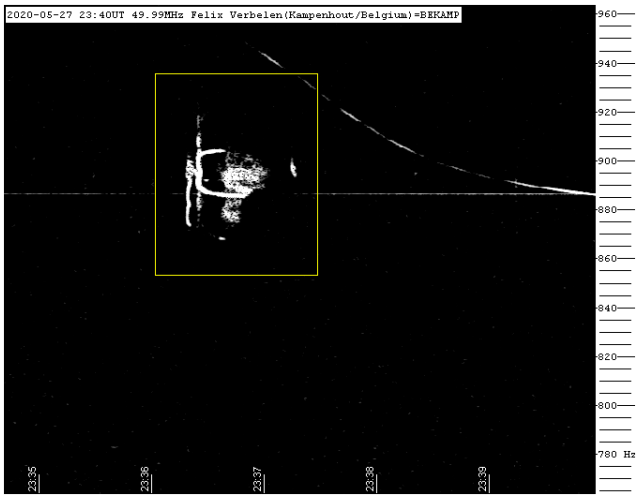

Figure 16 – 2020 May 27 at 23^h40^m UT.

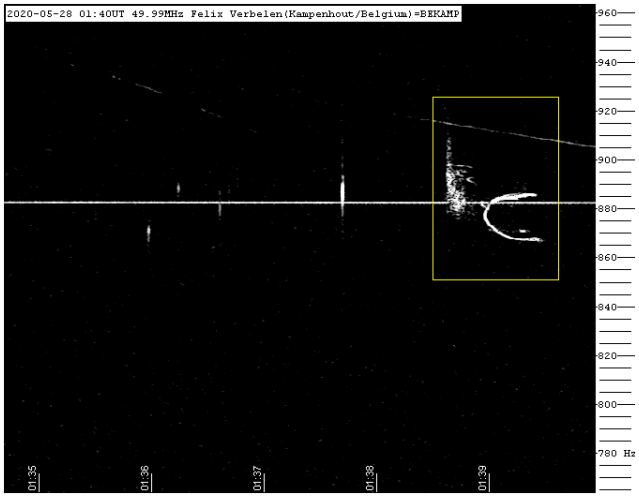

Figure 17 – 2020 May 28 at 01^h40^m UT.

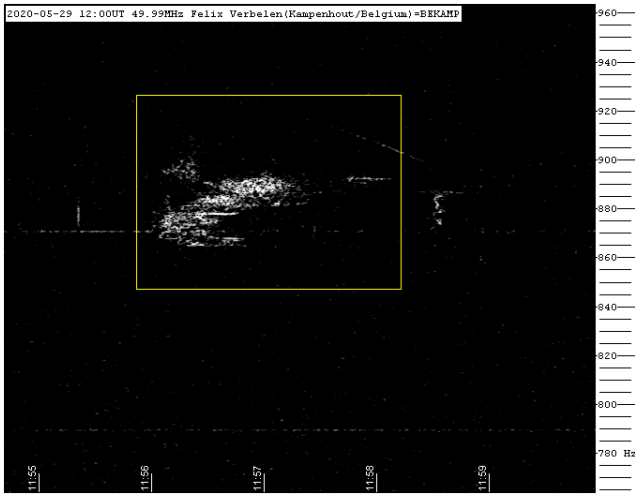

Figure 18 – 2020 May 29 at 12^h00^m UT.

A bright fireball over the state of Rio Grande do Sul

M. Zurita[1,2], R. Damiglê[1,3], J. Agustoni[1], C. Di Pietro[1], M. Domingues[1,4], L. Trindade[1], J. de Souza[1], A. Lima[1], G. Gonçalves[1,5], D. C. Mourão[1,6] and A. S. Betzler[1,7]

[1] **Brazilian Meteor Observation Network (BRAMON)**
agustoni@yahoo.com, carlos.pbella@gmail.com, lauristontrindade@yahoo.com.br, jocimarjustino@hotmail.com, arrowgreenflash@gmail.com

[2] **Associação Paraibana de Astronomia (APA)**
marcelozurita@gmail.com

[3] **Universidade Estadual do Ceará (UECE)**
rubens.damigle@aluno.uece.br

[4] **Clube de Astronomia de Brasília (CAsB)**
marcelo@casb.com.br

[5] **Instituto de Química/Universidade de São Paulo (IQ/USP)**
g_goncalves_silva@hotmail.com

[6] **Departamento de Matemática/Universidade Estadual Paulista - Guaratinguetá (UNESP)**
daniela.mourao@unesp.br

[7] **Universidade Federal do Recôncavo da Bahia (UFRB)**
a_betzler@yahoo.com

On June, 7th, 2019, around 01h33m (UT), inhabitants from Brazil (mainly in the Southern Region states), Argentina, Paraguay and Uruguay observed a very bright fireball which was also recorded by two meteor monitoring stations of BRAMON. The fireball entered in the atmosphere with a velocity of 14.3 km/s at an altitude of 104 km over the south of Paraguay, travelling 393 km until reaching its dark flight at an altitude of 27.4 km over the state of Rio Grande do Sul. The calculated energy corresponds to an entry mass between 3.25×10^3 kg and 5.75×10^3 kg (this corresponds to a meteoroid with a diameter of 1.2 m to 1.4 m). It is believed that about 10% of the original mass reached the ground. The shallow trajectory created a large meteorite strewn field that could extend from the cities of Jari to Santa Maria (Rio Grande do Sul, Brazil). Teams conducted a meteorite search in the area, with no success so far.

1 Introduction

Some countries, like Morocco, have developed recently a culture of meteorite trade, making people more aware of bright meteors (Ibhi, 2014), allowing the recovery of 11 meteorite falls in the last 20 years. In the United States, a country with a much larger surface, the use of technology is a key factor that has helped the recovery of meteorite falls. In the last 20 years, at least 14 of the 19 falls were recorded by cameras, detected by radars or satellites. In Brazil, only two meteorites (Porangaba and Varre-Sai) of the six falls from the last 20 years were recorded (Meteoritical Bulletin Database, 2020)[18]. The Porangaba meteorite is the first, and so far, the only Brazilian meteorite with an estimated orbit and published orbital elements (Ferus et al., 2020).

BRAMON (Brazilian Meteor Observation Network) is a meteor monitoring network created to, among other goals,

Figure 1 – Meteor as seen from Monte Castelo (Santa Catarina state) JJS2 BRAMON station and Caxias do Sul (Rio Grande do Sul state) camera of the project Clima Ao Vivo.

[18] Meteoritical Bulletin Database, 2020, https://www.lpi.usra.edu/meteor/, May 9th, 2020.

monitor meteors and help to improve the detection of possible meteorite dropping events in Brazil (Amaral et al., 2018). In this case the atmospheric trajectory, heliocentric orbit and pre-atmospheric mass of the progenitor of the meteor seen from southern Brazil, northern Argentina, Paraguay and Uruguay (*Figure 1*) are evaluated and the mass of the meteorite fragments that could have reached the ground has been estimated.

2 Methods

Location and equipment

The trajectory was estimated using the UFOOrbit© software (SonotaCo, 2009), triangulating and comparing the duration of the event captured by a security camera in Porto Alegre and a camera of the project Clima Ao Vivo in Caxias do Sul, both in Rio Grande do Sul state, and two BRAMON monitoring stations (JJS2 and JJS3) in Monte Castelo and Santa Catarina state. The cameras had a CCD of similar sensibility curve, a quantum efficiency peak near 90% (around 650 nm) (Gural, 2014). The security and weather monitoring cameras had a cutoff for wavelengths exceeding 750 nm (removed in the BRAMON stations), the frame rate 30 / s, the luminous fluxes about 0.1 lx and a FOV of about 120 deg^2 (plate scale of hundreds of arcsec/pixel).

Analysis

In the absence of bright stars as references, the street lamps were used for photometric calibration. The light curve of the Caxias do Sul video was used as reference to synchronize each recording. The atmospheric trajectory and the heliocentric orbit were calculated using the right ascension and declination of the beginning and end of the meteor and its duration. The approximate azimuth and altitude of the cameras FOV centers were inferred by information provided by the owners (Zurita et al., 2019).

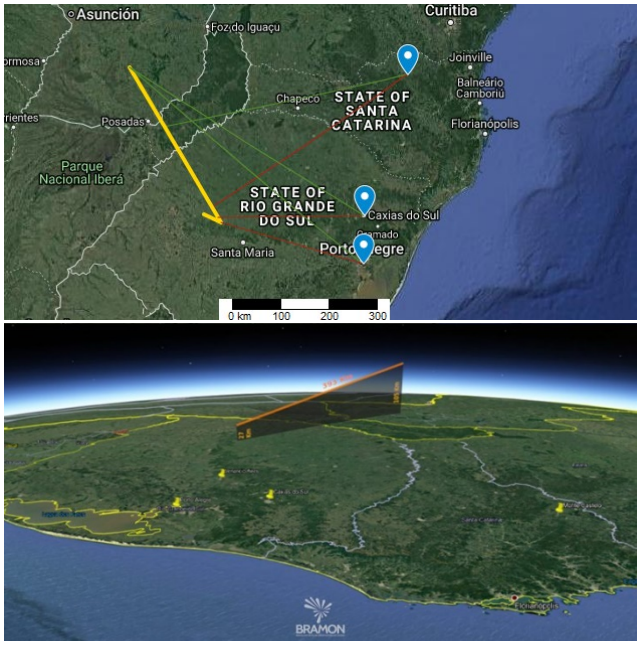

Figure 2 – Top: Position of each camera and the meteor trajectory. Bottom: Side view of the downward trajectory.

3 Results and discussion

Atmospheric trajectory, photometry and orbit

The meteor was very long and lasting and began at an altitude of 104 km over southern Paraguay (relative to sea level) with a geocentric velocity (v_g) of 14.3 km/s. For 27.5 seconds, it crossed 393 km through the atmosphere travelling to SSE and passing over parts of Argentina and the Northwest of the Rio Grande do Sul state, disappearing at 27.4 km altitude above the town of Jari (*Figure 2*). It reached a peak of absolute magnitude equal to –13, with a relative deviation of 20%. The light curve is shown in *Figure 3*. The orbital elements are shown in the *Table 1* (with a relative deviation of about 10%) and the orbit is shown in *Figure 4*. It was classified as a sporadic meteor and could be associated with the Atens near-Earth asteroids group.

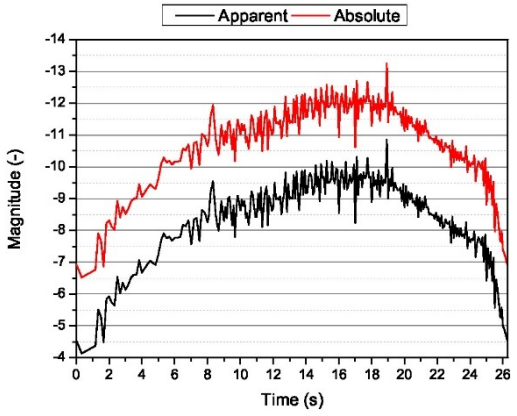

Figure 3 – The meteor light curve from Caxias do Sul (Rio Grande do Sul state) video.

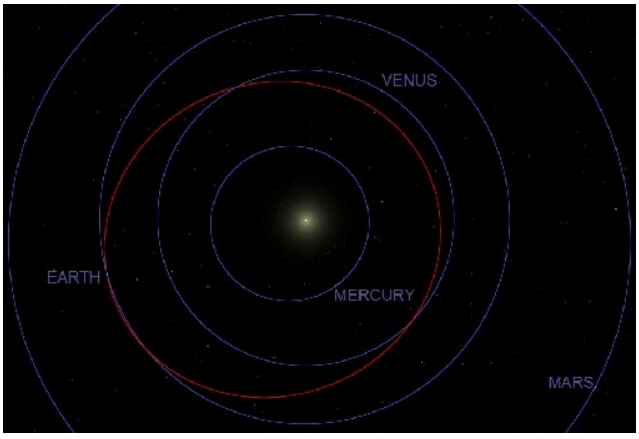

Figure 4 – Top view of the meteor orbit (red) relative to the Inner Solar System.

Pre- and post-atmospheric mass

The analysis of the luminous intensity indicates an initial mass between 3.25×10^3 and 5.75×10^3 kg (Ceplecha et al., 1996), with an uncertainty which is caused by the inaccuracy of the luminous flux in different recordings (Romig, 1965). Using the average density of an ordinary chondrite meteorite, 3.84 g/cm^3 (Britt and Consolmagno, 2003), the diameter of the meteoroid size was estimated

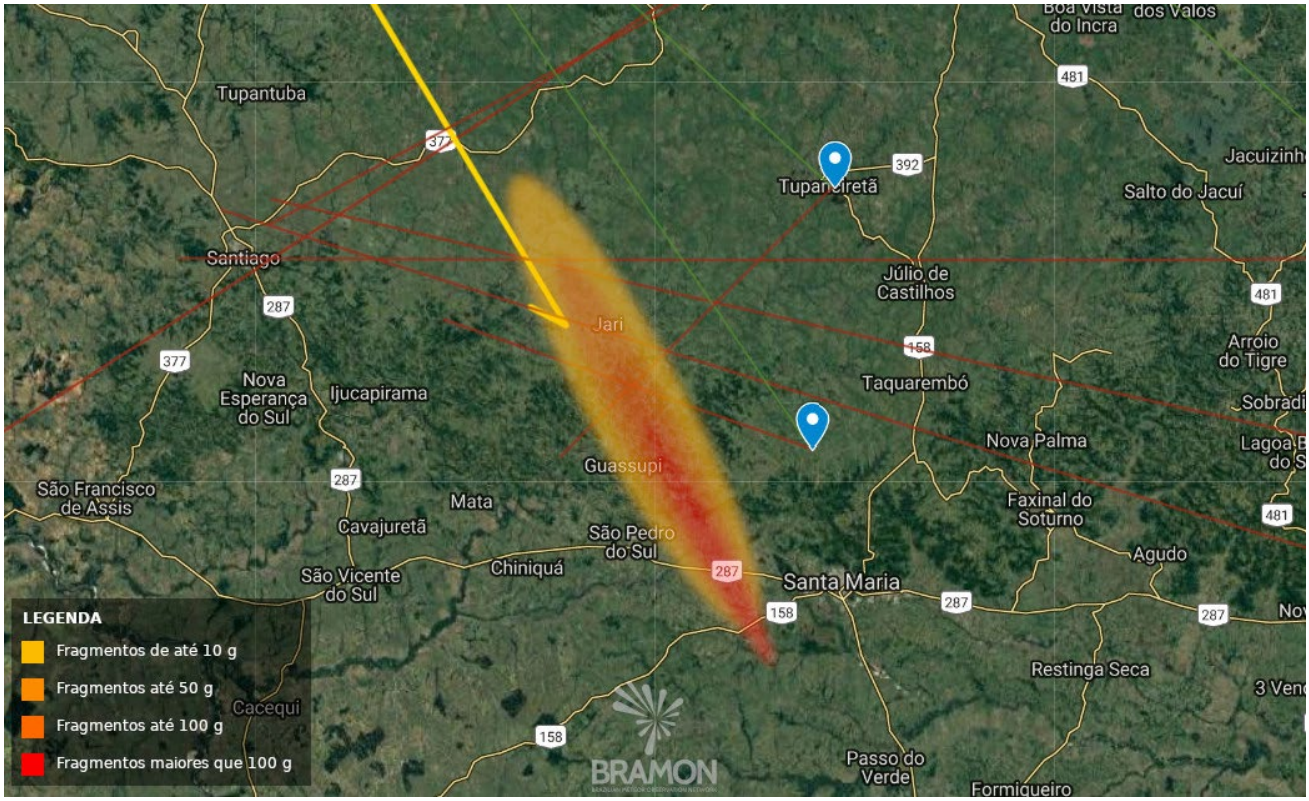

Figure 5 – Meteorite strewn field estimate.

between 1.2 m to 1.4 m. When applying the ablation model by Hawkins (1964), it seems that about 10% of the original mass reached the ground. The shallow trajectory and the low intensity of the winds over the area allowed the fragments to travel more than 50 km during the dark flight, creating a large strewn field (*Figure 5*) which could extend from the cities of Jari to Santa Maria (Rio Grande do Sul state). Teams went to the area and conducted searches, but no fragments were found so far. The area has plantations and cattle, making the search difficult.

Table 1 – Orbital elements of the fireball.

Elements	Value
a	0.817 AU
e	0.256 -
q	0.607848 AU
i	17.9°
Ω	255.8°
ω	194.2°
M	153°
P	0.738 years

4 Conclusions

The meteor travelled 393 km from south Paraguay towards mid-west Rio Grande do Sul with an entry velocity of 14.3 km/s. Its luminous trajectory began at 104 km with a peak in absolute magnitude of –13 until the fireball reached the dark flight at an elevation of 27.4 km. It had an entry mass over 3 metric tons (diameter over 1.2 m) and it is estimated that about 10% of the original mass fell between Jari and Santa Maria although no fragment was found until now.

Acknowledgements

The authors would like to thanks all the owners of the video recordings that kindly provided the videos used in this analysis (videos are available online[19]), all members of the BRAMON, and specially Jim Goodall and Professor Fabio Rodrigues.

References

Amaral L. S., Trindade L. S., Bella C. A. P. B., Zurita M. L. P. V., Poltronieri R. C., Silva G. G., Faria C. J. L., Jung C. F., Koukal J. A. (2018). "Brazilian Meteor Observation Network: History of creation and first developments". In, Gyssens M.; Rault J.-L., editors, *Proceedings of the International Meteor Conference*, Petnica, Serbia, 21-24 September, 2017. International Meteor Organization, pages 171–175.

Britt D. T. and Consolmagno S. J. (2003). "Stony meteorite porosities and densities: A review of the data through 2001". *Meteoritics & Planetary Science*, **38**, 1161–1180.

[19] https://www.tinyurl.com/BolideRS

Ceplecha Z., Spalding R. E., Jacobs C. and Tagliaferri E. (1996). "Luminous efficiencies of bolides". In, Timothy D. Maclay, Firooz A. Allahdadi; editors, Characteristics and Consequences of Orbital Debris and Natural Space Impactors, *SPIE*, **2813**, pages 46–56.

Ferus M., Petera L., Koukal J., Lenža L., Drtinová B., Haloda J., Matýsek D., Pastorek A., Laitl V., Poltronieri R. C., Domingues M. W., Gonçalves G., Sato R. O., Knížek A., Kubelík P., Křivková A., Srba J., di Pietro C. A., Bouša M., Vaculovič T., Civiš S. (2020). "Elemental composition, mineralogy and orbital parameters of the Porangaba meteorite". *Icarus*, **341**.

Gural P. S. (2014). "Offbeat and wacky projects using a video meteor camera". In, Rault J.-L., Roggemans P., editors, *Proceedings of the International Meteor Conference*, Giron, France, 18-21 September 2014. International Meteor Organization, pages 44–48.

Hawkins G. S. (1964). The Physics and Astronomy of Meteors, Comets, and Meteorites, 1964, McGraw-Hill Series in Undergraduate Astronomy, New York: McGraw-Hill.

Ibhi A. (2014). "Morocco Meteorite Falls and Finds: Some Statistics". *International Letters of Chemistry, Physics and Astronomy*, **20**, 18–24.

Romig M. F. (1965). "Physics of meteor entry". *AIAA Journal*, **3**, 385–394.

SonotaCo (2009). "A meteor shower catalog based on video observations in 2007-2008". *WGN, Journal of the International Meteor Organization*, **37**, 55–62.

Zurita M., Damiglê R., Di Pietro C., Trindade L., Silva G. G., Lima A., Mota A., Arthur R. and Betzler A. (2019). "A bright fireball over the coast of the state of Bahia". *Boletim da Sociedade Astronômica Brasileira*, **31**, 14–16.

Peculiar meteor above Belgium 2020 May 17

Paul Roggemans

Pijnboomstraat 25, 2800 Mechelen, Belgium
paul.roggemans@gmail.com

The trajectory and orbit calculated for a bright meteor that appeared on 2020 May 17 at 01h45m21s UT indicate it may be an outlier of the eta Aquariid meteor shower.

1 Introduction

During the night of 2020 May 17 at $01^h45^m21^s$ UT a peculiar bright meteor appeared above Belgium, not spectacular in brightness but with a very long trail at the sky. The event was captured by cameras of the CAMS BeNeLux network, BOAM, the Global Meteor Network and several all-sky cameras (*Figure 3 and 4*), including FRIPON stations. The meteor also caused some strong meteor echoes captured by BRAMS stations. The meteor caused some confusion as it appeared at the sky like a typical Eta Aquariid (ETA#031) for any observer while the calculated geocentric radiant position is rather far from the reference position.

2 The observational data

The meteor appeared very nicely in the field of view of the RMS camera BE0001 installed at Grapfontaine, Belgium (*Figure 1*) and in the upper right corner of RMS camera BE0003 installed at Genk, Belgium (*Figure 2*).

Figure 1 – Meteor 2020 May 17 at $01^h45^m21^s$ UT at Observatoire Centre Ardennes, Grapfontaine, Belgium.

Figure 2 – Peculiar meteor 2020 May 17 at $01^h45^m21^s$ UT at Cosmodrome, Genk, Belgium.

Figure 3 – Meteor 2020 May 17 at $01^h45^m21^s$ UT at Oostduinkerke, Belgium (courtesy Geert Vandenbulcke).

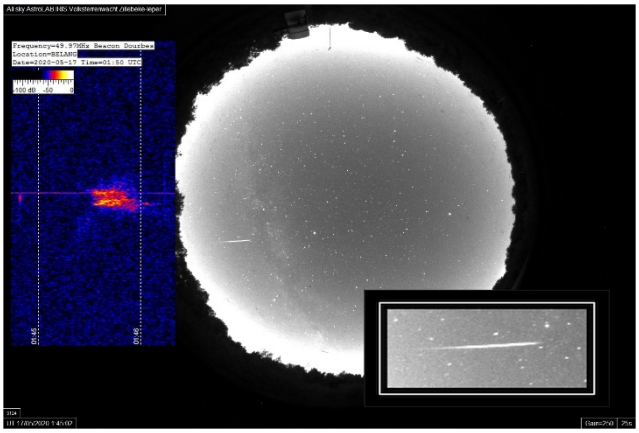

Figure 4 – Meteor 2020 May 17 at $01^h45^m21^s$ UT with the radio echo reflection of BRAMS at AstroLab, Zillebeke-Ieper, Belgium (courtesy Franky Dubois).

The FRIPON network registered the fireball at 7 stations:

- FRNP05 – Arras, France;
- FRNP02 – CappellelaGrande, France;
- NLWN01 – Noordwijk, Netherlands;
- BEBR01 – Bruxelles, Belgium;
- FRPI01 – Amiens, France;
- NLWN02 – Oostkapelle; Netherlands;
- BEWA01 – Liege, Belgium.

3 Orbit and trajectory

The multiple station data of CAMS BeNeLux, the French network BOAM (*Figure 5*) and FRIPON allowed to calculate the trajectory and orbit. The results can be compared in *Table 1*. Unfortunately, the GMN did not provide an orbit for this bright meteor as somehow the quality requirements were not met for the data of the RMS cameras.

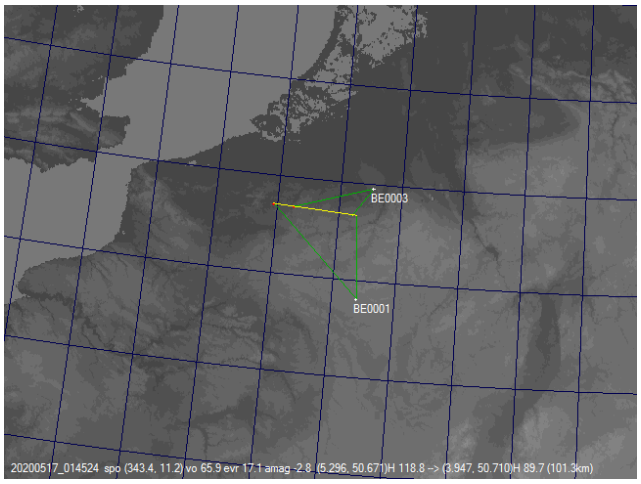

Figure 5 – Meteor 2020 May 17 at $01^h45^m21^s$ UT, trajectory calculated with SonotaCo software by Tioga Gulon.

The meteor appeared like an Eta Aquariid but the calculated geocentric radiant position is rather far from the references listed for this shower (α_g = 338°, δ_g = –1°). However, the orbital elements fit well with these of the Eta Aquariids, except for the inclination i = 144° against 164° for the eta Aquariids. Still it is very likely this meteoroid is an outlier of the eta Aquariid stream as a number of processes cause particles to get spread away from the main stream on slightly different orbits.

Table 1 – Orbit of the fireball of 17 May 2020 at $01^h45^m21^s$ UT by CAMS BeNeLux (Carl Johannink), BOAM (calculated with UFO Orbit by Tioga Gulon) compared to FRIPON (François Colas).

	CAMS BeNeLux	BOAM France	FRIPON
α_g	343.9°	343.8°	–
δ_g	+12.1°	+10.8°	–
H_b	130.1 km	118.8 km	–
H_e	87.0 km	89.6 km	–
v_∞	64.75 km/s	65.9 km/s	–
v_g	64.8 km/s	64.7 km/s	–
a	287.2 A.U.	17 AU	44.8±00.9 A.U.
q	0.6442 A.U.	0.644 A.U.	0.6379±0.004 A.U.
e	0.9978	0.963	0.9857±0.029
ω	105.8°	105.1°	104.83±0.96°
Ω	56.346°	56.352	56.346±0.0005°
i	144.4°	146.7°	144.99±0.72°

4 BRAMS radio echoes

Hervé Lamy reported that this fireball generated huge meteor reflections which completely saturated the receivers with very strong head echoes visible (*Figures 6 and 7*).

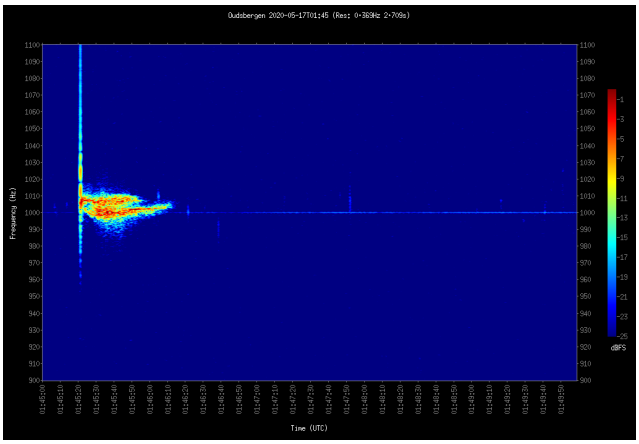

Figure 6 – Meteor 2020 May 17 at $01^h45^m21^s$ UT spectrogram at BRAMS station Oudsbergen (courtesy Hervé Lamy).

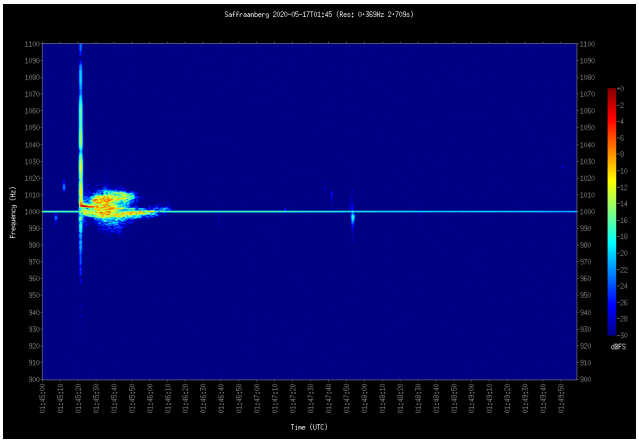

Figure 7 – Meteor 2020 May 17 at $01^h45^m21^s$ UT spectrogram at BRAMS station Saffraanberg (courtesy Hervé Lamy).

Acknowledgment

The author wishes to thank *François Colas* for providing the FRIPON data, *Tioga Gulon* for providing the BOAM trajectory and orbit data, *Carl Johannink* for providing the CAMS BeNeLux data, *Hervé Lamy* for providing the BRAMS data and *Franky Dubois* and *Geert Vandenbulcke* for their permission to include their images.

Figure 8 – Meteor 2020 May 17 at $01^{h}45^{m}21^{s}$ UT on Watec H2 Ultimate (CAMS 815) at Observatoire Centre Ardennes, Grapfontaine, Belgium.

The mission of MeteorNews is to offer fast meteor news to a global audience, a swift exchange of information in all fields of active amateur meteor work without editorial constraints. MeteorNews is freely available without any fee. To receive a notification: https://www.meteornews.net/newsletter-signup/.

You are welcome to contribute to MeteorNews on a regular or casual basis, if you wish to. Anyone can become an author or editor, send an email to us. For more info read: https://meteornews.net/writing-content-for-emeteornews/

The running costs for website hosting are covered by a team of sponsors. We want to thank Anonymous (2x), Nigel Cunnington, Kai Frode Gaarder, Pierre Tioga Gulon, J Andreas Howell, Koen Miskotte, Paul Roggemans, Peter Stewart and Mark Upton for their financial contributions.

Gifts are welcome to share the maintenance costs. To join the team of sponsors send your donation by PayPal: https://www.paypal.com/pools/c/8ks6DnMamJ

Webmaster & account administrator:

Richard Kacerek (United Kingdom): rickzkm@gmail.com

Contributing to this issue:

- **J. Agustoni**
- **A. S. Betzler**
- **R. Damiglê**
- **J. de Souza**
- **C. Di Pietro**
- **M. Domingues**
- **G. Gonçalves**
- **C. Johannink**
- **R. Kacerek**
- **M. Koseki**
- **A. Lima**
- **K. Miskotte**
- **D. C. Mourão**
- **H. Ogawa**
- **P. Roggemans**
- **T. Sekiguchi**
- **R. Sparrius**
- **L. Trindade**
- **F. Verbelen**
- **M. Zurita**

ISSN 2570-4745 Online publication https://meteornews.net

Listed and archived with ADS Abstract Service: https://ui.adsabs.harvard.edu/search/q=eMetN

MeteorNews Publisher:

Valašské Meziříčí Observatory, Vsetínská 78, 75701 Valašské Meziříčí, Czech Republic